Chapter 4
Water Balance Analysis by Using Remote Sensing

CHAPTER 4 WATER BALANCE ANALYSIS BY USING REMOTE SENSING TECHNIQUES

Water balance and groundwater recharge in each sub-basin were analyzed by using meteorological and hydrological data and remote sensing technique. Three kinds of water balance analyses were implemented. The detailed water balance was concentrated to the sub-basin G to know detailed distribution of the infiltration potential under consideration of surface water runoff. The second analysis, simplified water balance, was applied to each sub-basin to grasp the distribution of the infiltration potential in rainy season. The third analysis, monthly macro water balance, was aimed at roughly grasping the monthly change and annual amount of groundwater recharge potential among sub-basins in the Internal Drainage Basin (IDB).

4.1 Purpose of Analysis

The purposes of the analysis are as follows:

- To evaluate evapotranspiration with the help of hydrology and remote sensing technology.
- To delineate the area with high infiltration potential (high groundwater resource potential) in IDB in consideration of water balance of each sub-basin.

4.2 Survey Area

(1) Detailed Water Balance Analysis Area

Taking the Phase I study results into consideration, including ground water potential, fluoride contamination and population regards, the sub-basin G area was selected as a detailed analysis area of interest (Figure 4-1).

The sub-basin G is located in the southern central part of IDB. The topographic features characterizing the basin are divided into two regions by ENE-WSW trending fault. Mountainous and high altitudes areas, approximately 1,000-1,800m in elevation, are distributed in the northern area, and low plain, Bahi swamp and gentle hills, approximately 800-1,000m in elevation, are widely spread in the southern area. Drainages developed in this area converge to the Bahi swamp, and main drainage is Bubu River which flows north to the Bahi swamp.

(2) Simplified Water Balance Analysis Area

Simplified water balance analysis was applied to all sub-basins of IDB.

(3) Macro Water Balance Analysis Area

Macro water balance analysis was applied to all sub-basins of IDB.

4.3 Detailed Water Balance Analysis for the Sub-basin G

Water balance analysis was conducted to estimate volumes of rainfall, evapotranspiration, runoff and infiltration, comparing bi-temporal LANDSAT ETM+ data to observation data in the field. The data acquisitions of LANDSAT ETM+ are in February 2000 and in September 2000, corresponding to rainy and dry seasons respectively (Table 4-1).

Table 4-1 List of LANDSAT ETM Data Used for Detailed Analysis

No.	Path	Row	Acquisition Date	
1	168	63	2000/2/21	Rainy season
2	168	64	2001/3/11	
3	168	65	2000/2/21	
4	169	63	2000/2/12	
5	169	64	2000/2/12	
1	168	63	2000/9/16	Dry season
2	168	64	2000/9/16	
3	168	65	2000/9/16	
4	169	63	2000/9/23	
5	169	64	2000/9/23	

LANDSAT false colour images, SAVI (Soil adjusted vegetation index) images, VSW (Vegetation-Soil-Water) images and land cover maps of each season were prepared as a basic data set for this analysis. These images are shown in Figure 4-1 to Figure 4-4 respectively. In these Figures a high contrast of vegetation activity is clear in each season, which is closely related to water content of the soil. Therefore, these processed remote sensing data could be used as one of the important information to understand the water balance of the sub-basin.

The water balance is expressed by following equation.

$$P = E + R \pm I \qquad \cdots\cdots (1)$$

Where, P is rainfall, E is evapotranspiration, R is runoff and I is infiltration.

Observed meteorological data and hydrological data used in this calculation are as follows,

- Temperature and evaporation data in February and September 2000, derived from "Tanzania Meteorological Agency".
- Rainfall data in February and September, derived from "Summary of rainfall in Tanzania"(1975: East Africa Community, Nairobi).
- Hydrometric gauging station data of river water level shown in Table 4-2.

Table 4-2 Used Hydrometric Gauging Station Data of River Water Level

Hydrometric Gauging Station		Observation Period
2R1A	Bubu at Farkwa	1957 – 1989
2R23	Mponde	1969 – 1985
2R25	Msememb o	1970 – 1991
2R26	Madumu at Makuru	1970 – 1990
2R29	Bubu at Thawi	1972 – 1985

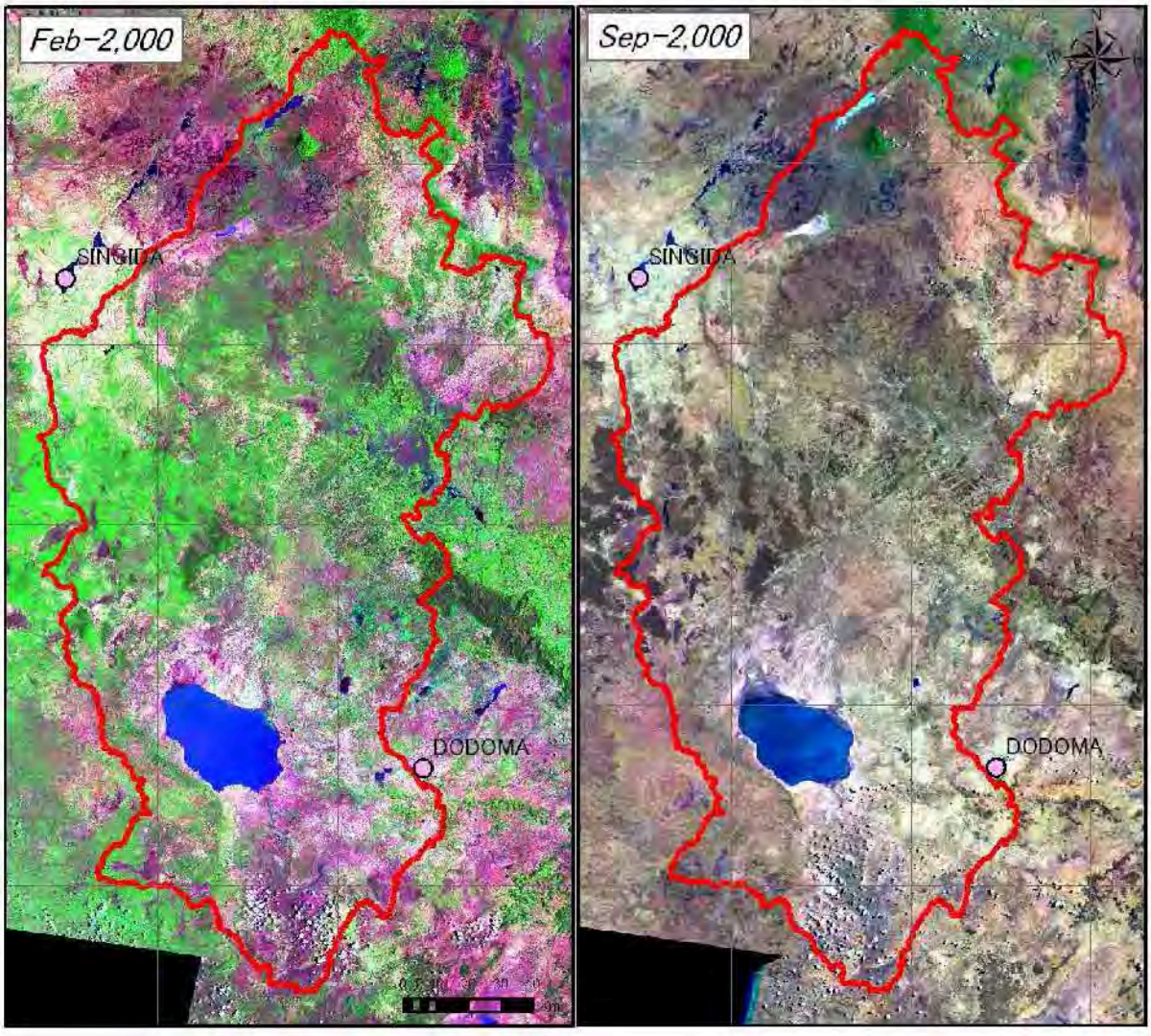

Figure 4-1 LANDSAT ETM+ False Colour Images (B, G, R : Band2, Band4, Band5)

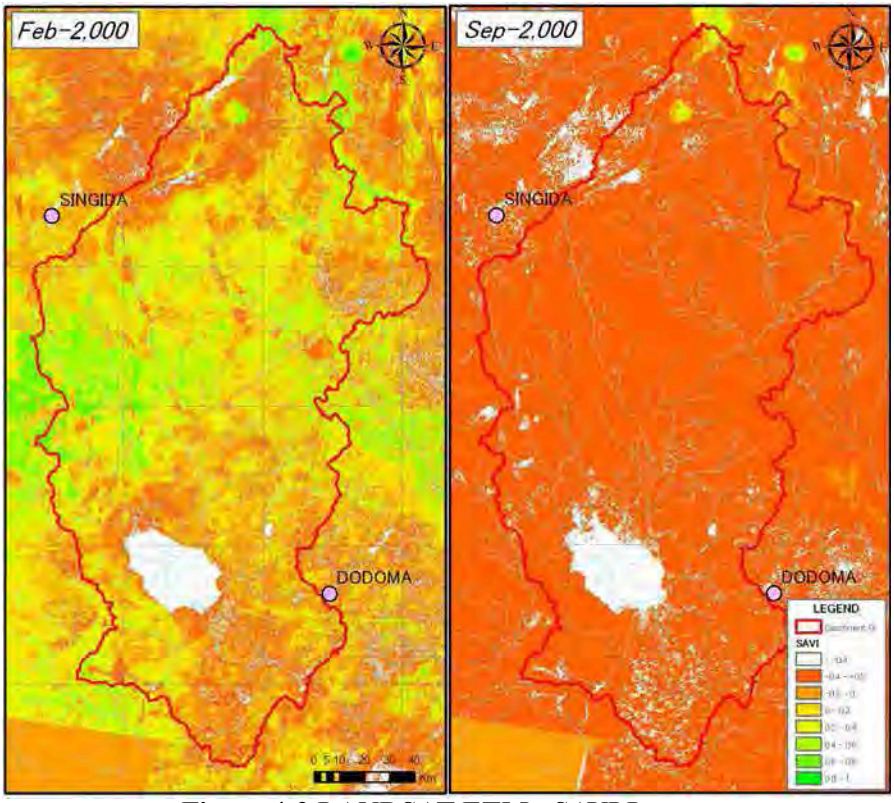

Figure 4-2 LANDSAT ETM+ SAVI Images

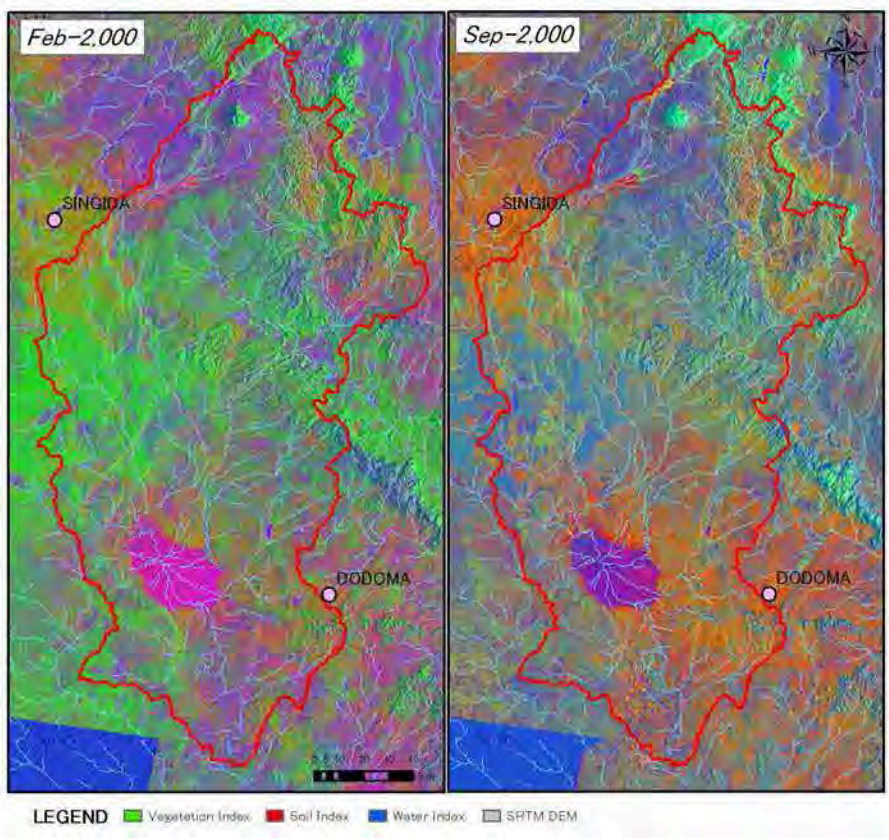

Figure 4-3 LANDSAT ETM+ VSW Images

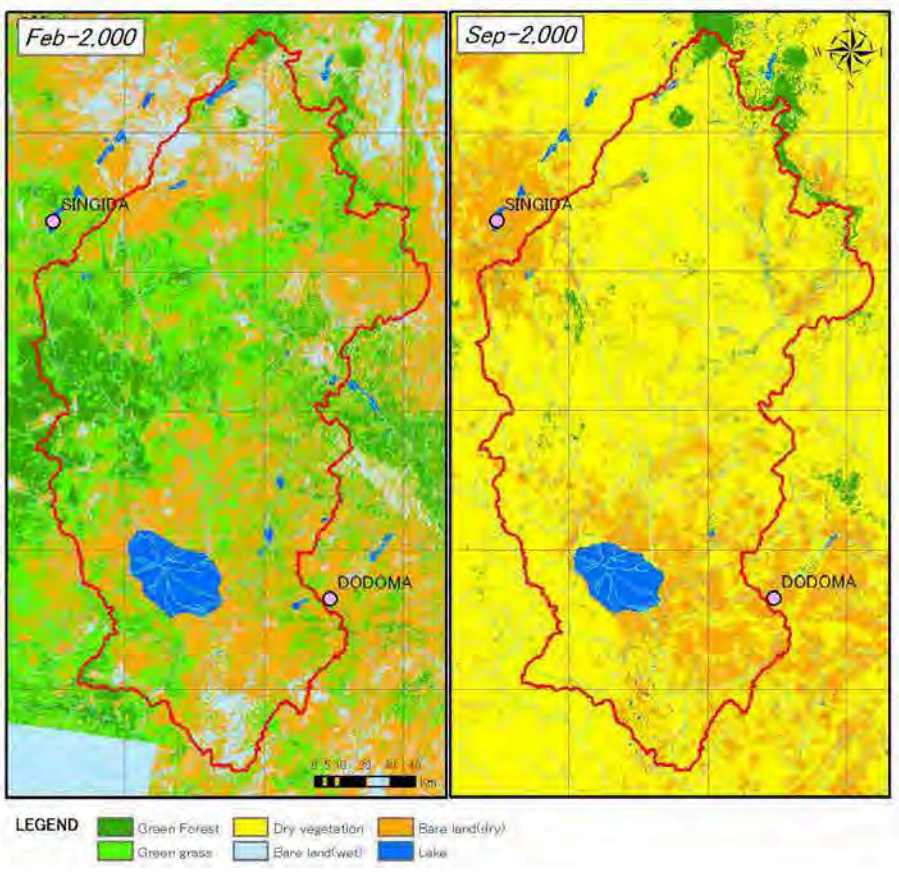

Figure 4-4 Land Cover Maps

Using these images and observed data mentioned above, evapotranspiration maps, rainfall maps and infiltration maps were composed in the area of sub-basin G. The composition methods of each map are explained below.

4.3.1 Evapotranspiration

Makkink equation (Makkink, 1957) was applied to the sub-basin G to estimate potential evapotranspiration ET (mm/day). The equation is defined as follows,

$$ET_{mak} = \frac{\Delta}{\Delta+\gamma} \frac{Rs}{\lambda} \quad \cdots\cdots (2)$$

In addition, following equation (ERSDAC, 2005, Nagai, 1993) were proposed because of various ground condition of the whole sub-basin G.

$$ET = \alpha[(a - A) \frac{\Delta}{\Delta+\gamma} \frac{Rs}{\lambda} + b] \quad \cdots\cdots (3)$$

Where, Rs (cal/cm^2/day) is the total solar radiation, Δ (mbar/°C) is the slope of the saturation vapour

pressure curve, γ (in mbar/°C) is the psychrometric constant, λ (cal/g) is the latent heat, a and b are local constant values, A is Albedo and α is conversion value to actual evapotranspiration ($0< \alpha =<1.0$). And Rs, the total solar radiation, is calculated by using following equation.

$$Rs = Ra (0.18+0.55n/N)$$

Where, Ra is the outer space solar radiation, n is the observed sunshine hours and N is the possible sunshine duration.

$\{\Delta / (\Delta + \gamma)\}$ is dimensionless parameter and approximated by using the following equation.

$$\frac{\Delta}{\Delta + \gamma} = 1 / [1.05 + 1.4 \exp (-0.0604T)]$$

Where, T is the observed temperature. λ (latent heat) is calculated by using following equation.

$$\lambda = 2.5-0.0025T$$

The estimation method of each term of Makkink equation is summarized as follows.

Terms of Makkink equation	Necessary basic data
Albedo	1) Processed satellite images into classified land covers. 2) Correlation of land covers and Albedo values.
Total solar radiation	Sunshine hours distribution
Slope of the saturation vapour pressure curve	Temperature distribution
Psychrometric constant	Temperature distribution
Latent heat	Temperature distribution
Local constant values (a, b)	Pan evaporation data and albedo of evaporation pan

(1) Temperature and Sunshine Hours

The calculation of total solar radiation {Rs} can be obtained from the sunshine hours data, and the calculation of both of dimensionless parameter $\{\Delta / (\Delta+\gamma)\}$ and latent heat {λ} can be obtained from temperature data. Therefore, temperature maps and sunshine hours maps covering the sub-basin G in each season are processed proportionately by using observed meteorological data in Arusha, Kilimanjaro airport, Moshi, Tabora and Dodoma. The processed values of temperature in this way should be rectified by an altitude effect through SRTM DEM data. The altitude effect of temperature is estimated at 0.7°C/100m (commonly used 0.6°C/100m) using regression analysis between observed temperature data and elevation of each meteorological station.

These temperature maps and sunshine hour maps for rainy and dry seasons are shown in Figure 4-5 and Figure 4-6, respectively.

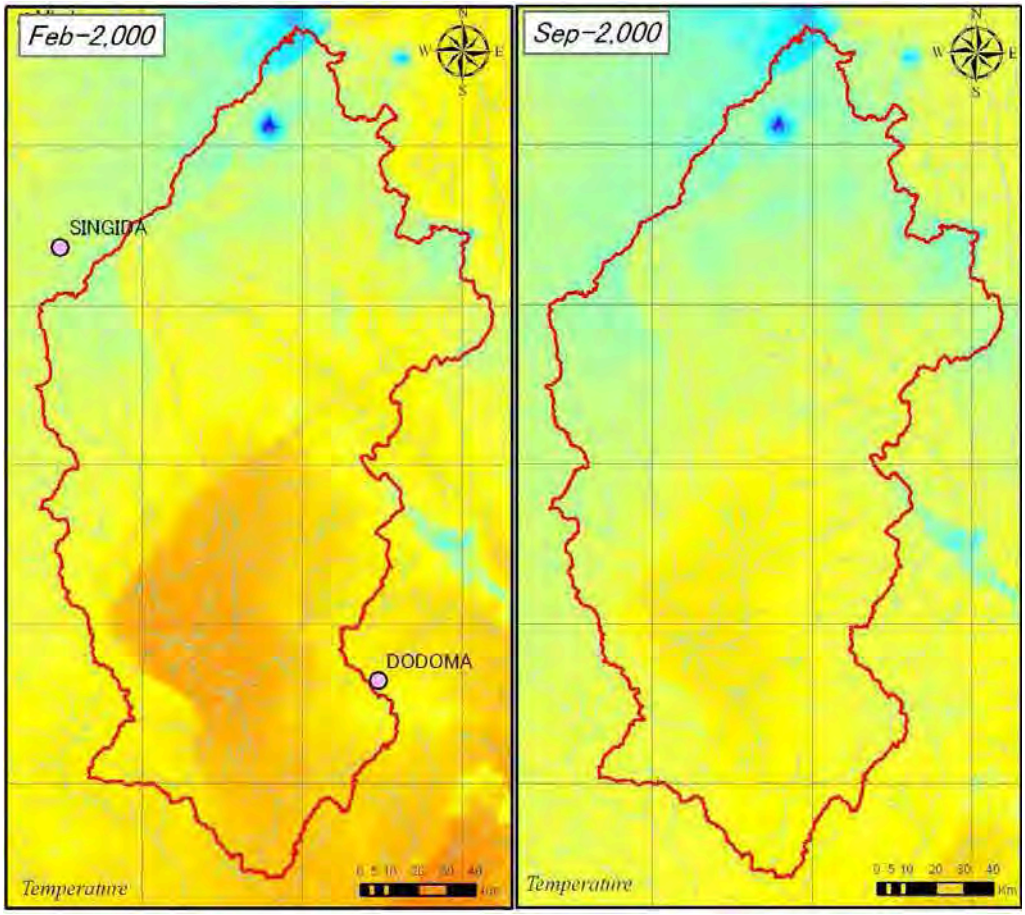

Figure 4-5 Temperature Maps

The temperature distributions on February and September 2000 have similar tendency because the temperature distributions highly depend on the altitude. The temperature is higher in southern low land areas, and lower in northern high land areas. The point of the lowest temperature is the summit of Mt. Hanang located in northern area in the sub-basin G.

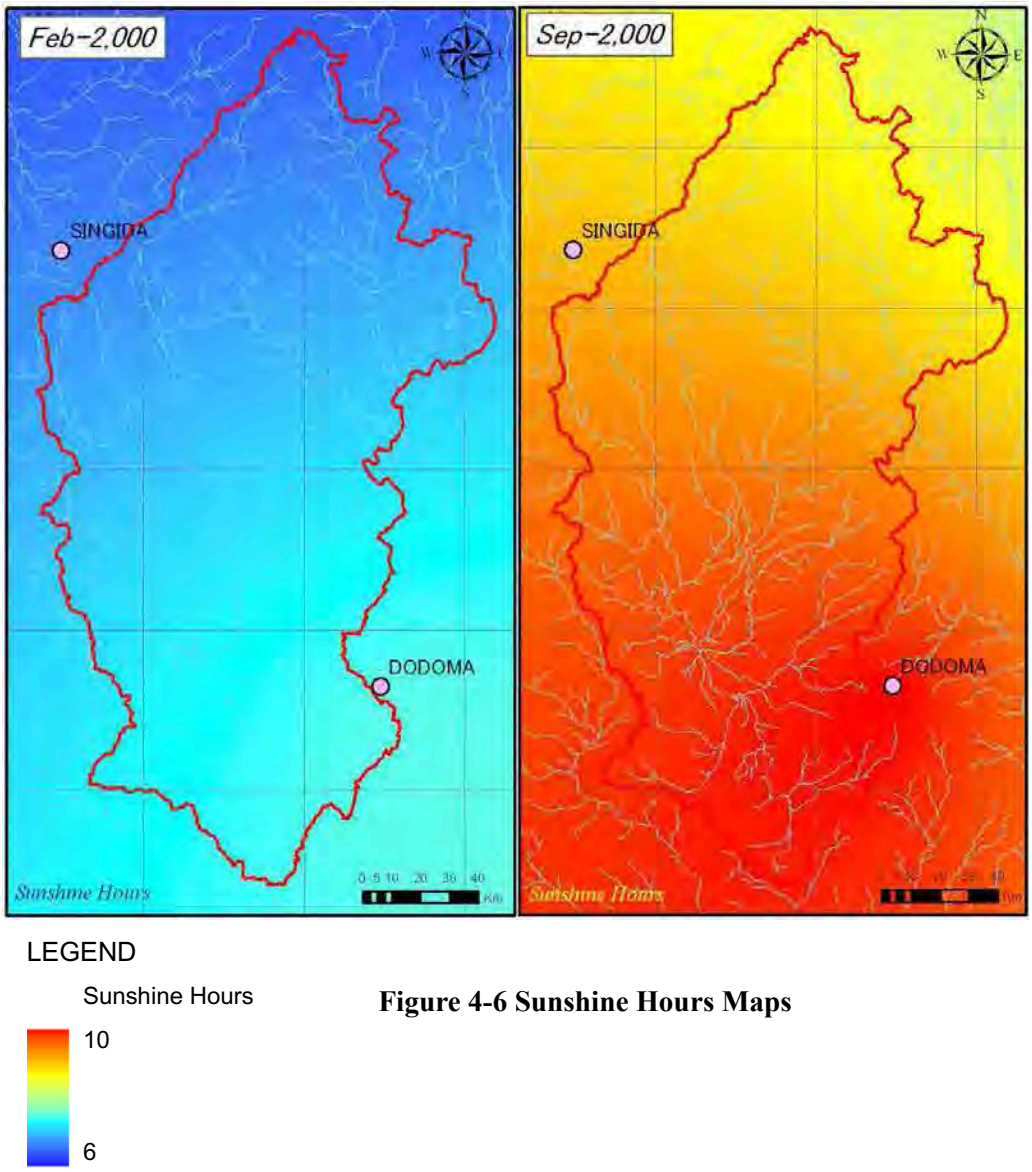

Figure 4-6 Sunshine Hours Maps

The sunshine hours distributions in the sub-basin G on February and September 2000 has the same pattern, that is, the sunshine hours are longer in northern areas than in southern areas. The sunshine hour on February is shorter than that on September because February is in rainy season.

(2) Local Constant Values {a, b}

The local constant values {a, b} are calculated from the data both of the monthly observed evaporation and estimated monthly evapotranspiration (ET_{mak}) through equation (2) for a year duration. As an example, the calculation at Dodoma is described next. The used meteorological data and estimated ET_{mak} are shown in Table 4-3. The scatter diagram in monthly mean of the observed evaporation versus monthly mean of the estimated ET_{mak} is shown in Figure 4-7. In this diagram, x-coefficient 1.04 and y-intercept 0.76 correspond to local constant value {a-A} and {b}

respectively. The albedo {A} of the observed evaporation pan water surface was adopted to be 0.05 to determine the value {a}

Table 4-3 Observed Monthly Weather Data of Dodoma 2004 and Estimated Monthly Evapotranspiration (ET mak)

2,004	T(℃)	Sunshine hours	Evaporation (mm)	Δ/(Δ+γ)	Rs	λ	Estimated ET_{mak} (mm)
Jan	24.9	267		0.73	20.14	2.44	188
Feb	24.3	210	175.2	0.73	17.85	2.44	149
Mar	24.1	239	185.8	0.73	20.22	2.44	186
Apr	23.1	234	157.2	0.72	19.30	2.44	170
May	22.4	304	194.0	0.71	22.67	2.45	203
Jun	20.3	306	196.5	0.68	21.63	2.45	181
Jul	20.0	329	215.0	0.68	23.20	2.45	200
Aug	20.9	326	241.5	0.69	26.04	2.45	228
Sep	22.3	303	262.0	0.71	23.66	2.45	205
Oct	23.9	329	302.7	0.72	25.42	2.44	234
Nov	24.7	300	282.5	0.73	22.34	2.44	201
Dec	24.4	158	212.5	0.73	14.71	2.44	136

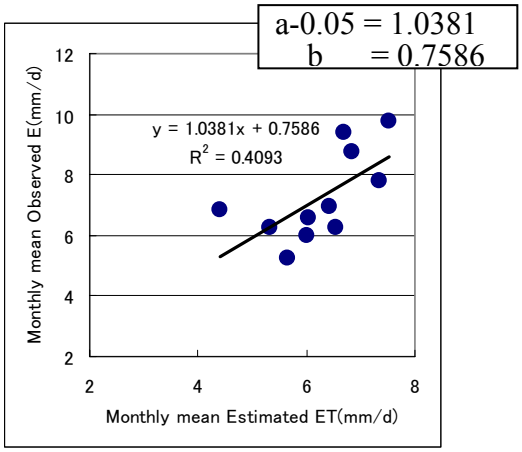

Figure 4-7 Scatter Diagram of Observed E (evaporation) and Estimated ET_{mak}

Table 4-4 Local Constant Value a and b

Meteorological Station	a-0.05	b	R^2
Dodoma	1.04	0.76	0.4
Arusha	1.27	-1.54	0.71
Kilimanjaro	1.36	-2.39	0.66
Moshi	1.69	-3.37	0.79
Tabora	1.04	-0.71	0.56
Average	1.28	-1.452	

Table 4-4 summarizes the local constant values calculated from five meteorological stations. An average of five stations data is adopted as representative local constant value of IDB area, those are {a-0.05} equals 1.28 and {b} does -1.45.

As a result, the evapotranspiration in sub-basin G is estimated by using following equation. (This equation can be applied to the other sub-basins in the IDB.)

$$ET = \alpha \left[(1.28 + 0.05 - A) \frac{\Delta}{\Delta + \gamma} \frac{Rs}{\lambda} - 1.452 \right] \quad \cdots\cdots (4)$$

(3) Albedo

Albedo is a value corresponding to the ratio between incidence and reflection lights at surface. It could be estimated by the results of principal component analysis using LANDSAT ETM+ band1 to band5 data. The first principal component (PC1) ranging from visible to near infrared bands seems to be albedo. Therefore, in order to convert PC1 into albedo, the conversion rate value was necessary to calculate from correlation between recommended Albedo value (Table 4-5) and PC1 scores, using typical data at places of lake, green forest and bare land where field survey about land cover class was conducted in advance.

The scatter diagram is shown in Figure 4-8. The Albedo Maps on February and September 2000 are shown in Figure 4-9.

Table 4-5 Recommended Values of Albedo (ERSDAC 2005)

Land cover class	Albedo
Open water	0.08
Tall forest	0.11-0.16
Grass and pasture	0.20-0.26
Bare soil	0.10(wet)-0.35(dry)

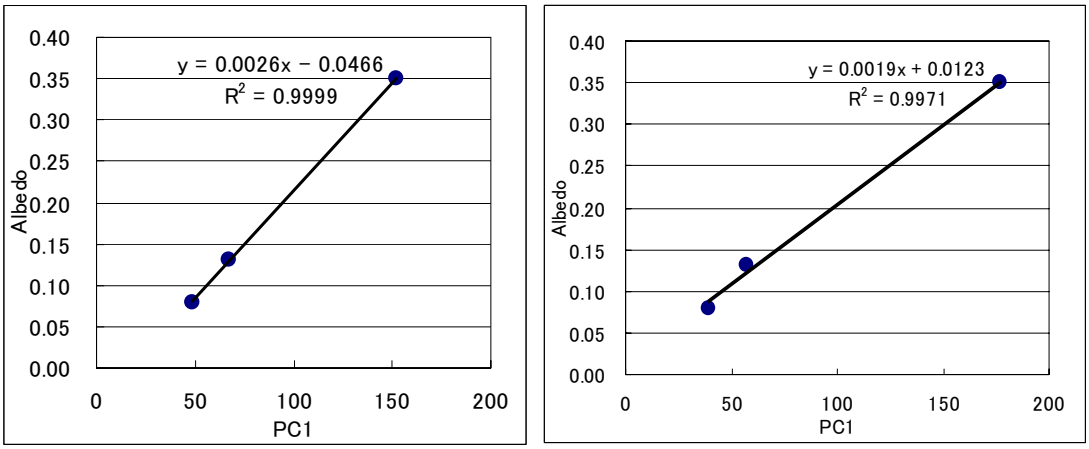

Figure 4-8 Scatter Diagrams of Albedo and First Principal Component of LANDSAT ETM+ Data

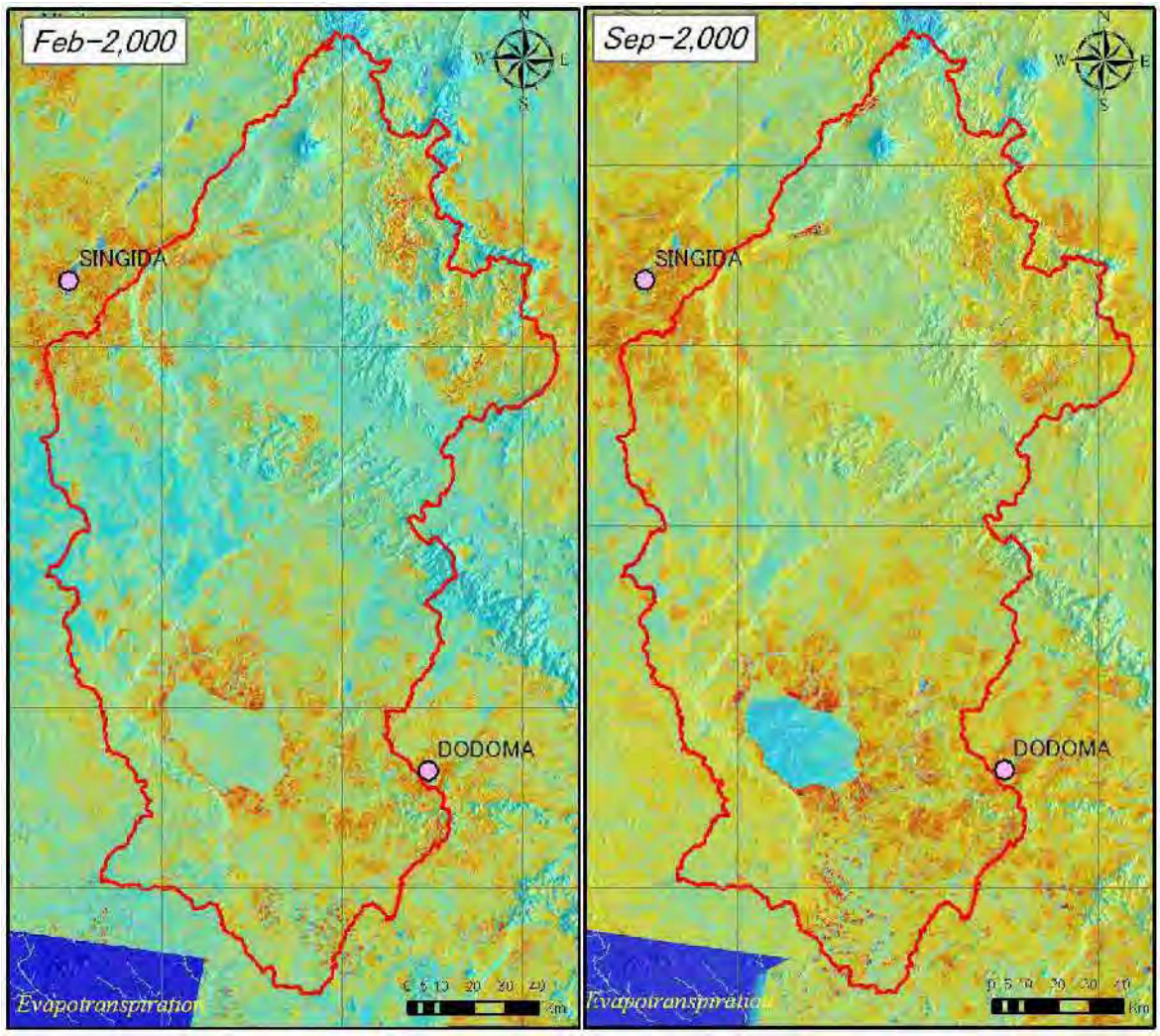

Figure 4-9 Albedo Maps

The albedo of Bahi swamp in September (dry season) has lower value than that in February (rainy season). This result comes from the violet colour of Bahi swamp in Figure 4-3 LANDSAT ETM+ VSW Images. One of the possible reasons is the existence of Mbuga clay because it has dark colour itself.

(4) Conversion Value to Actual Evapotranspiration α

As a general value, 0.6 was adopted to the conversion value α.

(5) Evapotranspiration

The actual evapotranspiration maps in February and September 2000 processed through equation (3) are shown in Figure 4-10. In sub-basin G, the calculated actual evapotranspiration in February was 40 to 80 mm/month, and in September was 60 to 105 mm/month. The actual evapotranspiration estimated here is not necessarily mean real evapotranspiration. It needs water resource, soil moisture, to evaporate. Therefore it should be called actual possible evapotranspiration precisely.

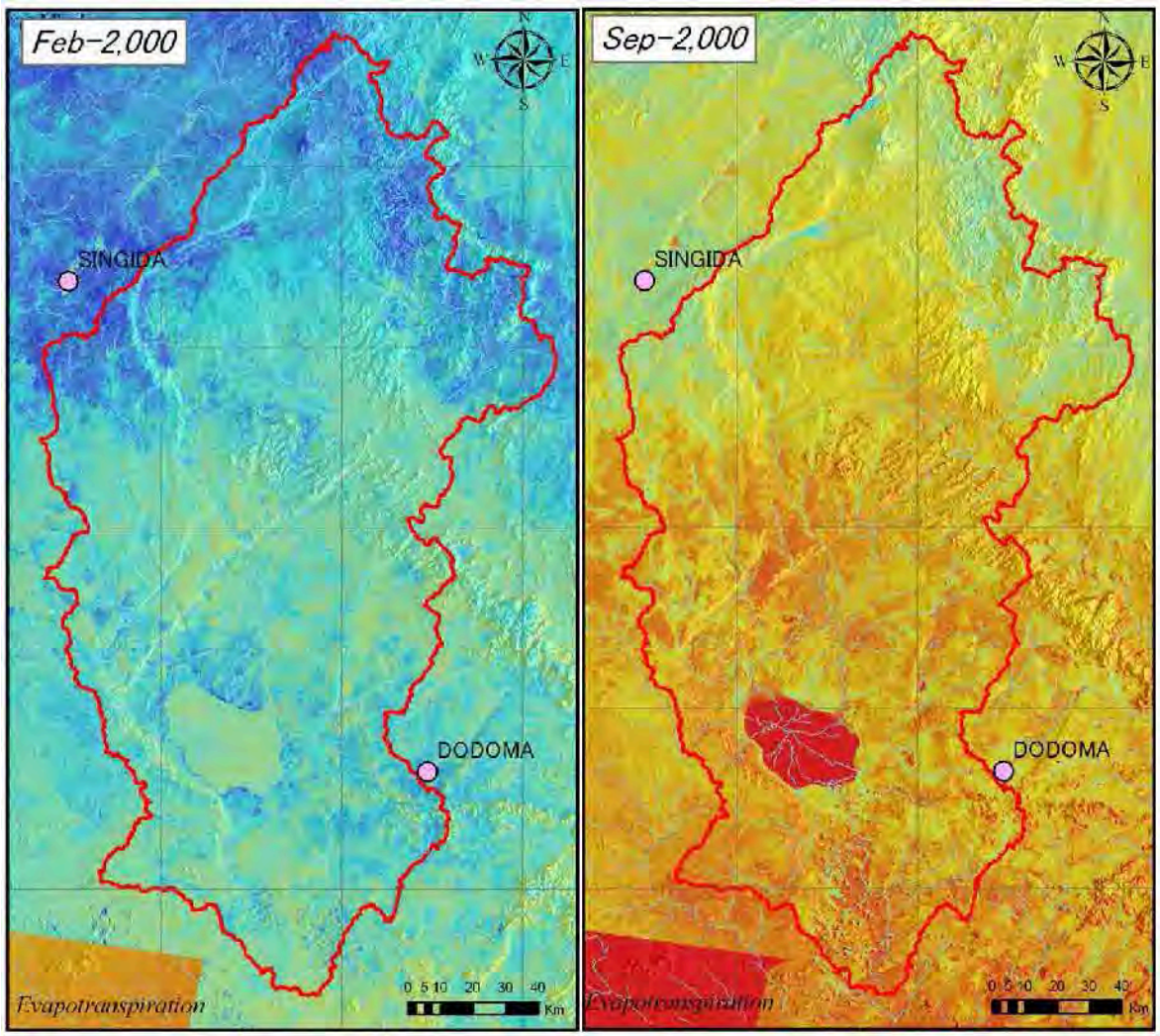

Figure 4-10 Evapotranspiration Maps

4.3.2 Rainfall

Monthly rainfall map in February and September were processed from observed rainfall data. As a precise rainfall data is not available in this area, "Summary of rainfall in Tanzania" (1975) is used for the purpose. Figure 4-11 shows the monthly rainfall maps in February and September. The rainfall in February, rainy season, is about 110mm/month, in September, dry season, is just a few mm/month over sub-basin G.

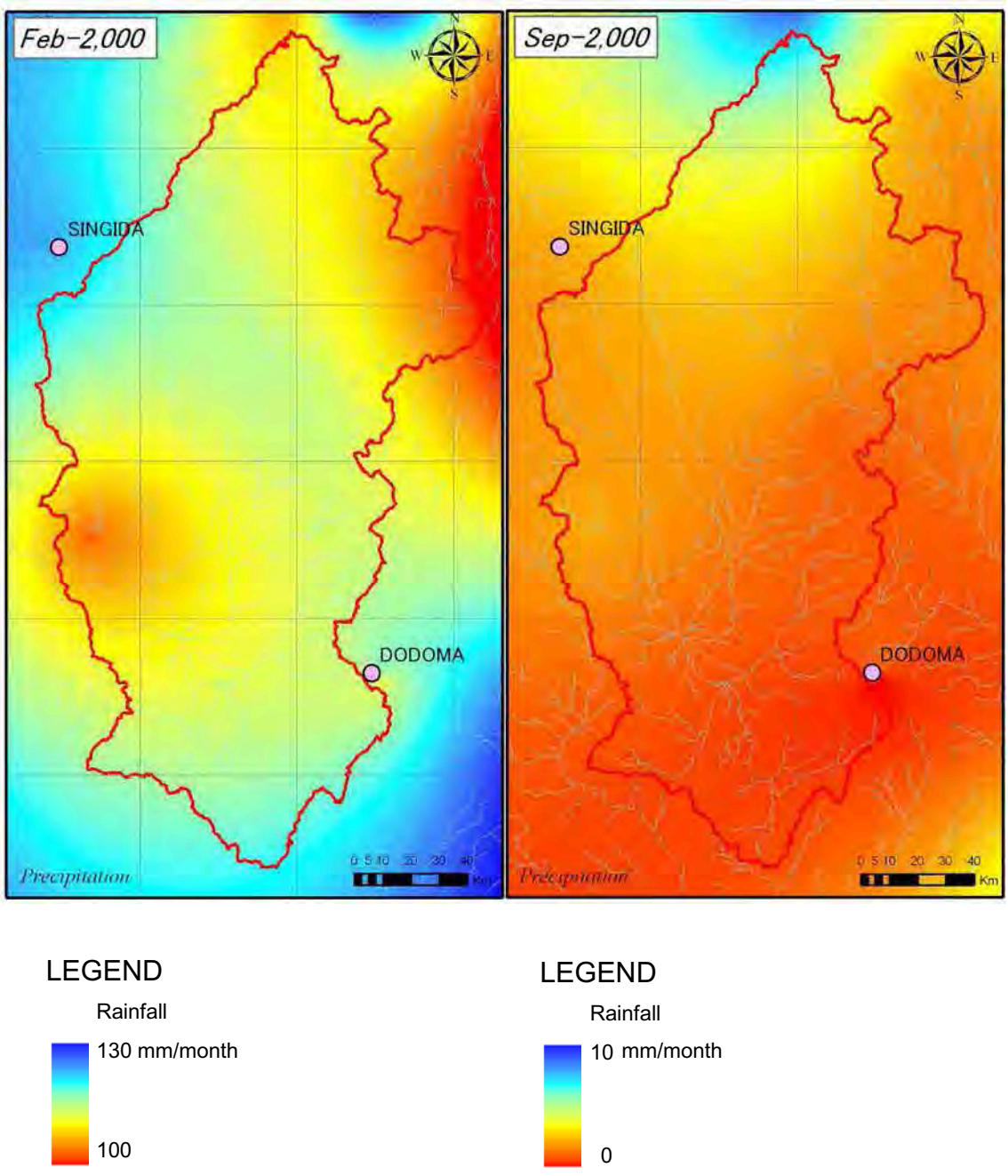

Figure 4-11 Rainfall Maps

4.3.3 Runoff

Figure 4-12 shows locations of hydrometric gauging stations in the sub-basin G and also shows areas of water catchment where stations 2R1A, 2R23, 2R25, 2R26 and 2R29 are located.

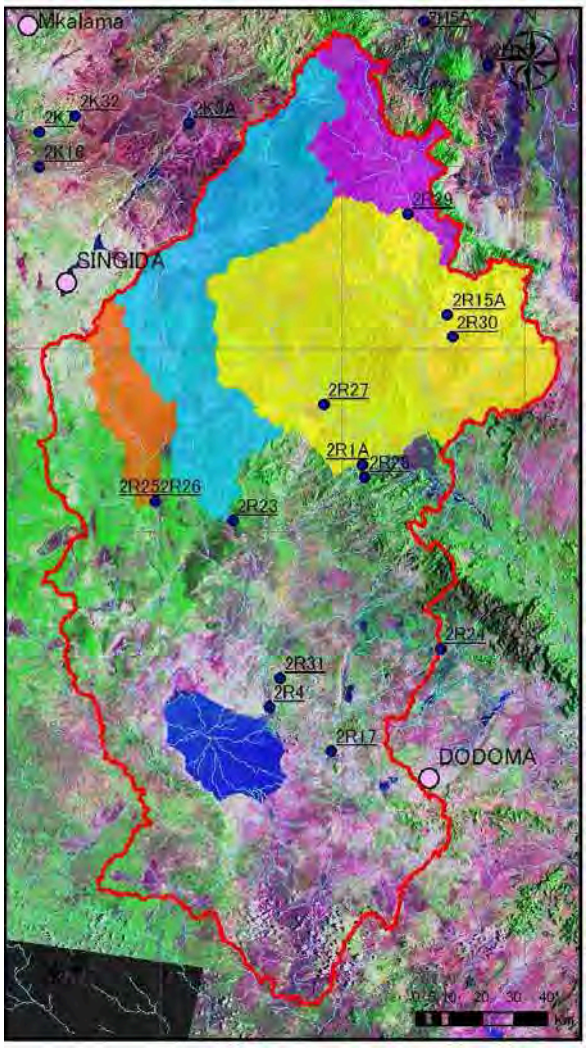

Figure 4-12 Hydrometric Gauging Stations of Sub-basin G and those Water Catchment Areas

For estimating runoff coefficient (Ra), following equation (5) was used.

$$Ra = \frac{R}{P} \qquad \cdots\cdots (5)$$

Where, R is total monthly runoff (m^3) and P is total monthly rainfall (m^3).

The runoff coefficient and observed data are shown in Table 4-6 and Table 4-7.

Table 4-6 Average River Water Discharge in February and September

Hydrometric Gauging Station		Average monthly discharge (m^3/month)		Observation Period
		February	September	
2R1A	Bubu at Farkwa	51,690,062	0	1957 - 1989
2R23	Mponde	5,623,853	0	1969 – 1985
2R25	Msemembo	6,292,870	0	1970 - 1991
2R26	Madumu at Makuru	4,684,244	0	1970 - 1990
2R29	Bubu at Thawi	14,215,652	0	1972 - 1985

Table 4-7 Runoff Coefficients of the Drainages in the Sub-basin G

Hydrometric Gauging Station		Monthly discharge (R) on February (m^3)	Monthly Rainfall (P) on February (m^3)	Runoff coefficient (Ra=R/P)
2R1A	Bubu at Farkwa	51,690,062	731,358,639	0.071
2R23	Mponde	5,623,853	384,674,589	0.015
2R25	Msemembo	6,292,870	94,040,806	0.067
2R26	Madumu at Makuru	4,684,244	94,040,806	0.050
2R29	Bubu at Thawi	14,215,652	132,959,443	0.107

4.3.4 Infiltration

Infiltration maps of sub-basin G in February and September were calculated from rainfall, evapotranspiration and runoff, using equation (6).

$$I = P - ET - Ra \times P \qquad \cdots\cdots (6)$$

Where, I is monthly infiltration, P is monthly rainfall (Figure 4-11), ET is monthly evapotranspiration (Figure 4-10) and Ra is runoff coefficient (Table 4-7).

The Infiltration map of each water catchment area along with gauging stations listing up on Table4-6 is shown in Figure 4-13.

Figure 4-14 shows the possible infiltration map of whole sub-basin G, processed from simple difference between Rainfall and Evapotranspiration using following equation (7).

$$I = P - ET \qquad \cdots\cdots (7)$$

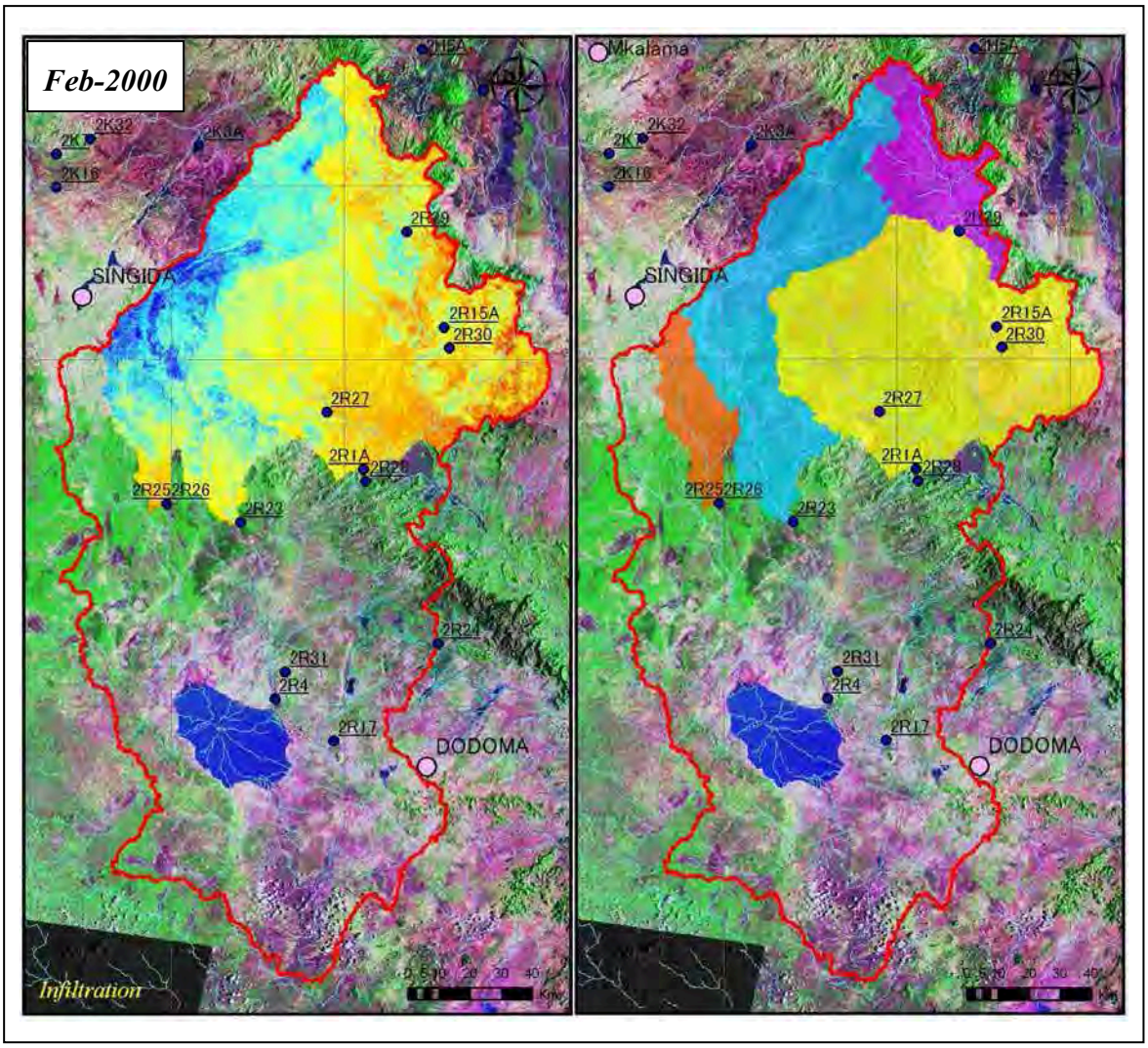

Figure 4-13 Infiltration Map (I = P－ET－Ra×P)
of 2R1A, 2R23, 2R25, 2R26 and 2R29

It is necessary to notice that the infiltration in September is almost zero. The right map shows only the catchment area of each gauging station.

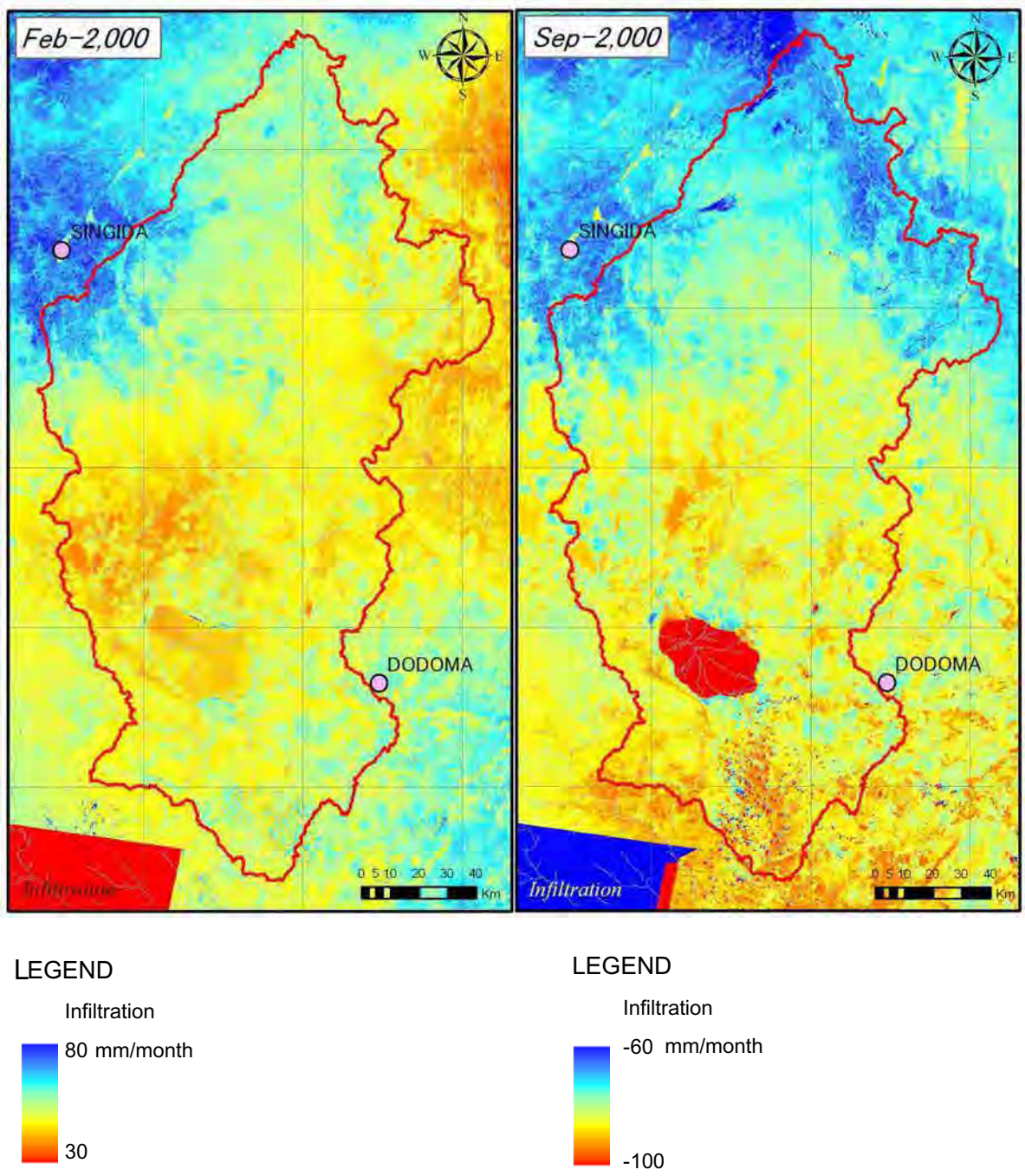

Figure 4-14 Possible Infiltration Maps (I=P-ET) of Sub-basin G

It is necessary to notice that the possible infiltration in September takes minus value. It should be read that there was no possible infiltration.

4.3.5 The Results of Detailed Water Balance of Sub-basin G

The results of water balance analysis for the sub-basin G are summarized in Table 4-.8 and Table 4-.9

Table 4-8 Results of Detailed Water Balance Analysis for Sub-basin G on February

Hydrometric gauging station	Area (Km2)	Rainfall (m3/month)	Evapotranspiration (m3/month)	Runoff (m3/month)	Infiltration (m3/month)	Infiltration Rate (%)
2R1A	6,649	731,358,639	389,602,243	51,690,062	290,066,334	40
2R23	3,374	384,674,589	192,337,295	5,623,853	186,713,441	49
2R25	811	94,040,806	45,399,010	6,292,870	42,348,926	45
2R26	811	94,040,806	45,399,010	4,684,244	43,146,856	46
2R29	1,220	132,959,443	64,650,004	14,215,652	54,093,786	41
Whole G	26,445	2,961,784,657	1,613,114,858	0	1,348,669,799	46

Table 4-9 Results of Detailed Water Balance Analysis for Sub-basin G on September

hydrometric gauging station	Area (Km2)	Rainfall (m3/month)	Evapotranspiration (m3/month)	Runoff (m3/month)	Infiltration (m3/month)	Infiltration Rate (%)
2R1A	6,649	13,297,430	519,298,097	0	(-506,000,667)	0
2R23	3,374	10,460,449	263,198,403	0	(-252,737,954)	0
2R25	811	1,540,324	62,423,638	0	(-60,883,315)	0
2R26	811	1,540,324	63,234,335	0	(-61,694,011)	0
2R29	1,220	4,879,246	89,046,232	0	(-84,166,987)	0
Whole G	26,445	44,955,660	2,194,893,987	0	(-2,149,938,327)	0

The infiltration values for the whole sub-basin G in the tables above mean the possible infiltrations because there are no considerations of runoff terms. The minus values of the infiltrations in the Table 4-9 mean no infiltration in practice.

4.4 Simplified Water Balance Analysis for the Sub-basins in IDB

The methodology of simplified water balance for the Sub-basins in IDB is completely the same as the method applied to sub-basin G. The simplified water balance analysis is a way which applied to only rainy season. The data acquisition of LANDSAT ETM+ was in February 2000, rainy season (Table 4-1). Hereinafter the analysis results are described below.

Used observed meteorological data and hydrological data are as follows,

- Temperature and evaporation data in February and September, 2000 derived from "Tanzania meteorological Agency".
- Rainfall data in February derived from "Summary of rainfall in Tanzania"(1975: East Africa Community, Nairobi).
- River water level data and River discharge rating curves of hydrometric gauging stations shown in Table 4-10.

Table 4-10 Used River Water Level Data of Hydrometric Gauging Station

Hydrometric Gauging Station		Observation Period
2K7	Ndurumo	1962 - 1984
2K11	Manonga	1969 - 1981
2K15	Mhwala	1969 - 1982

Figure 4-15 shows the locations of hydrometric gauging stations in IDB area and water catchment area of stations where river flow discharge data acquired. Temperature map, sunshine hours map, rainfall map, evapotranspiration map and infiltration map in February are shown in Figure 4-16 to Figure 4-20 respectively.

The rainfall map shows that the southern area of Ngorongoro Crater (north sides of Lake Eyasi and Lake Manyara) and the Tabora region have much rainfall than the others. On the other hand, the Masai Steppe (the sub-basin I) has little rainfall.

The evapotranspiration distribution in the whole IDB is strongly affected by the sunshine hours. And in addition, the evapotranspiration in areas where have especially higher elevation such as Mt. Kilimanjaro and Mt. Hanang is affected by the temperature. The evapotranspiration in southern sub-basins has higher value than that in northern sub-basins.

The Figure 4-20, the possible infiltration map (P-ET) on February, shows that the infiltration in the IDB has its highest values at Tabora region and the area between Ngorongoro Crater and Mt. Hanang/Mt. Leya. It is necessary to pay attention to the fact that this tendency will be changed corresponding to target month because of the difference of rainfall and evapotranspiration distribution on each month during rainy season.

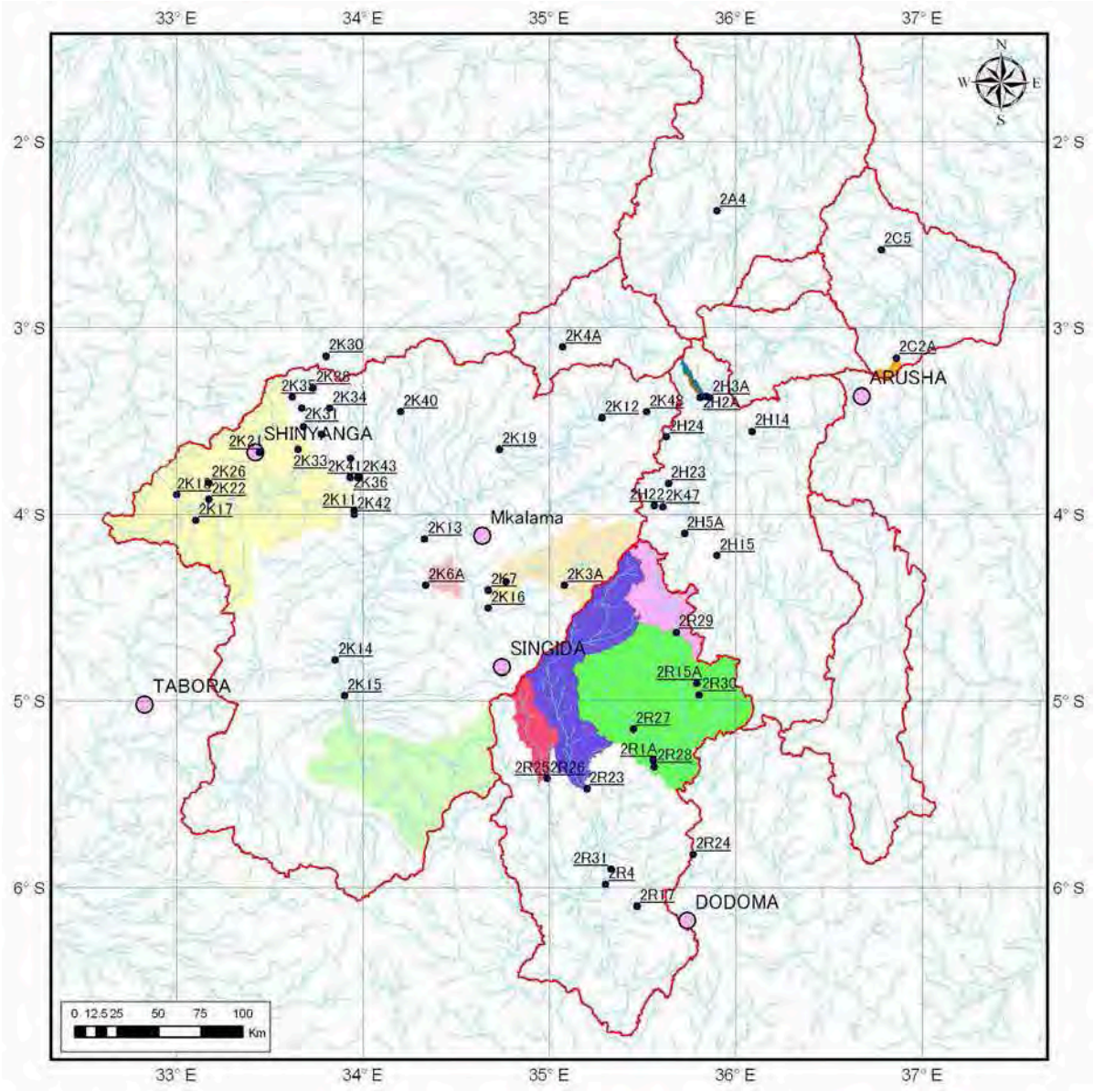

Figure 4-15 The Hydrometric Gauging Stations of IDB Area

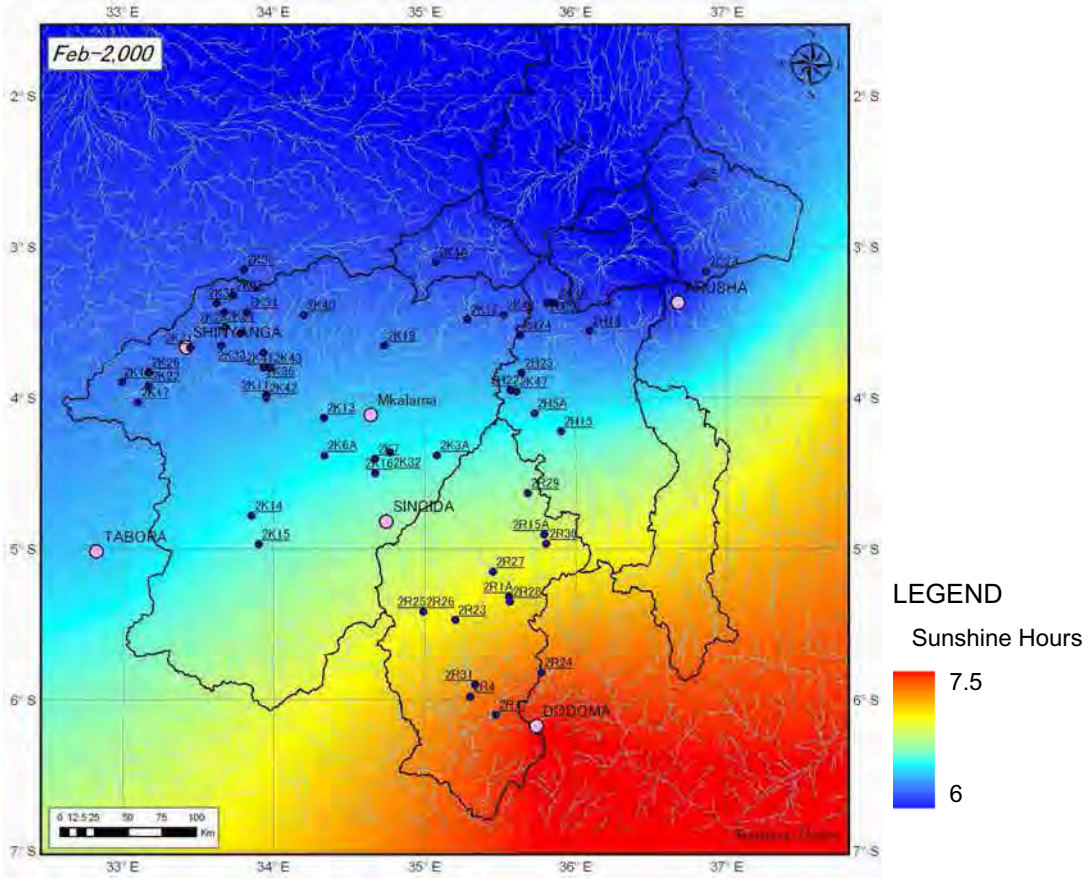

Figure 4-16 Sunshine Hours Map

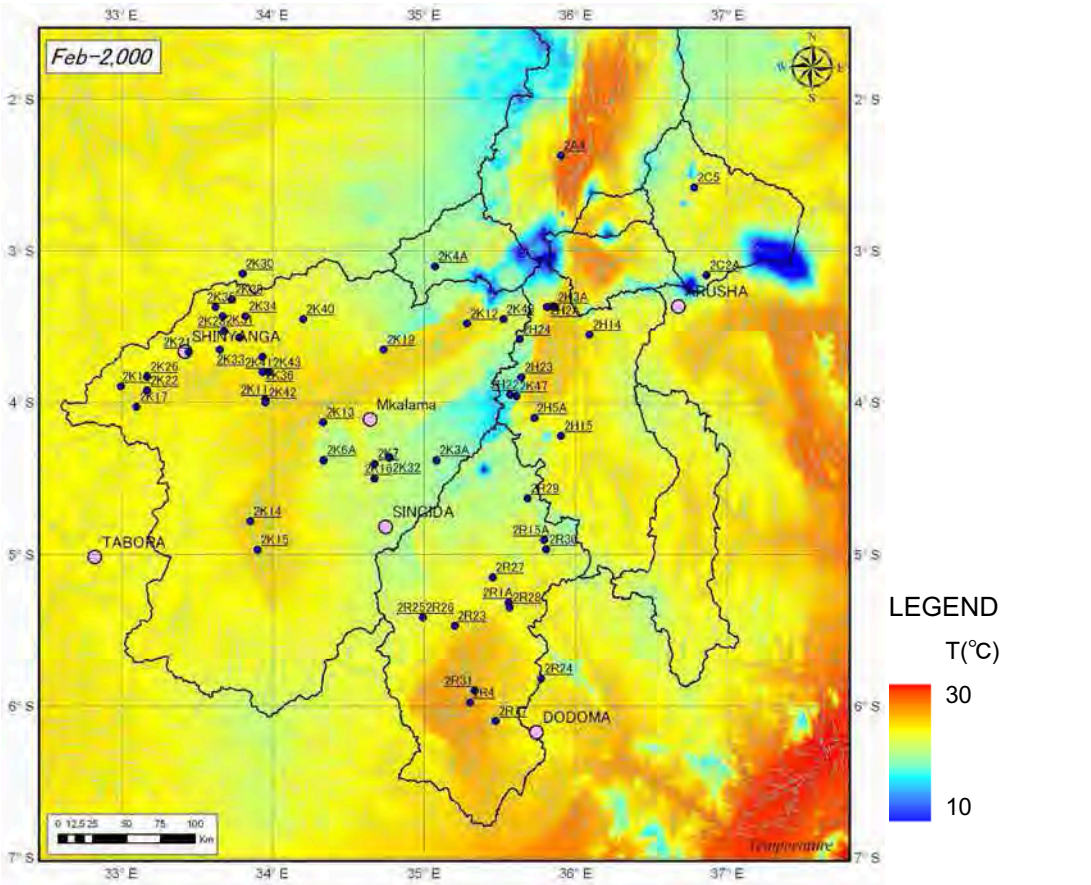

Figure 4-17 Temperature Map

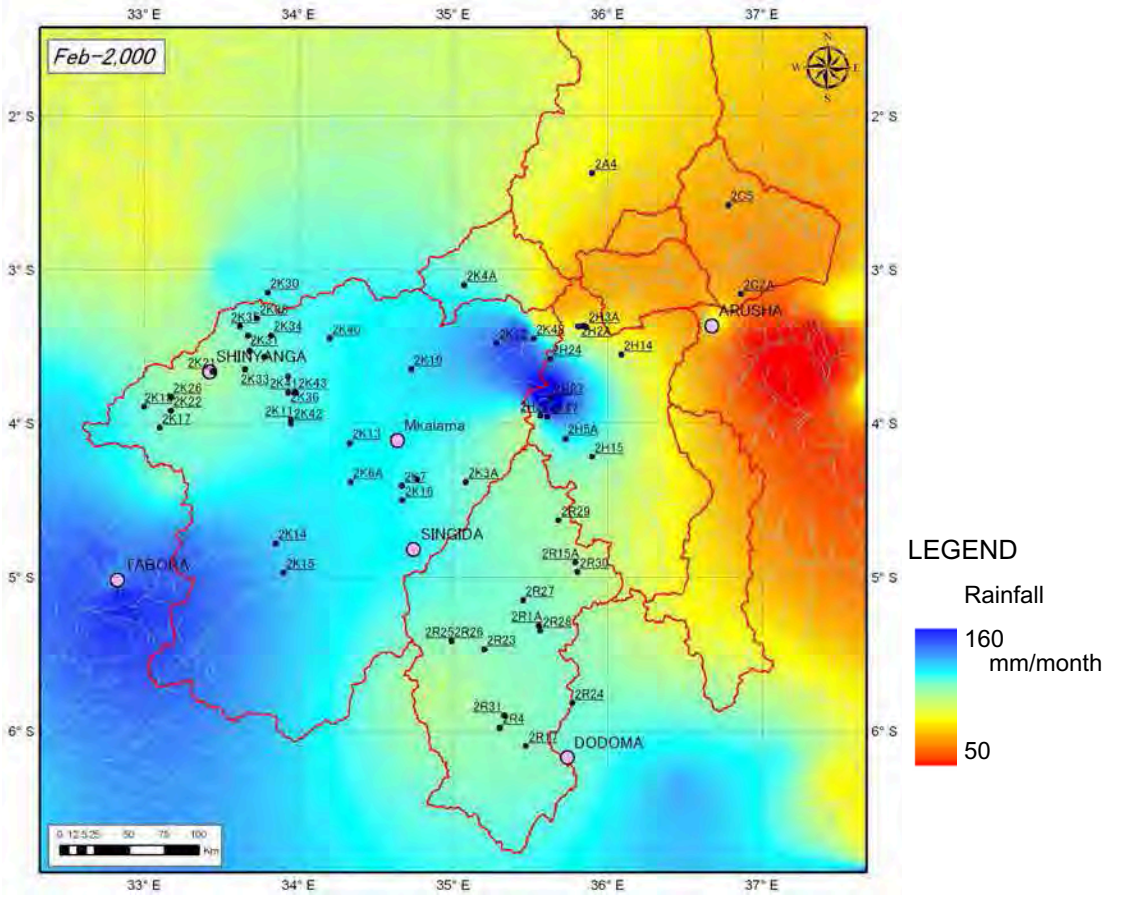

Figure 4-18 Rainfall Map

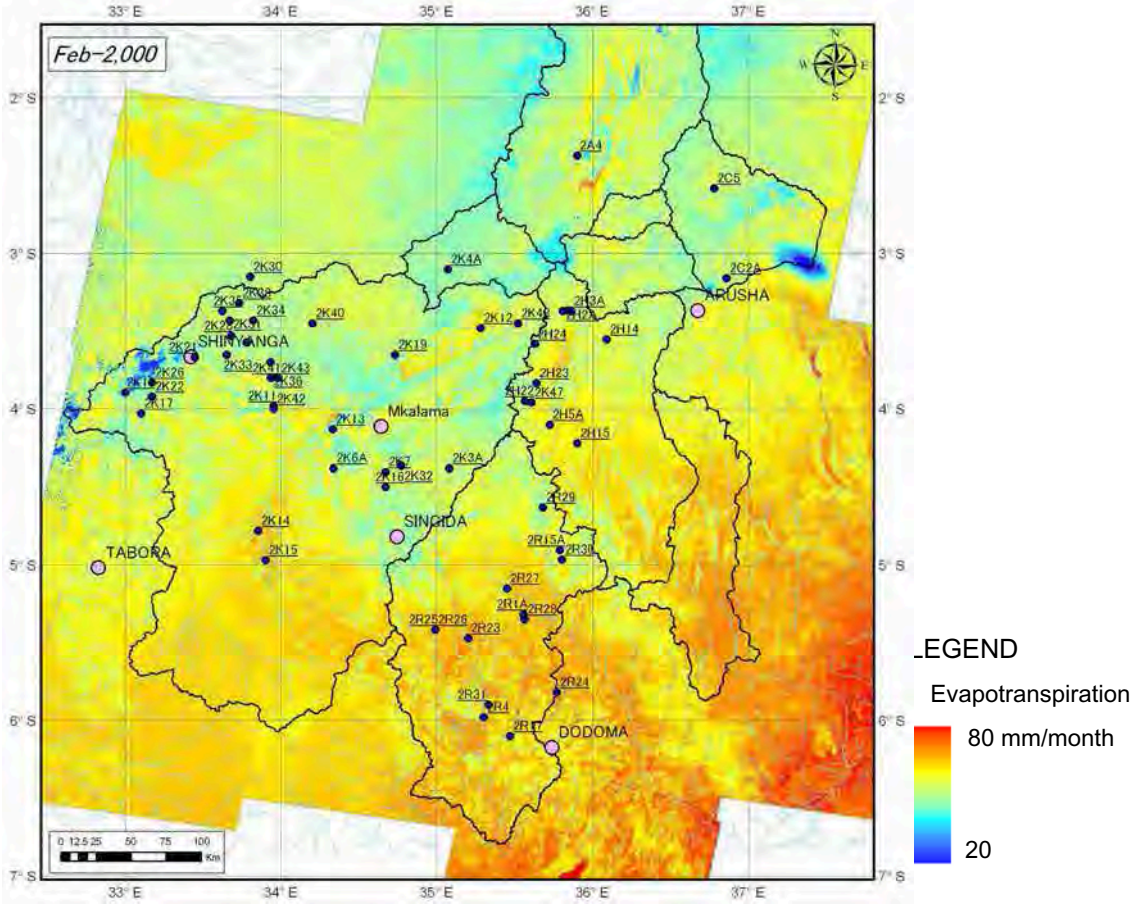

Figure 4-19 Evapotranspiration Map

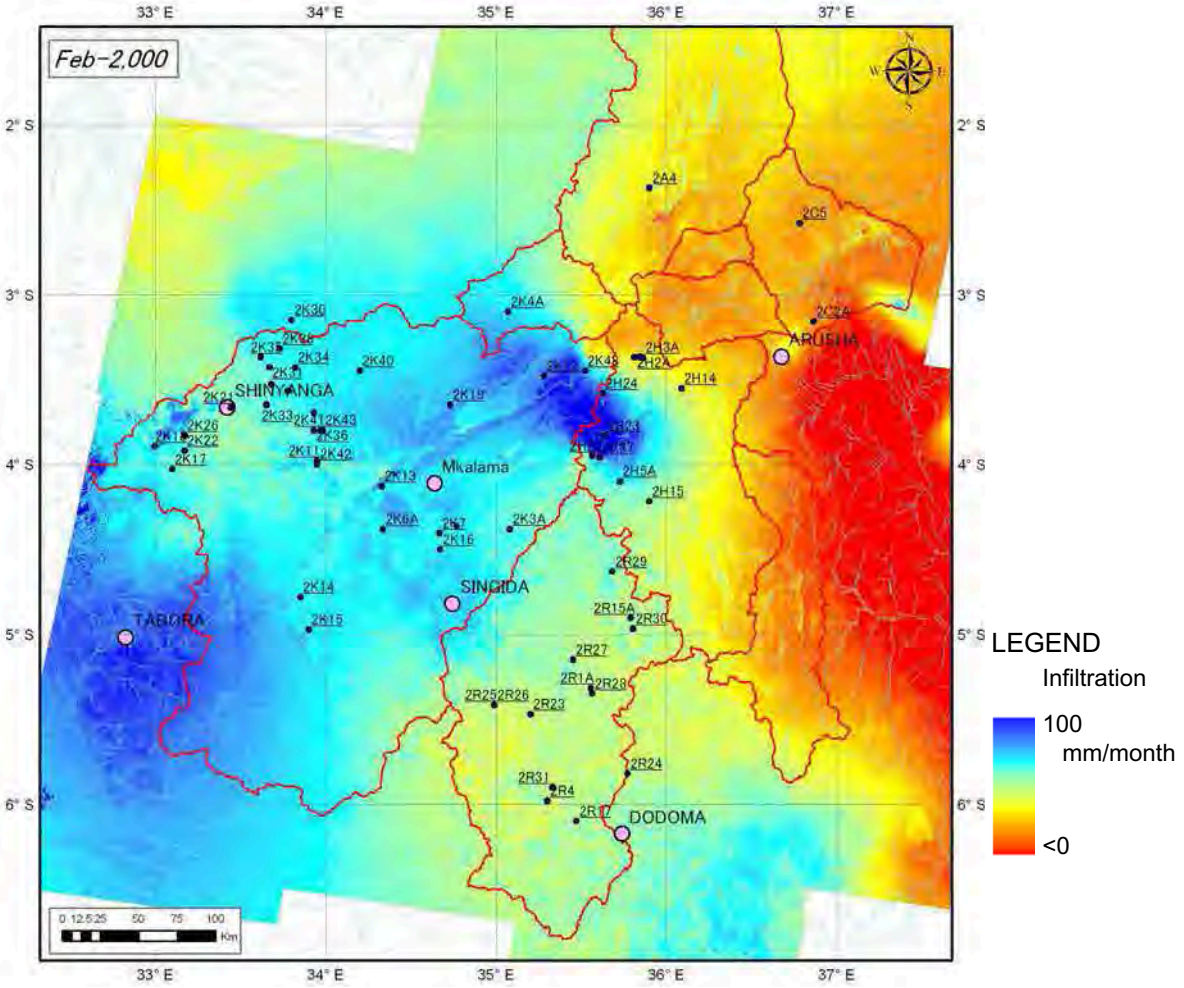

Figure 4-20 Possible Infiltration Map (P-ET)

4.4.1 Sub-basin A (Lake Eyasi Sub-basin)

The Average river water discharge of sub-basin A in February is shown in Table 4-11.

Table 4-11 Average River Water Discharge in February

hydrometric Gauging Station		Average monthly discharge on February (m^3/month)	Observation Period
2K7	Ndurumo	2,825,426	1962 – 1984
2K11	Manonga	4,8276,780	1969 – 1981
2K15	Mhwala	19,190.868	1969 – 1982

The estimation for runoff coefficient of sub-basin A area is shown in Table 4-12.

Table 4-12 Estimation for Runoff Coefficient of Sub-basin A Area

hydrometric Gauging Station		Monthly discharge (R) on February (m^3)	Monthly Rainfall (P) on February (m^3)	Runoff coefficient (Ra=R/P)
2K7	Ndurumo	2,825,426	265,194,016	0.011
2K11	Manonga	4,8276,780	964,000,975	0.050
2K15	Mhwala	19,190.868	576,210,218	0.033

The results of water balance analysis for sub-basin A area are shown in Table 4-13.

Table 4-13 Results of Water Balance Analysis for Sub-basin A

hydrometric gauging station	Area (km^2)	Rainfall (m^3/month)	Evapotranspiration (m^3/month)	Runoff (m^3/month)	Infiltration (m^3/month)	Infiltration Rate (%)
2K7	2,326	265,194,016	120,965,692	2,825,426	141,402,899	53
2K11	8,456	964,000,975	431,263,594	48,276,780	484,460,600	50
2K15	4,647	576,210,218	288,105,109	19,190.868	268,914,241	47
Whole A	64,545	8,068,158,307	3,549,989,655	0	4,518,168,652	56

4.4.2 Sub-basin B [Monduli Sub-basin (1)]

The result of water balance analysis for sub-basin B area is shown in following table.

Table 4-14 Results of Water Balance Analysis for Sub-basin B

Area (km^2)	Rainfall (m^3/month)	Evapotranspiration (m^3/month)	Possible Infiltration (m^3/month)	Infiltration Rate (%)
4,115	296,263,129	213,967,815	82,295,314	28

4.4.3 Sub-basin C [Monduli Sub-basin (2)]

The result of water balance analysis for sub-basin C area is shown in following table.

Table 4-15 Results of Water Balance Analysis for Sub-basin C

Area (km^2)	Rainfall (m^3/month)	Evapotranspiration (m^3/month)	Possible Infiltration (m^3/month)	Infiltration Rate (%)
1,385	99,738,967	72,033,698	27,705,269	28

4.4.4 Sub-basin D (Lake Manyara Sub-basin)

The result of water balance analysis for sub-basin D area is shown in following table.

Table 4-16 Results of Water Balance Analysis for Sub-basin D

Area (km_2)	Rainfall (m^3/month)	Evapotranspiration (m^3/month)	Possible Infiltration (m^3/month)	Infiltration Rate (%)
18,491	1,886,068,302	1,072,470,211	813,598,091	43

4.4.5 Sub-basin E (Lake Natron Sub-basin)

The result of water balance analysis for sub-basin E area is shown in following table.

Table 4-17 Results of Water Balance Analysis for Sub-basin E

Area (km^2)	Rainfall (m^3/month)	Evapotranspiration (m^3/month)	Possible Infiltration (m^3/month)	Infiltration Rate (%)
26,224	2,229,016,075	1,180,067,334	1,048,948,741	47

4.4.6 Sub-basin F (Olduvai Sub-basin)

The result of water balance analysis for sub-basin F area is shown in following table.

Table 4-18 Results of Water Balance Analysis for Sub-basin F

Area (km^2)	Rainfall (m^3/month)	Evapotranspiration (m^3/month)	Possible Infiltration (m^3/month)	Infiltration Rate (%)
4,577	475,996,291	219,690,596	256,305,695	54

4.4.7 Sub-basin G (Bahi (Manyoni) Sub-basin)

Refer to the Clause 4.3.

Table 4-19 Results of Water Balance Analysis for Sub-basin G

Area (km^2)	Rainfall (m^3/month)	Evapotranspiration (m^3/month)	Possible Infiltration (m^3/month)	Infiltration Rate (%)
26,445	2,961,784,657	1,613,114,858	1,348,669,799	46

4.4.8 Sub-basin H (Masai Steppe Sub-basin)

The result of water balance analysis for sub-basin H area is shown in following table.

Table 4-20 Results of Water Balance Analysis for Sub-basin H

Area (km^2)	Rainfall (m^3/month)	Evapotranspiration (m^3/month)	Possible Infiltration (m^3/month)	Infiltration Rate (%)
9,313	763,696,310	596,055,656	167,640,653	22

4.4.9 Sub-basin I (Namanga Sub-basin)

The detailed results of water balance analysis for sub-basin I area are shown in following table.

Table 4-21 Results of Water Balance Analysis for Sub-basin I

Area (km^2)	Rainfall (m^3/month)	Evapotranspiration (m^3/month)	Possible Infiltration (m^3/month)	Infiltration Rate (%)
14,080	985,600,000	704,000,000	281,600,000	29

4.4.10 Summary of the Water Balance in February (Rainy Season)

The possible infiltrations of each sub-basin in February were summarized in below Table 4-22 and Figure 4-21. The possible infiltration quantity (mm) and infiltration rate has the highest value in the sub-basin A. The second highest group consists of sub-basin D (Lake Manyara sub-basin), E (Lake Natron sub-basin), F (Olduvai sub-basin) and G (Bahi sub-basin). The lowest possible infiltration group consists of sub-basin B {Monduli (1) sub-basin}, C {Monduli (2) sub-basin}, H (Masai Steppe sub-basin) and I (Namanga sub-basin).

Table 4-22 Summary of Water Balance Analysis for IDB on February

Sub-basin		Area (km^2)	Rainfall (m^3/month)	Evapo -transpiration (m^3/month)	Possible Infiltration		
					(m^3/month)	(%)	(mm/month)
A	Lake Eyasi	64,545	8,068,158,307	3,549,989,655	4,518,168,652	56	70
B	Monduli (1)	4,115	296,263,129	213,967,815	82,295,314	28	20
C	Monduli (2)	1,385	99,738,967	72,033,698	27,705,269	28	20
D	Lake Manyara	18,491	1,886,068,302	1,072,470,211	813,598,091	43	44
E	Lake Natron	26,224	2,229,016,075	1,180,067,334	1,048,948,741	47	40
F	Olduvai	4,577	475,996,291	219,690,596	256,305,695	54	56
G	Bahi (Manyoni)	26,445	2,961,784,657	1,613,114,858	1,348,669,799	46	51
H	Masai Steppe	9,313	763,696,310	596,055,656	167,640,653	22	18
I	Namanga	14,080	985,600,000	704,000,000	281,600,000	29	20

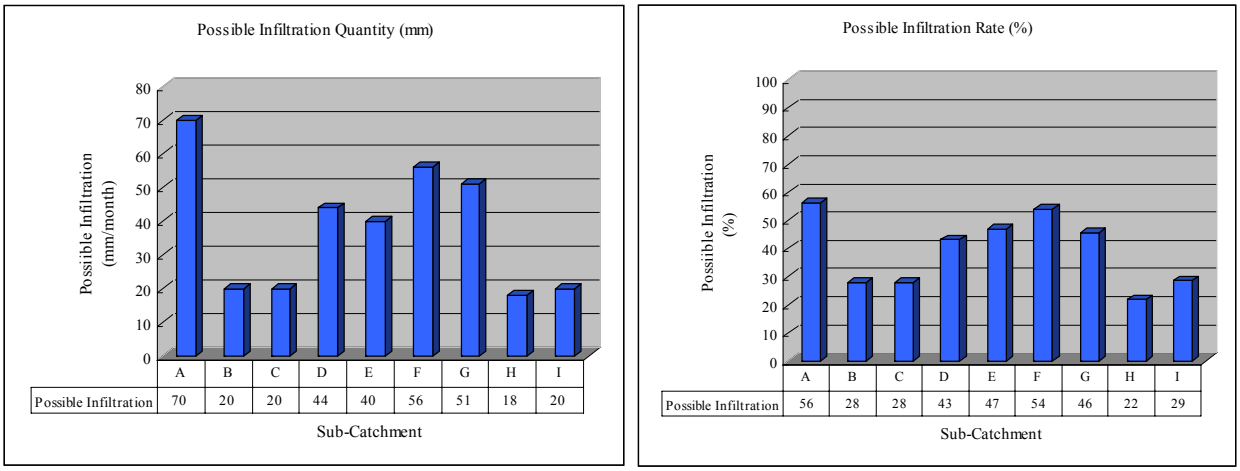

Figure 4-21 Possible Infiltration on February

4.5 Macro Water Balance Analysis

Macro water balance analysis was implemented using monthly mean data for each sub-basin in the IDB. The used method and data were as follows:

(1) The Used Method

The possible monthly infiltration of each whole sub-basin was processed from simple difference between monthly rainfall and evapotranspiration using following equation (8).

$$I = P - ET \quad \cdots (8)$$

Each sub-basin in the IDB has no runoff to outside of itself so that the runoff term is not included in the macro water balance.

The monthly rainfall of each whole sub-basin was estimated by spatially average of the observed rainfall data.

The monthly evapotranspiration of each whole sub-basin was estimated from modified Makkink equation (9).

$$ET = \alpha \left[(a - A) \frac{\Delta}{\Delta + \gamma} \frac{Rs}{\lambda} + b \right] \quad \cdots (9)$$

The detailed explanation about each term in the above equation is shown in section 4.3.1. Taking the detailed and simplified analysis results into consideration, the following values were adopted for the macro water balance analysis: the conversion value to actual evapotranspiration α =0.6, the local constant values a=1.28 + 0.05, b=-1.452 and the albedo A in Table 4-23 for each land cover.

Table 4-23 Albedo Values

Land cover class	Albedo
Forest	0.14
Grass and pasture	0.23
Bare soil – wet	0.10
Bare soil – dry	0.35

The land covers in each sub-basin are classified by the results of principal component analysis using LANDSAT ETM+ band1 to band5 data at February 2000. The classified area of each land cover is shown in Table 4-24 and Figure 4-22, and applied to the evaluation of the evapotranspiration in whole year. This means that the seasonal change of the land covers is neglected in the estimation because it has no effect on the estimation of infiltration in dry season due to almost no rainfall.

Table 4-24 Land Covers of Sub-basins in February 2000 by Remote Sensing

Sub-basin	Catchment Area (km2)	Land Cover Area (km2)			
		Forest	Grass	Bare land-wet	Bare land-dry
A	64,545	10,033	18,091	7,143	29,278
B	4,115	228	195	567	3,125
C	1,385	29	47	246	1,062
D	18,491	1,144	1,932	7,617	7,798
E	26,224	312	846	10,433	14,633
F	4,577	295	311	838	3,133
G	26,445	3,700	8,311	3,066	11,368
H	9,313	836	1,971	2,871	3,636
I	14,080	339	765	3,120	9,856
Total	169,175	16,916	32,469	35,901	83,889

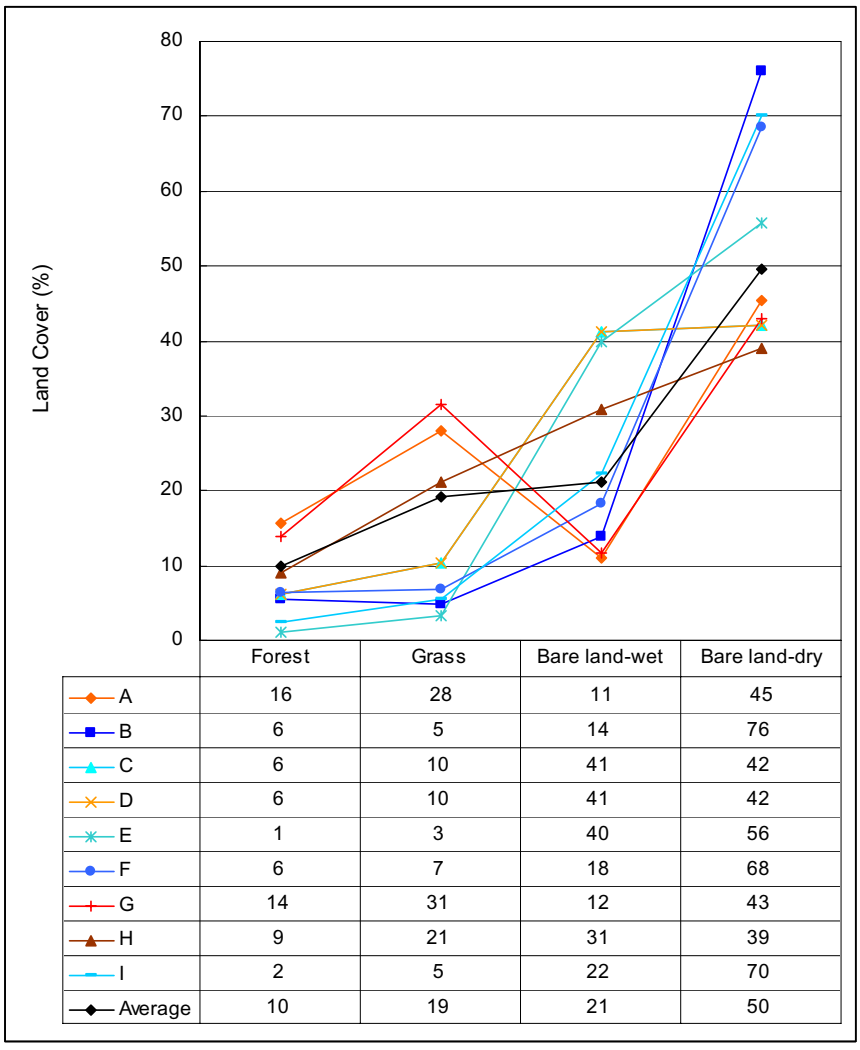

	Forest	Grass	Bare land-wet	Bare land-dry
A	16	28	11	45
B	6	5	14	76
C	6	10	41	42
D	6	10	41	42
E	1	3	40	56
F	6	7	18	68
G	14	31	12	43
H	9	21	31	39
I	2	5	22	70
Average	10	19	21	50

Figure 4-22 Land Cover Ratio of Each Sub-basin

The averaged land cover on February 2000 shows that forest land 10%, grass land 19%, bare land-wet 21% and bare land-dry 50%.

The other terms of the evapotranspiration were determined by observed sunshine hours and Temperature.

(2) The Used data

Observed meteorological data used in this calculation are as follows,

- Temperature, sunshine hours and evaporation data from 1975 to 2004, derived from "Tanzania meteorological Agency".
- Rainfall data in every month, derived from "Summary of rainfall in Tanzania" (1975: East Africa Community, Nairobi).
- LANDSAT ETM+ band1 to band5 data at February 2000

(3) Results

The estimation results are shown in Figure 4-23 to Figure 4-27.

1) Rainfall;

In the northern sub-basins monthly rainfall has its maximum value on April; on the other hand, in the southern sub-basins monthly rainfall has no major peak. They have rather stable values during rainy season.

2) Evapotranspiration;

Monthly evapotranspiration in southern sub-basins has higher value than that in northern sub-basins. Each sub-basin has its highest evapotranspiration on October.

3) Possible infiltration;

Monthly possible infiltration in the IDB occurs only in rainy season. Annual possible infiltration is 155 mm/year on the average in the whole IDB. The F sub-basin has the highest annual possible infiltration, and the H sub-basin has the lowest value in the IDB. These values highly depend on the quantities of rainfall in each sub-basin.

It is necessary to take notice that even if "annual summation of monthly rainfall" minus "annual summation of calculated monthly evapotranspiration" is less than zero, there are still infiltrations during rainy season. Shortly, there are no waters for evapotranspiration in dry season so that calculated evapotranspiration can not occur.

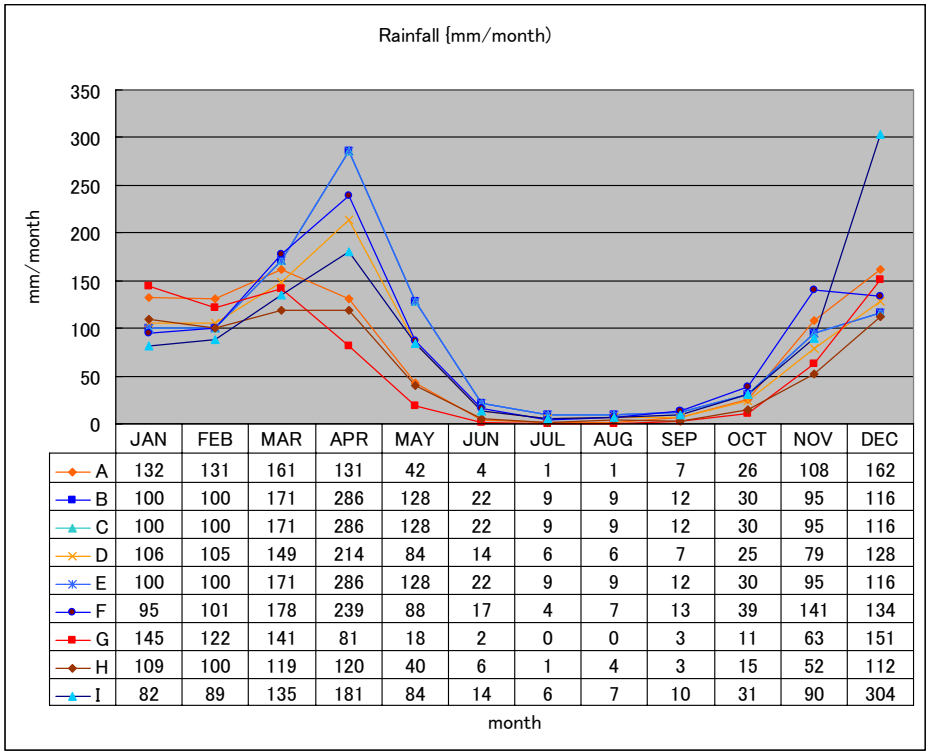

	JAN	FEB	MAR	APR	MAY	JUN	JUL	AUG	SEP	OCT	NOV	DEC
A	132	131	161	131	42	4	1	1	7	26	108	162
B	100	100	171	286	128	22	9	9	12	30	95	116
C	100	100	171	286	128	22	9	9	12	30	95	116
D	106	105	149	214	84	14	6	6	7	25	79	128
E	100	100	171	286	128	22	9	9	12	30	95	116
F	95	101	178	239	88	17	4	7	13	39	141	134
G	145	122	141	81	18	2	0	0	3	11	63	151
H	109	100	119	120	40	6	1	4	3	15	52	112
I	82	89	135	181	84	14	6	7	10	31	90	304

Figure 4-23 Monthly Rainfall Change in Each Sub-basin

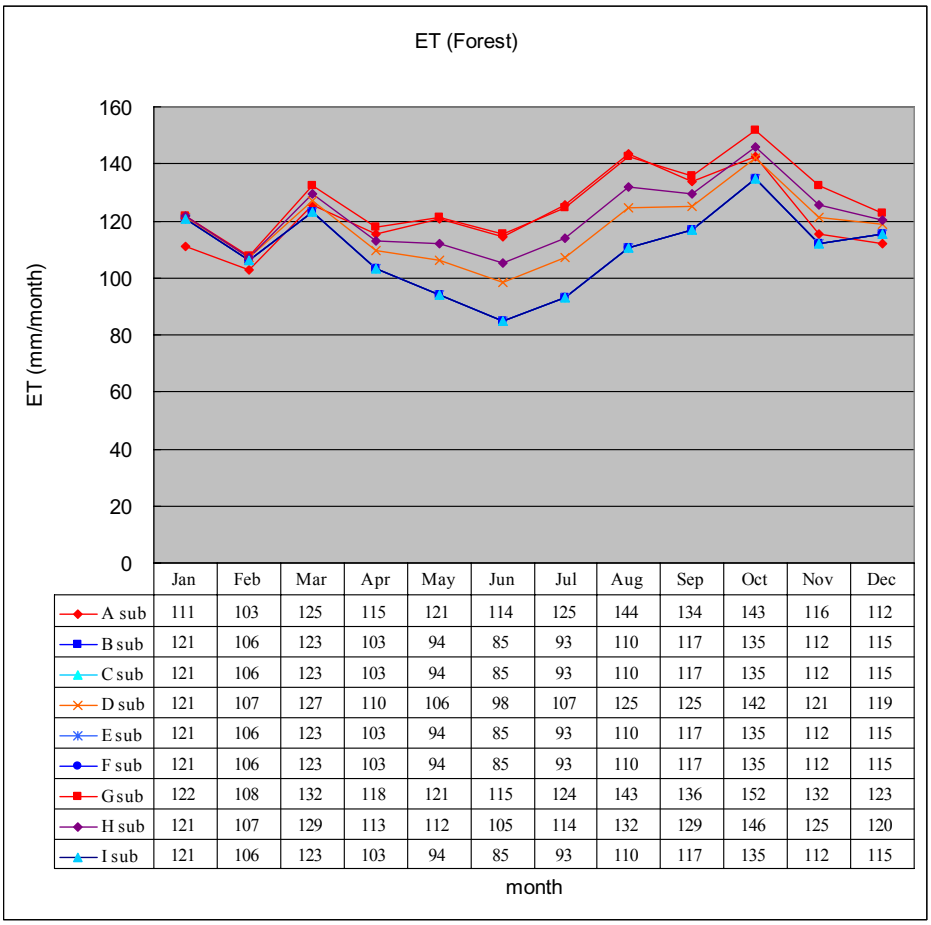

	Jan	Feb	Mar	Apr	May	Jun	Jul	Aug	Sep	Oct	Nov	Dec
A sub	111	103	125	115	121	114	125	144	134	143	116	112
B sub	121	106	123	103	94	85	93	110	117	135	112	115
C sub	121	106	123	103	94	85	93	110	117	135	112	115
D sub	121	107	127	110	106	98	107	125	125	142	121	119
E sub	121	106	123	103	94	85	93	110	117	135	112	115
F sub	121	106	123	103	94	85	93	110	117	135	112	115
G sub	122	108	132	118	121	115	124	143	136	152	132	123
H sub	121	107	129	113	112	105	114	132	129	146	125	120
I sub	121	106	123	103	94	85	93	110	117	135	112	115

Figure 4-24 Monthly Evapotranspiration Change in Each Sub-basin

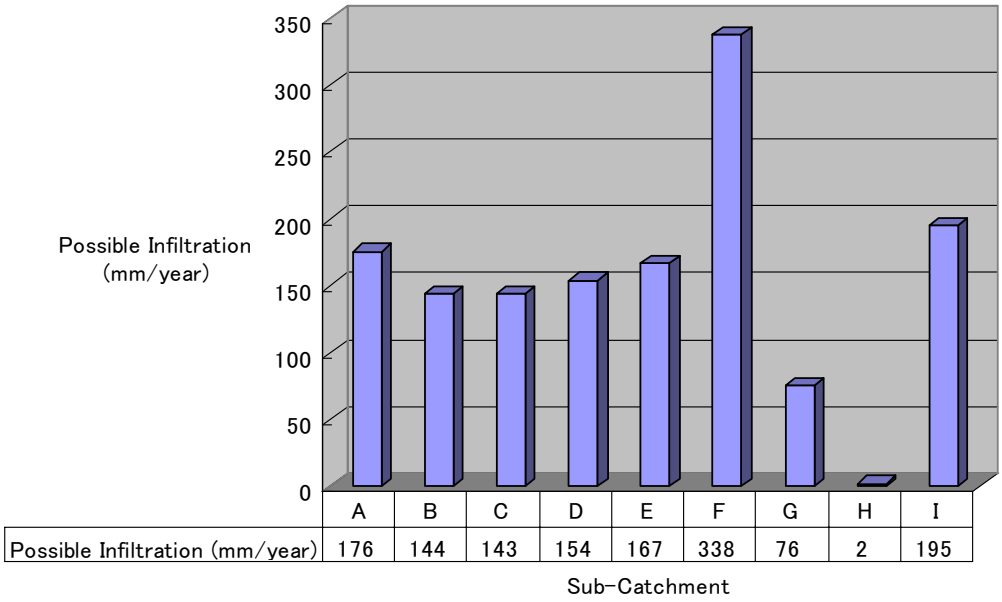

	A	B	C	D	E	F	G	H	I
Possible Infiltration (mm/year)	176	144	143	154	167	338	76	2	195

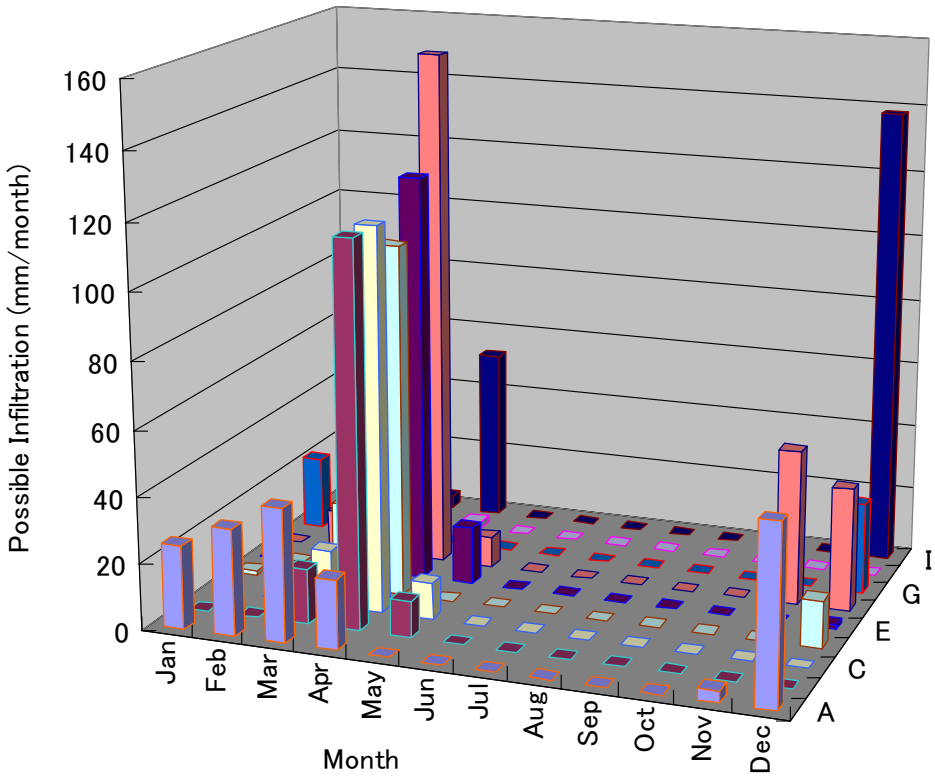

	Jan	Feb	Mar	Apr	May	Jun	Jul	Aug	Sep	Oct	Nov	Dec
A	25	32	40	21	0	0	0	0	0	0	3	53
B	0	0	17	116	11	0	0	0	0	0	0	0
C	0	0	17	116	11	0	0	0	0	0	0	0
D	1	6	26	106	0	0	0	0	0	0	0	14
E	0	0	26	123	17	0	0	0	0	0	0	1
F	0	12	76	157	9	0	0	0	0	0	47	37
G	22	15	11	0	0	0	0	0	0	0	0	28
H	0	0	0	2	0	0	0	0	0	0	0	0
I	0	0	4	52	0	0	0	0	0	0	0	139

Figure 4-25 Monthly Change of Possible Infiltration (1) (unit: mm)

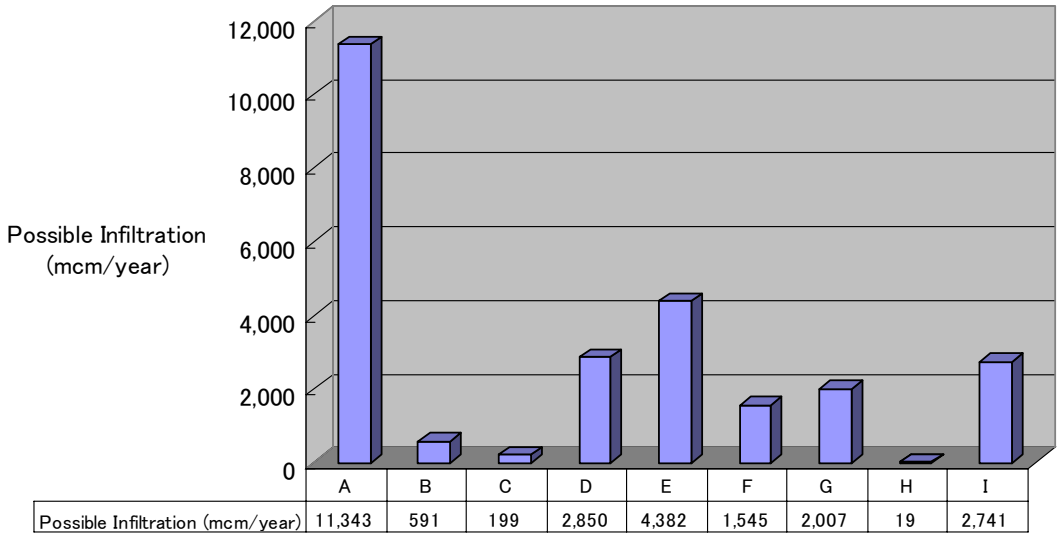

	A	B	C	D	E	F	G	H	I
Possible Infiltration (mcm/year)	11,343	591	199	2,850	4,382	1,545	2,007	19	2,741

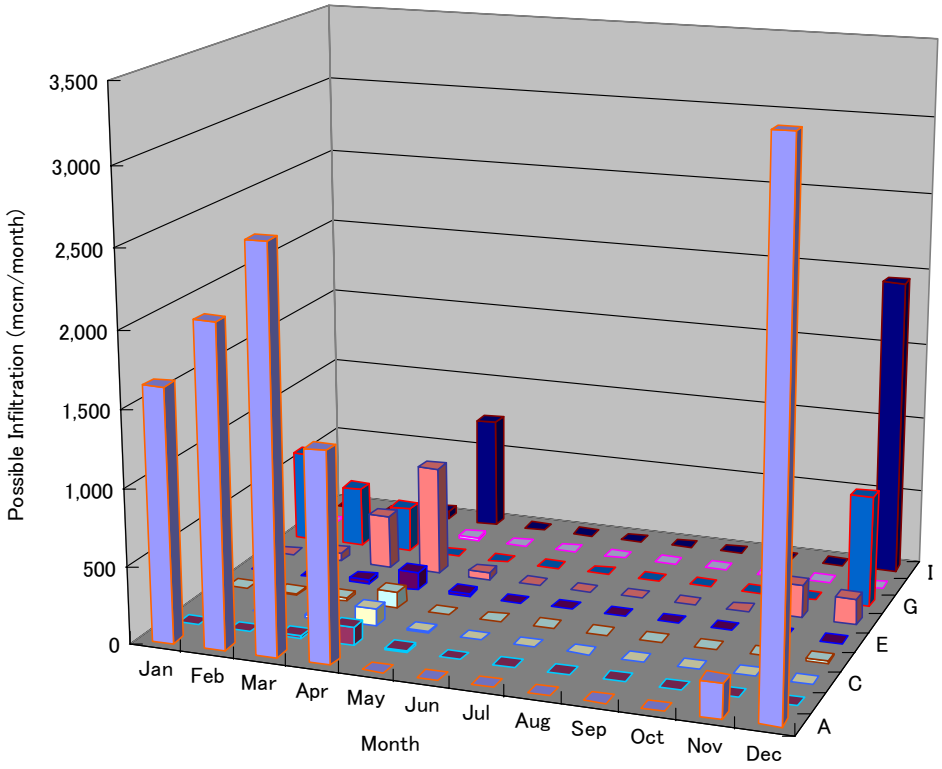

	Jan	Feb	Mar	Apr	May	Jun	Jul	Aug	Sep	Oct	Nov	Dec
A	1,641	2,079	2,595	1,353	0	0	0	0	0	0	224	3,451
B	0	0	17	116	11	0	0	0	0	0	0	0
C	0	0	17	116	11	0	0	0	0	0	0	0
D	1	6	26	106	0	0	0	0	0	0	0	14
E	0	0	26	123	17	0	0	0	0	0	0	1
F	0	54	347	717	42	0	0	0	0	0	215	170
G	593	392	294	0	0	0	0	0	0	0	0	728
H	0	0	0	19	0	0	0	0	0	0	0	0
I	0	0	52	736	0	0	0	0	0	0	0	1,952

Figure 4-26 Monthly Change of Possible Infiltration (2) (unit: mcm)

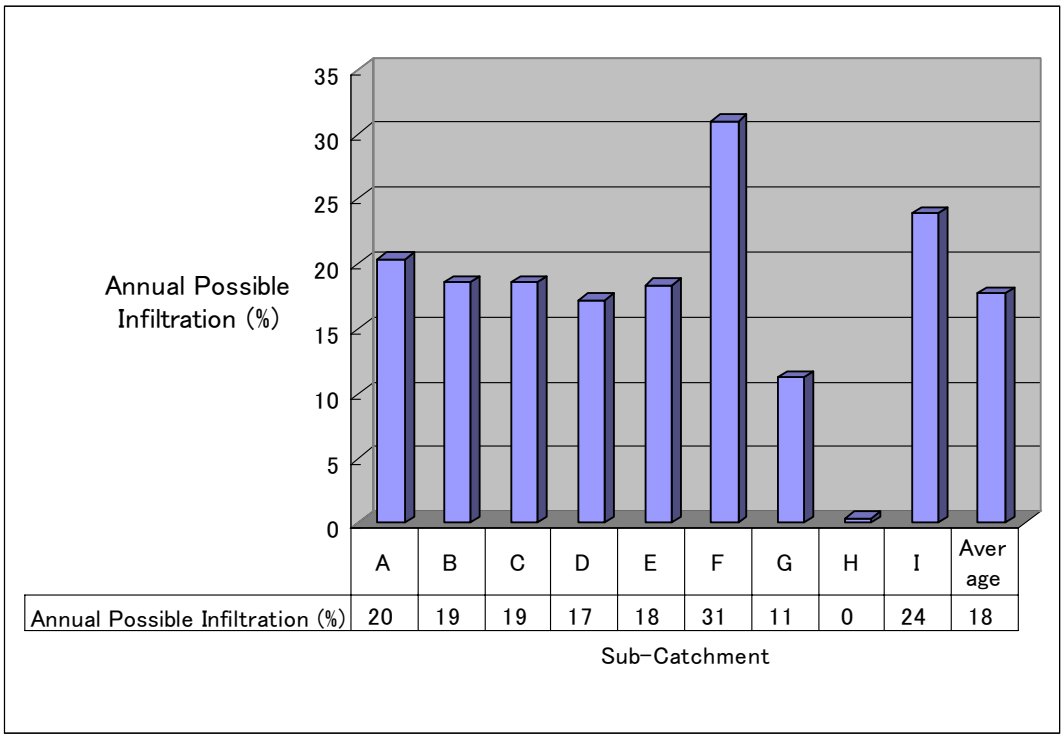

Figure 4-27 Annual Possible Infiltration Rate (%)

Reference (1)

Land covers of catchment for each hydrometric gauging station and sub-basin in February are calculated using remote sensing data. The results are shown in Tables below.

Gauging station	Catchment area (km^2)	Land Cover (km^2)			
		Forest	Grass	Bare land-wet	Bare land-dry
2C2A	85	11	28	21	25
2H1A	73	25	16	24	8
2H2A	26	1	2	18	5
2K6A	303	10	117	13	163
2K7	2,326	94	437	603	1,192
2K11	8,456	676	1,935	526	5,319
2K15	4,647	2,398	1,587	62	599
2R1A	6,649	705	2,344	554	3,045
2R23	3,374	418	927	611	1,418
2R25	811	272	379	9	150
2R26	811	272	379	9	150
2R29	1,220	134	297	232	557

Gauging station	Catchment area (km2)	Land Cover (%)			
		Forest	Grass	Bare land-wet	Bare land-dry
2C2A	85	13	33	24	29
2H1A	73	34	22	33	11
2H2A	26	3	7	69	21
2K6A	303	3	39	4	54
2K7	2,326	4	19	26	51
2K11	8,456	8	23	6	63
2K15	4,647	52	34	1	13
2R1A	6,649	11	35	8	46
2R23	3,374	12	27	18	42
2R25	811	34	47	1	19
2R26	811	34	47	1	19
2R29	1,220	11	24	19	46

Reference (2)

- Earth Remote Sensing Data Analysis Center (ERSDAC), 2005, Applicability of ASTER Data for Integrated Water Management Project in Tuul River, Mongolia, Report of research and development of remote sensing technology for Non-renewable resources.
- Makkink GF., 1957, Testing the Penman formula by means of lysimeters, Journal of the Institution of Water Engineers, 11, 277-288.
- Nagai, 1993, Estimation of Pan Evaporation by Makkink Equation, J. Japan Soc, Hydrol and Water Resour, Vol.6, No.3, pp283-243.
- East Africa Meteorological Department (East Africa Community, Nairobi), 1975, Summary of Rainfall in Tanzania for the Year 1973.

Chapter 5
Geophysical Survey

CHAPTER 5 GEOPHYSICAL SURVEY

Resistivity survey and magnetic survey were carried out as geophysical survey in this study. Since resistivity generally varies with rock composition, grain size, compaction and water contents, the hydrogeological structure can be practically figured out based on the resistivity survey analysis. Therefore, resistivity survey has been used generally for groundwater survey to clarify the hydrogeological structure and aquifer zone. On the other hand, magnetic property is varied by rock material: especially igneous rock has high magnetic susceptibility. Magnetic survey is applied for the hydrogeological survey at the places where igneous rocks and sediments are contacted each other.

5.1 Outline of Survey

Geophysical survey was planned for two aims: namely, the geological structure survey and the drilling site survey. As for the geological structure survey, Vertical Electrical Sounding (VES) was planned at 120 survey points and for the drilling site survey, VES was planned three points in each village and two-dimensional resistivity survey and magnetic survey was planned in several villages.

5.1.1 Purpose of Survey

The purpose of this geophysical survey is shown as follows:

- To figure out the geological structure of the whole Internal Drainage Basin (IDB)
- To select the site of test borehole drilling
- To clarify the aquifer structure around the survey points.

5.1.2 Planned Survey Location

Survey points were selected by the procedure as follows:

- To disperse VES points to the whole area of IDB
- To locate VES points in each geological unit based on the geological classification
- To conduct VES at several points to select the appropriate sites for test borehole drilling in IDB
- To conduct two-dimensional resistivity survey or magnetic survey to detect geological structure for drilling.

5.1.3 Survey Quantity

The number of survey points by survey items is shown in **Table 5-1**.

Table 5-1 Number of Survey Points for Geophysical Survey

Purpose	Survey Method	Quantity
Geological Structure	Vertical Electrical Sounding	114 points
Investigation for Test Borehole Drilling Site	Vertical Electrical Sounding	76 points
	2-D Resistivity Survey	2 lines
	Magnetic Survey	12 places

5.2 Survey Methodology

Three kinds of geophysical survey technique were applied in this study. These are vertical electrical sounding, two-dimensional resistivity survey and magnetic survey.

5.2.1 Vertical Electrical Sounding

Vertical electrical sounding was conducted to figure out general geological structure of IDB and to determine the test borehole drilling sites.

Although most of all fresh bedrocks have quite high resistivity except for mudstone or shale, an actual resistivity of the strata usually are dominated by the resistivity of the groundwater in pore spaces. Pore spaces in fault and fracture zones are often larger than the pore spaces of the original rocks. Such a zone with high water content: namely, fracture zone, usually has considerably low resistivity. In addition, the resistivity of the fresh rocks remarkably decreases since weathering or alteration transforms them into sandy or clayey materials. Consequently, rock resistivity usually varies widely: e.g. about 10^{-1} ohm-m for fault clay to about 10^{5} ohm-m for fresh rocks. Therefore, resistivity should be dealt with an effective index for detecting anomalous zones in strata for groundwater exploration.

Figure 5-1 and **5-2** show the conceptual diagram about resistivity and the range of resistivity for each rock and soil respectively.

Resistivity	Small ⟷ Large
Soil	(Clay) (Silt) (Sand) (Gravel)
Particle size	Small ⟷ Large
Water saturation	Large ⟷ Small
Water contents (Porosity*Saturation)	Large ⟷ Small
Electric Conductivity (EC) of groundwater	Large ⟷ Small

Figure 5-1 Conceptual Diagram of the Factor which Defines Resistivity

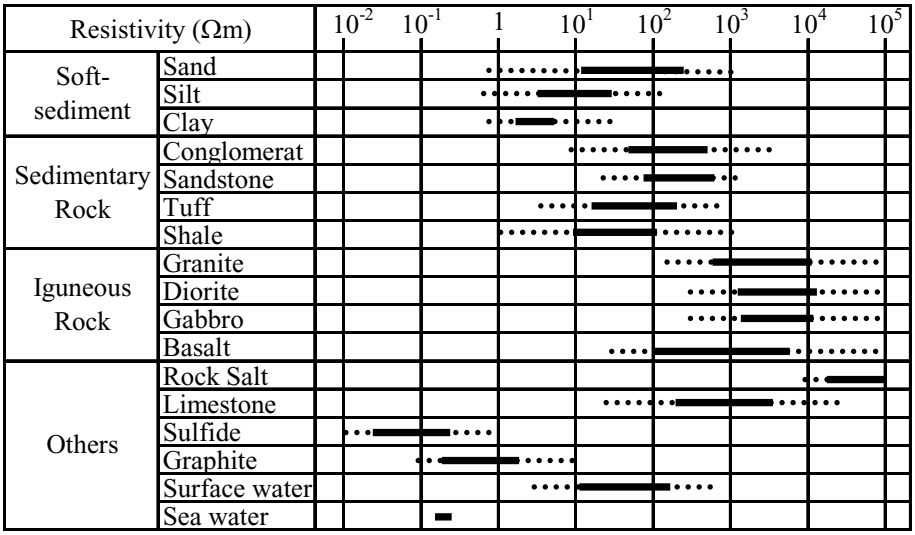

After "Zukai Buturi Tansa (in Japanese)"

Figure 5-2 Range of Resistivity Values for Various Materials

(1) Principle

Schlumberger electrode array (Schlumberger configuration) is used for vertical electrical sounding. A pair of current electrodes is arranged around the measurement point on the both sides symmetrically. The spacing of the current electrodes (A-B) has to be more than three times of the spacing of electric potential electrodes (M-N). Electric potentials were measured by the Schlumberger configuration shown in Figure 5-3.

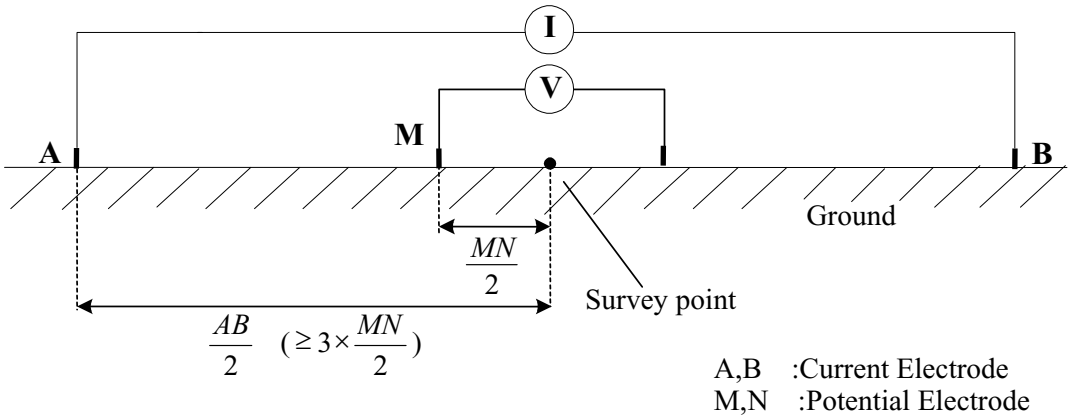

Figure 5-3 Schematic Diagram of Schlumberger Configuration

When the electrical current is injected from the current electrodes put on the outside, the electric potential difference (voltage) around the center is measured between potential electrodes. An apparent resistivity value can be calculated from the electrode spacing, the electric current value and the electrical potential difference value that these are measured at that time. As the actual ground is not homogeneous, apparent resistivity value shows the average resistivity in hemisphere, which makes an electrode spacing at that time a diameter. In general, the data in the depth direction are acquired by extending electrode spacing gradually from the little one to the big part. If electrode

spacing is small, apparent resistivity value reflects the resistivity of the shallow part. If electrode spacing is big, the value which contains information on the resistivity of deeper part is measured. Therefore, the analysis of the underground structure becomes possible if electrode spacing is changed and a series of measurement is done and apparent resistivity is obtained as a function of the electrode spacing.

Vertical electrical sounding can be applied in case that underground has an approximately horizontally layered structure.

(2) Field Measurement

VES uses two types of electrodes: current electrodes (A, B) and potential ones (M, N) which are driven into the ground as shown in **Figure 5-4**. The measurement point is the center of the pair electrodes. The current electrodes inject electrical current into the ground and the potential electrodes measure electrical potential.

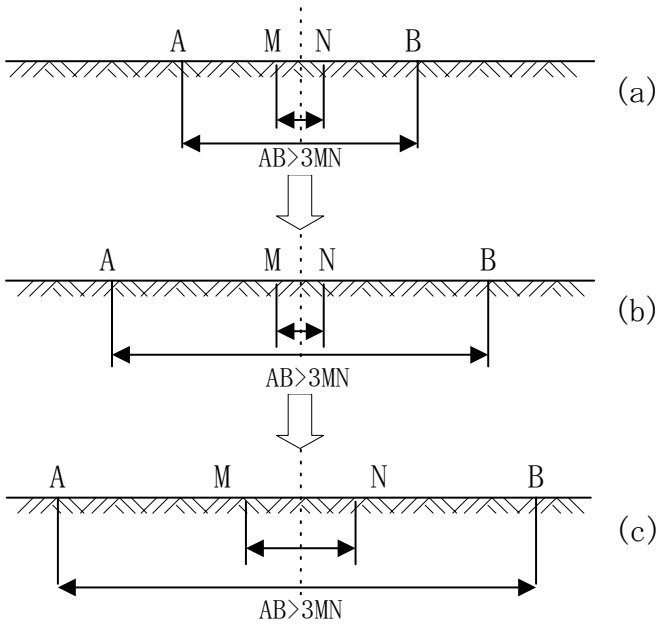

Figure 5-4 Schematic Diagram of Field Measurement and Measurement Procedure

Table 5-2 Measurement Schedule of Schlumberger Electrode Array

AB/2 (m)	MN/2 (m)	K
1.5	0.5	6.2832
2	0.5	11.781
2.5	0.5	18.85
3	0.5	27.489
4	0.5	49.48
5	0.5	77.754
6	0.5	112.31
8	0.5	200.28
10	0.5	313.37
10	2.5	58.905
12	2.5	86.551
15	2.5	137.44
20	2.5	247.4
25	2.5	388.77
30	2.5	561.56
30	5	274.89
40	5	494.8
50	5	777.54
50	10	376.99
60	10	549.78
75	10	867.87
100	10	1555.1
100	25	589.05
125	25	942.48
150	25	1374.4
180	25	1996.5
200	25	2474

Two sets of electrodes spread out by turns based on the measurement schedule as shown in **Table 5-2**. The distance between A and B are maintained at least three times more than the distance between M and N. K is a coefficient to calculate an apparent resistivity that is explained in the following section:

It is regarded that the electric potential gradient can be measured between the current electrodes in the case of Schlumberger configuration. The current electrodes spacing must be more than three times of the spacing of electric potential electrode in order to assure above mentioned assumption. However, it is very difficult to measure electrical potential by the resistivity meter when the spacing of current electrodes (A-B) is more than 30 times of the spacing of potential electrodes (M-N). Therefore, the current electrode spacing is between 3-30 times of the potential electrode spacing in the potential electrode.

(3) Analysis

The flow chart of the automatic inversion is shown in **Figure 5-5**. This is based on an iterative method.

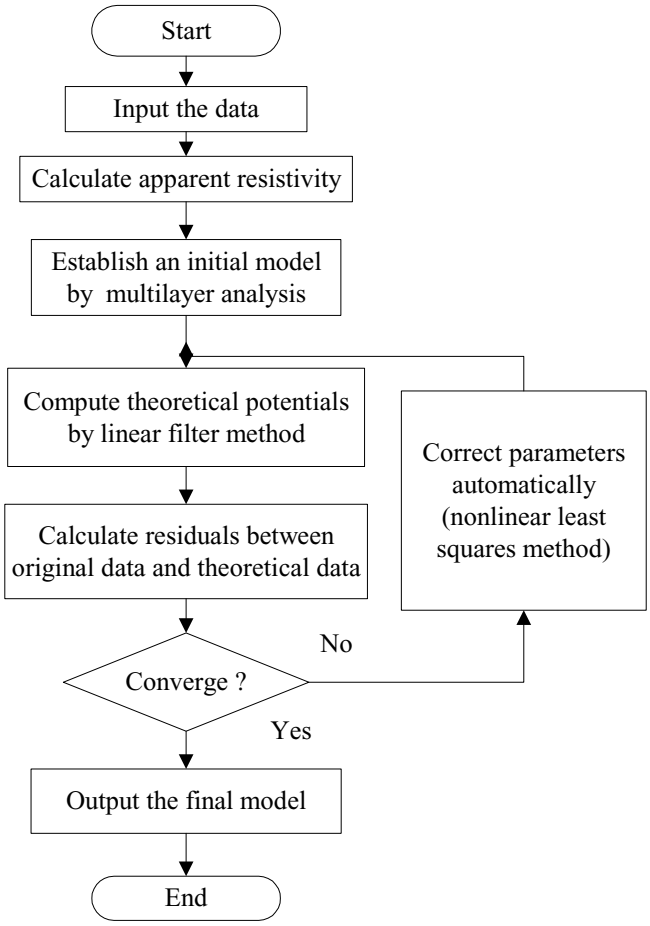

Figure 5-5 Flow Chart of Automatic Analysis

First, an apparent resistivity is calculated from the collected data by following equation.

$$\rho_a = \pi \frac{AB^2 - MN^2}{4 \cdot MN} \cdot \frac{V}{I} = K \cdot \frac{V}{I}$$

This apparent resistivity is plotted in graphical paper on logarithmic scale. An abscissa is electrode spacing corresponding to the prospecting depth.

Next, theoretical potential data corresponding to the model are computed. Alternatively, if the underground has an approximately horizontally layered structure, the digital linear filter method can be used to conduct continuous one-dimensional inversion. After theoretical potential data are calculated, the model is modified to reduce the residuals between the theoretical data and the measured data. To find the model giving the minimum residuals, the non-linear least squares technique is applied. This modification process is iterated until the residuals become sufficiently small or subsequent changes to the model no longer improve the fitting. At this point, the inversion is considered to have converged. An analysis program called ELPAC1 developed by OYO Corporation was used for the study. The specifications of our geophysical survey equipments are shown in following table. How to read the figure of analysis result for VES is as follows (See **Figure 5-6**):

An analysis result is shown on both logarithm graphs, which a vertical axis is depth or electrode spacing, a horizontal axis is apparent resistivity or resistivity. The point of " ■ " shows the measured apparent resistivity value, The hatched block shows the resistivity structure model of the underground, and the curve connected with line "-" is the apparent resistivity curve computed from the model.

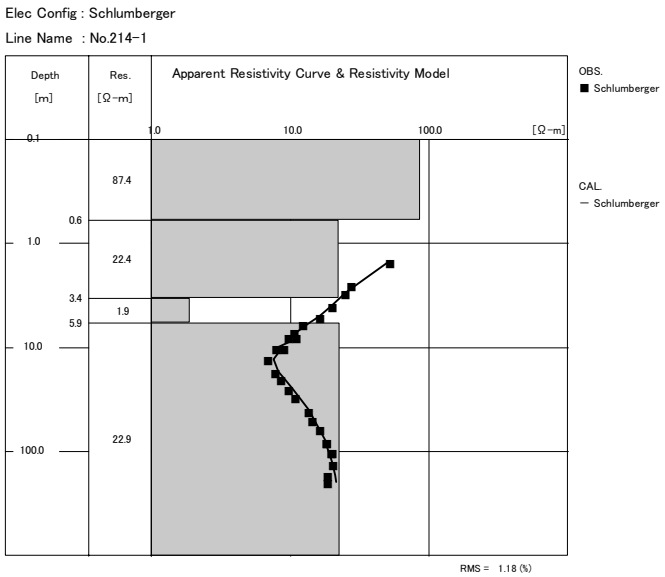

Figure 5-6 Example of VES Analysis

If obtained data "■" and computed curve are fit well, a residual error is small, the resistivity structure of the underground can be explained with this model, and this model becomes an analysis result. “RMS” shows a root mean square of residual error.

Table 5-3 Specification of Vertical Electrical Sounding Equipments

Name	Specification	Number	Manufacturer
Resistivity meter (SAS-300C)	Transmitter Voltage: 400 V (Max) Maximum current: 1.0A Maximum power: 100W Receiver Resolution: 30nV (Theoretical) Input impedance: 10Mohm Power 12V DC Dimension: 105 x 325 x 300 mm Weight: 4.6kg	1	ABEM Instruments AB (Sweden)
Cable	200m with cable dram	4	-
Electrode	Form: f10mm x 1000mm Material: Copper Steel	20	-
Battery	12V, 70Ah	2	-

5.2.2 Two-dimensional Resistivity Survey

Two-dimensional resistivity survey was conducted to detect fracture zone in rocky areas where In Vertical electrical sounding is not suitable because it is not estimated horizontal layered structure. Since the structure of those areas is more complicated than sedimentary strata area, this method was applied to determine the drilling points.

(1) Principle

Horizontal Electrical survey is one of the resistivity surveys that lateral resistivity changes can be detected. Vertical sounding was explained in above section as the method which vertical resistivity changes can be detected. Two-dimensional resistivity survey can be considered as a combined method of the horizontal survey and the vertical sounding. Two-dimensional resistivity survey uses inversion techniques to analyze a two-dimensional resistivity distribution and displays the results as a color profile. These analysis results show a more detailed and reliable resistivity distribution than vertical sounding. Electric potentials are measured by the pole-pole electrode array shown in **Figure 5-7**.

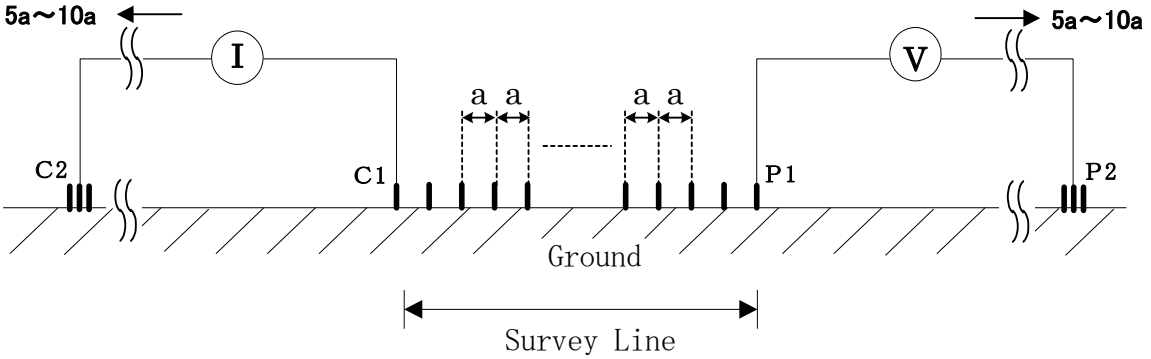

C1:Cureent Electrode (moving)
C2:Cureent Electrode (remote)
P1:Potential Electrode (moving)
P2:Potential Electrode (remote)

Figure 5-7 Schematic Diagram of Pole-pole Electrode Array

In general, the relation between resistance R (Ω) and resistivity ρ ($\Omega \cdot m$) obtained by pole-pole array is expressed as equation (1).

$$R = \rho \cdot \frac{l}{S} \qquad \text{--- (1)}$$

And electric potential V (volt) by Ohm's low is

$$V = R \cdot I = \rho \cdot \frac{l}{S} \cdot I \qquad \text{--- (2)}$$

where l is length, S is the area section, I (ampere) is the intensity of the injected current.

In hemisphere in flat ground (see **Figure 5-8**), electric potential difference $V_{r_0 - r_1}$ between radius r_0 and r_1 is obtained as:

$$V_{r0-r1} = \rho \cdot \frac{l}{S} \cdot I \qquad \text{--- (3)}$$

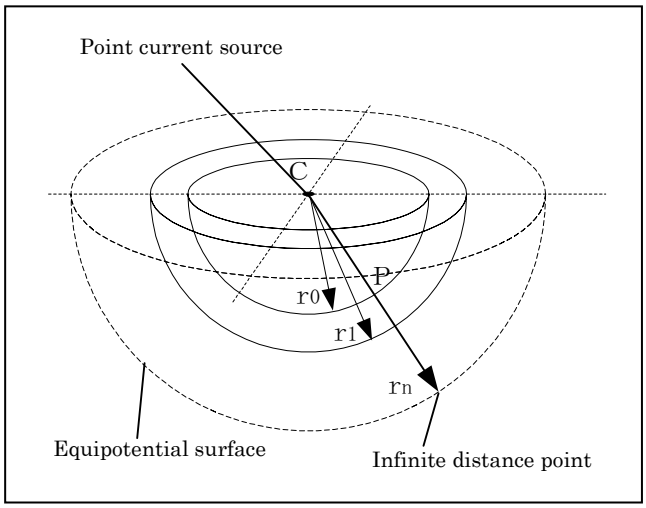

Figure 5-8 Potential Distribution with Point Current Source

Surface area of hemisphere S is

$$S = \frac{4\pi r^2}{2} = 2\pi r^2 \qquad \text{--- (4)}$$

If $r_0 \cong r_1$, then e.q. (4) gives

$$S = 2\pi r^2 = 2\pi r_0 r_1 \qquad \text{--- (4)'}$$

Since $l = r_1 - r_0$, e.q. (3) is written as:

$$\begin{aligned} V_{r_0 - r_1} &= \rho \cdot \frac{r_1 - r_0}{2\pi r_0 \cdot r_1} \cdot I \\ &= \frac{\rho I}{2\pi} \cdot \left(\frac{1}{r_0} - \frac{1}{r_1} \right) \end{aligned} \qquad \text{--- (5)}$$

Electric potential at P is obtained the sum of electric potential difference from equipotential surface at radius r_n to r_0.

$$\begin{aligned} V_P &= V_{r_0 - r_1} + V_{r_2 - r_2} + \cdots + V_{r_0 - r_1 - r_n} \\ &= \frac{\rho I}{2\pi} \cdot \left(\frac{1}{r_0} - \frac{1}{r_1} + \frac{1}{r_1} - \frac{1}{r_2} + \cdots + \frac{1}{r_{n-1}} - \frac{1}{r_n} \right) \qquad \text{--- (6)} \\ &= \frac{\rho I}{2\pi} \cdot \left(\frac{1}{r_0} - \frac{1}{r_n} \right) \end{aligned}$$

r_n is defied as an infinite distance point from current point source (C). Thus e.q. (6) is given as:

$$V = \frac{\rho \cdot I}{2\pi} \cdot \frac{1}{r_0} \qquad \text{--- (7)}$$

where $\frac{1}{r_n} = 0$.

In the case of homogeneous, resistivity ρ is given as

$$\rho = 2\pi r \frac{V}{I} \qquad \text{--- (8)}$$

(2) Field Measurement

Figure 5-9 shows that simple diagram of field measurement of pole-pole array. In this array, one electrode: C1 injects electric current into the ground and another electrode: P1 measures the electric potential. These two electrodes are called “moving electrodes”. Another potential electrode: P2 is needed to provide a reference for the potential at P1. Electrodes C2 and P2 should be located very far from the moving electrode so that they have a negligible effect on the measurement. C2 and P2 are called as “remote electrode”.

For actual measurement, the distance between a remote electrode and a moving electrode is maintained at least five times than the maximum distance between the moving electrodes.

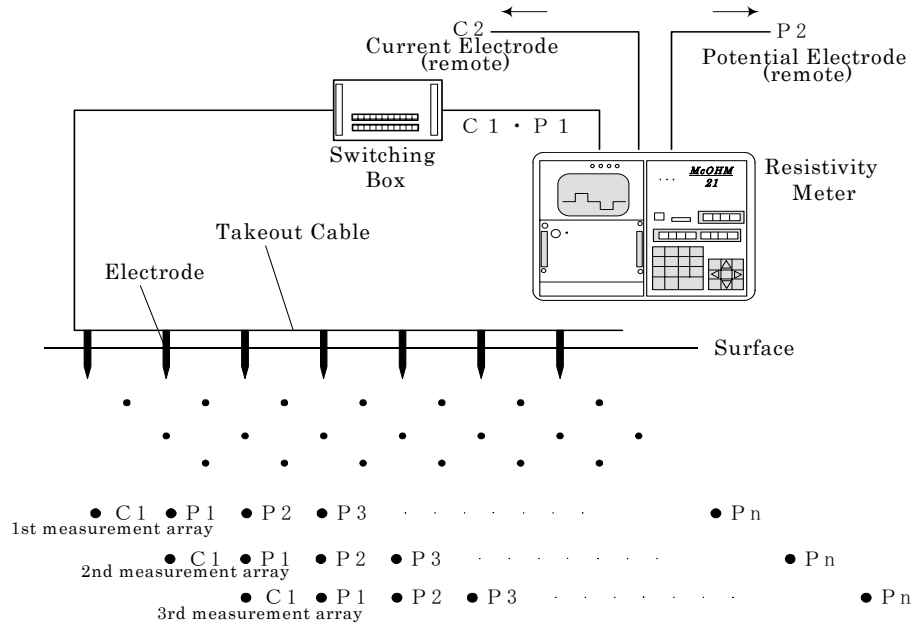

Figure 5-9 Schematic Diagram of Field Measurement and Process for two-dimensional Resistivity Survey

Table 5-4 Specification of Two-dimensional Resistivity Survey Equipments

Name	Specification	Number	Manufacturer
Resistivity meter (SYSCAL Jr.)	Transmitter Voltage: 50, 100, 200, 400V Maximum current: 1.2A Maximum power: 100W Receiver Resolution: 10μV Input impedance: 10Mohm Power 12V DC Dimension: 310 x 210 x 160 mm Weight: 5.0 kg	1	IRIS Instruments (France)
Switching Box	7 terminals x 3 (switchable)	1	OYO Corporation
Extension Box	7 terminals	3	OYO Corporatio
Cable	200m x 20 Takeout Cable (7 cores) 70m Extension Cable (7 cores) 70m	20 3 2	-
Electrode	Form: ϕ10mm x 1000mm Material: Copper Steel	40	-
Battery	12V, 70Ah	2	-

(3) Analysis

The flow chart of the automatic inversion is shown in **Figure 5-10**. This is based on an iterative method.

First, terrain effects are estimated using the finite element method (Coggon, 1971). These effects then are eliminated from the measured potential data. Next, an apparent resistivity pseudo-section is

produced from the corrected data. This pseudo-section is usually used as the initial model for the inversion. If the pseudo-section does not produce adequate convergence, an average model is used for the initial model.

Next, theoretical potential data corresponding to the model are computed. Alternatively, if the underground has an approximately horizontally layered structure, the digital linear filter method (Ghosh, 1971a, b) can be used to conduct Continuous one-dimensional inversion. After theoretical potential data are calculated. the model is modified to reduce the residuals between the theoretical data and the measured data. To find the model giving the minimum residuals, the non-linear least squares technique is applied. This modification process is iterated until the residuals become sufficiently small or subsequent changes to the model no longer improve the fitting. At this point. The inversion is considered to have converged.

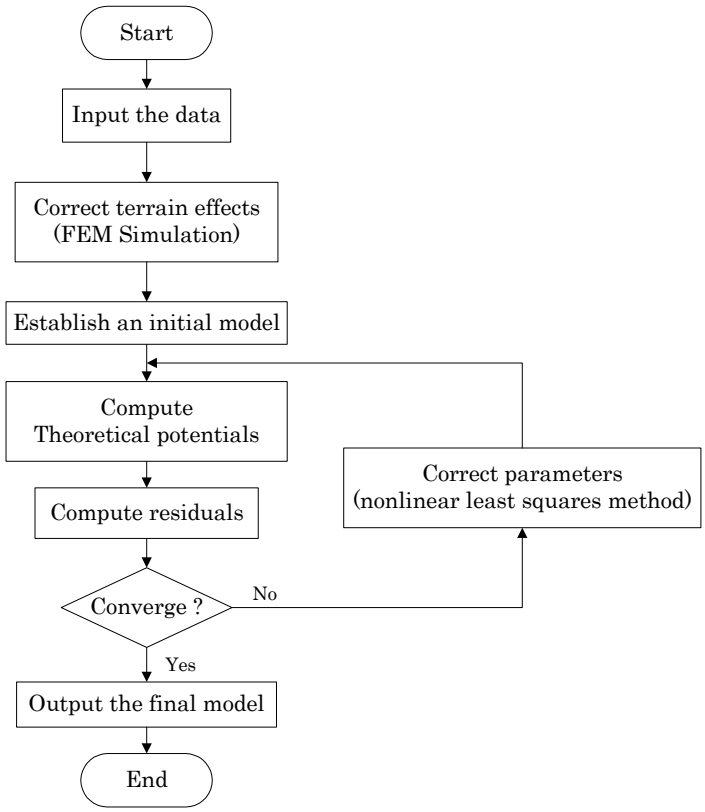

Figure 5-10 Automatic Inversion Flow Chart of Two-dimensional Resistivity Survey

Finally, resistivity model is displayed as a color profile that clearly shows the resistivity structure.

How to read the figure of analysis result for two-dimensional resistivity survey is as follows (See **Figure 5-11**):

An analysis result is shown on cross-section, which a vertical axis is depth, a horizontal axis is distance from the start point of the measurement. Red color shows high resistivity and blue shows low resistivity.

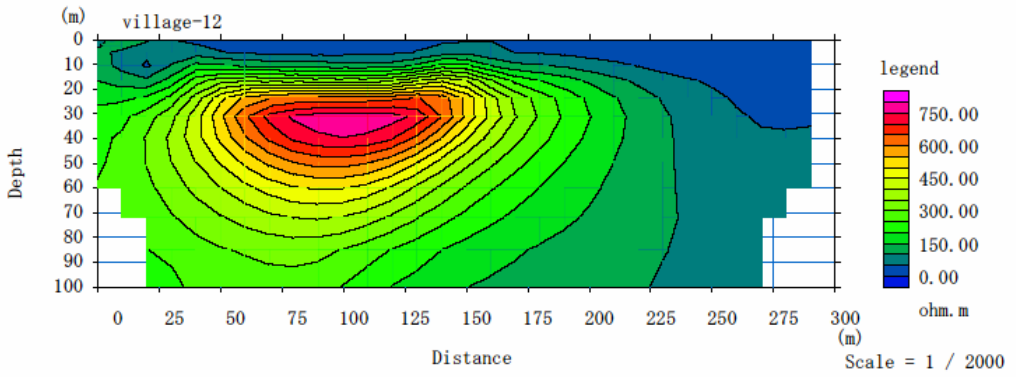

Figure 5-11 Example of Two-dimensional Resistivity Survey Analysis

5.2.3 Magnetic Survey

Magnetic survey was conducted to detect lateral change of geology by magnetic anomaly of rocks. Rocks have some magnetization which is characterized by magnetic susceptibility. Magnetic survey can detect as magnetic anomaly where different kinds of rocks are facing each other. This method was conducted to determine the drilling point too.

(1) Principle

Magnetic survey measures geomagnetism on the ground surface. Position of the source of magnetic anomaly is estimated by detecting the magnetic anomaly pattern in the distribution of magnetic field. Rock magnetism is described by magnetic susceptibility, for example, shown in **Figure 5-12**.

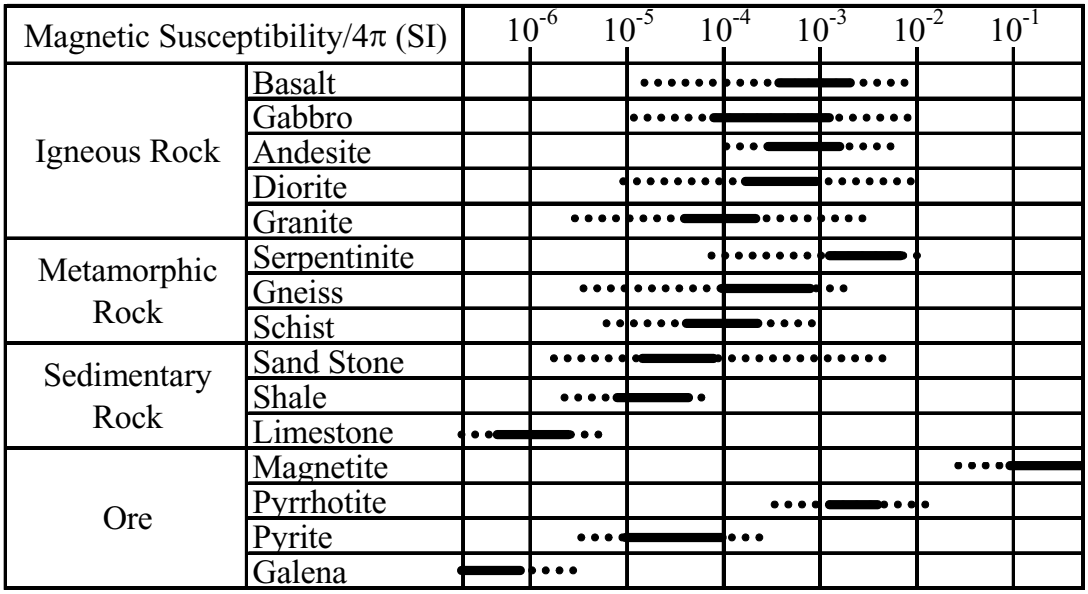

After "Zukai Buturi Tansa (in Japanese)"

Figure 5-12 Range of Magnetic Susceptibility Value for Various Materials

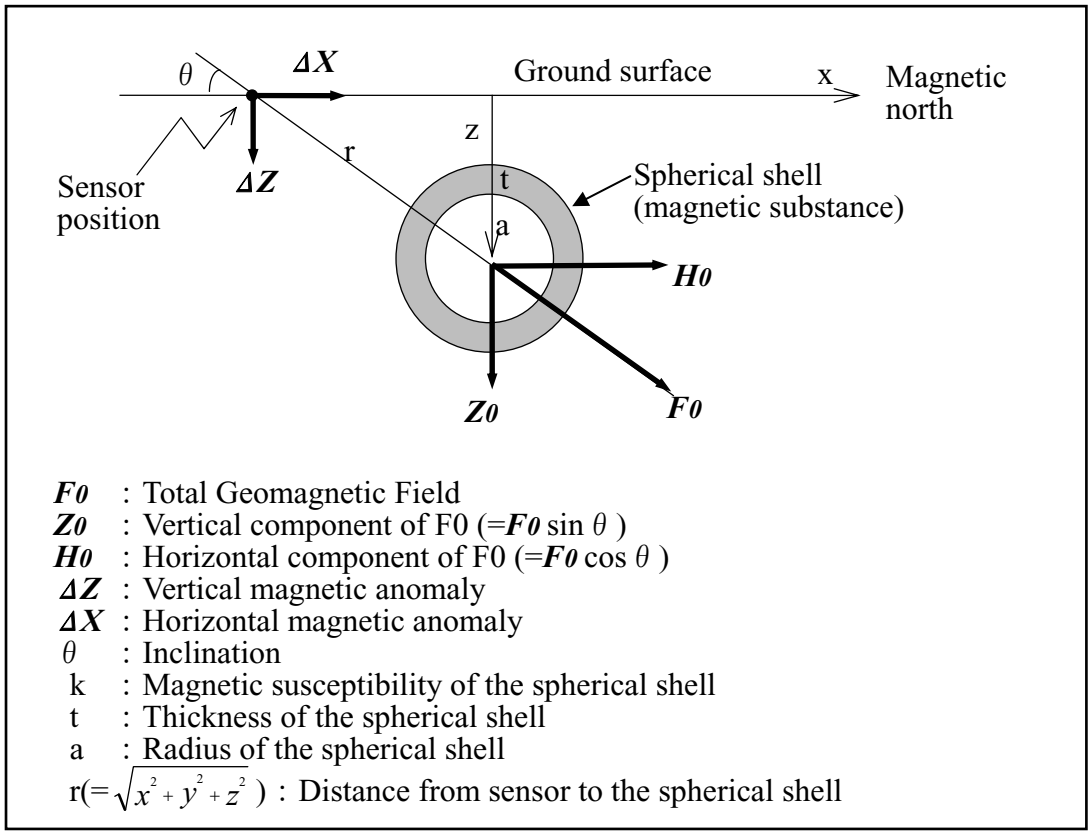

Figure 5-13 Schematic Diagram of the Model of Spherical Shell in the Geomagnetic Field

Geomagnetism is disturbed above the buried body of magnetic substance. It can be detected as a magnetic anomaly on the ground surface. When a spherical shell shown in **Figure 5-13** as a simplified model is considered, the magnetic anomaly which is occurred by this shell is shown in following equations.

Vertical magnetic anomaly ΔZ and horizontal magnetic anomaly ΔX at the sensor position in **Figure 5-13** are expressed as follows, respectively:

$$\Delta Z = \frac{kVZ_0}{r^5}\left\{\left(x^2 + y^2 - 2z^2\right) - 3xz\cot\theta\right\}$$
$$\Delta X = \frac{kVZ_0}{r^5}\left\{\left(-2x^2 + y^2 + z^2\right)\cot\theta - 3xz\right\}, \quad (5\text{-}1)$$

where, V is the volume of the shell. V is expressed as follows:

$V = 4\pi a^2 t$.

(2) Field Measurement

Magnetometer G-858 manufactured by Geometrics Inc. was used for magnetic survey measurement. G-858 is cesium magnetometer which is used that the energy level width of cesium atom in static magnetic field is proportional to intensity of magnetic field at the position. Since the cesium type

sensor is more stable than Fluxgate type magnetometer, the measurement is possible to shift 2 or 3 times faster. The specification of the magnetometer is shown in **Table 5-5**.

Table 5-5 Specification of Magnetic Survey Equipment

Name	Specification	Number	Manufacturer
G-858	Cesium Magnetometer Measurement range: 17,000nT～100,000nT Resolution: 0.05nT Memory: 250,000 data Power: Rechargeable Battery Data output: RS-232C	1	Geometrics (U.S.A.)

The measurement was conducted by two persons, one observer measured the magnetometer by shifting and the other measured the position of the sensor by GPS. The observers were not wearing any metal material. In order to avoid the diurnal variation of the magnetic field, the measurement point was duplicated to the first point several times in the measurement duration. The schematic diagram of measurement was shown in **Figure 5-14**.

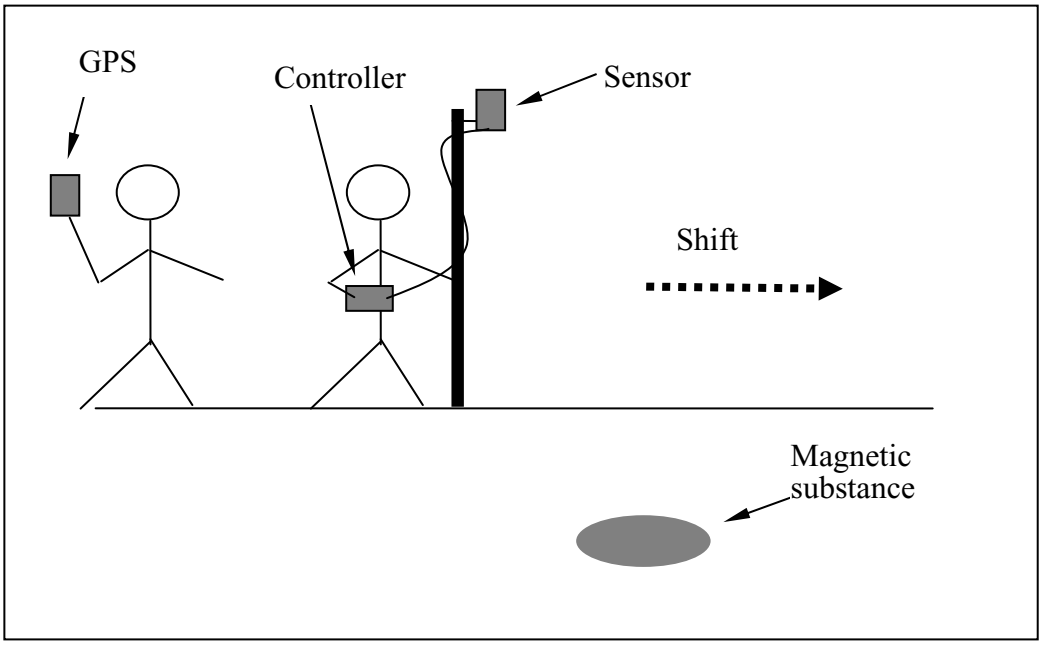

Figure 5-14 Schematic Diagram of Measurement for Magnetic Survey (G-858)

(3) Analysis

Analysis procedure is as follows:

- After transferring the data from G-858 to computer, the data are combined with position data observed by GPS.
- The diurnal variation was subtracted from each data.
- The data were drawn in magnetic force to distance graph.
- If the data were correct, the data were drawn to contour map in X-Y plane.

- The magnetic anomaly would be detected.

Figure 5-15 shows the flow chart of analysis for the magnetic survey.

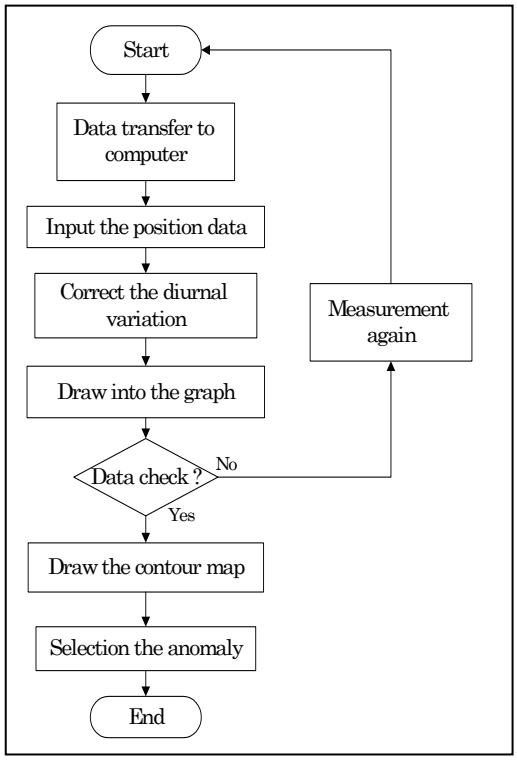

Figure 5-15 Analysis Flowchart for Magnetic Survey

5.3 Survey Result

Geophysical survey has two aims. One is to figure out the geological structure and the other is to select the test boreholes drilling sites. Vertical Electrical Sounding (VES) was conducted for the geological structure survey in a whole IDB. Three kinds of survey: VES, two-dimensional resistivity survey and magnetic survey were conducted in selected villages for the test borehole drilling site survey.

5.3.1 Geological Structure Survey (Vertical Electrical Sounding)

VES was conducted to figure out the outline of geological structure of whole IDB. Additionally, it was conducted to determine the sites for test borehole drilling survey. Total number of VES points was 166 points, 113 points for the geological structure survey and 53 points for test drilling site survey. The survey points are shown in the **Table 5-6**. The survey point name (ID number) for the survey of geological structure consists of “GS-” and the serial number of the planned point on the map. Furthermore, the survey name which was initiated with "T-" shows the ID number for the drilling site survey. For example, “T-1-1” means the first point of the test drilling number “1”.

The results of the geophysical survey in whole IDB are fundamental data to analyze the hydrogeological conditions. The survey points which VES was conducted are shown in **Figure5-16**

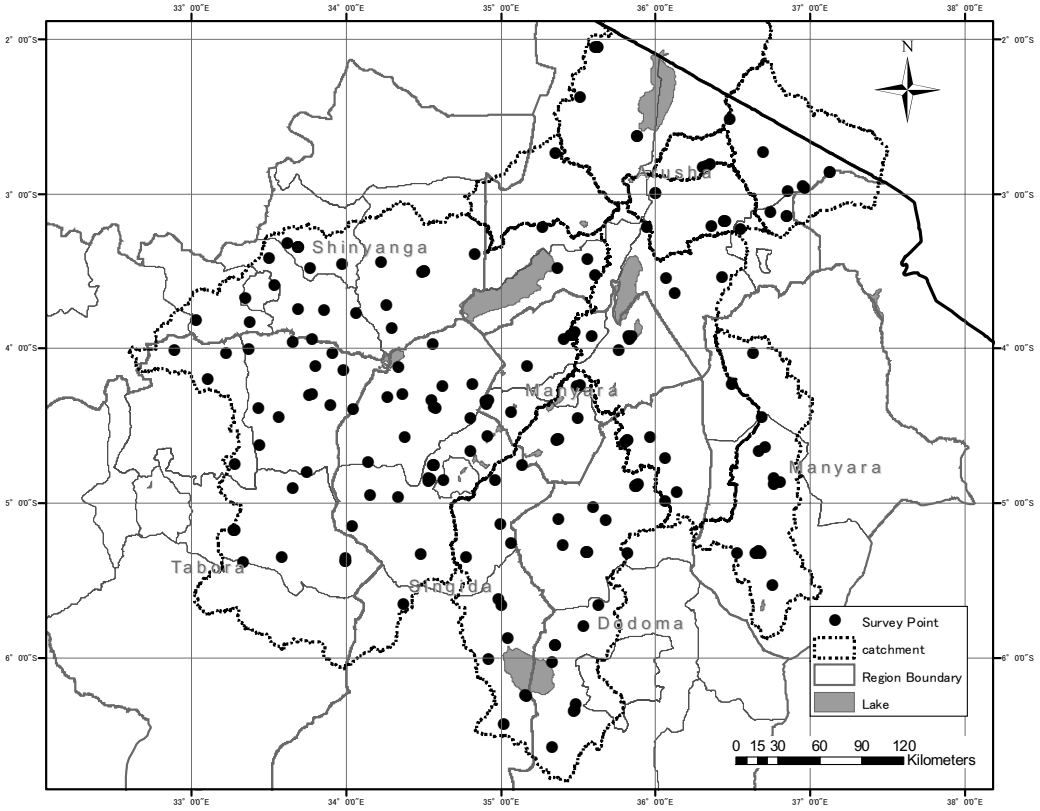

Figure 5-16 Location Map of Survey Points for Vertical Electrical Sounding

Table 5-6 Location and the Result of Vertical Electrical Sounding (1/4)

No	GS-No	Location					Position			Survey Date	Analysis Result								
		Region	District	Division	Ward	Village	Longitude	Latitude	Altitude		Rho-1 (Ωm)	Depth-1 (m)	Rho-2 (Wm)	Depth-2 (m)	Rho-3 (Wm)	Depth-3 (m)	Rho-4 (Wm)	Depth-4 (m)	Rho-5 (Wm)
1	GS-1	Arusha	Arumeru	Mukulat	Mwandej	Engalaoni	36.54937	-3.23247	1938	2006/8/1	274.5	0.9	62.8	2.8	12.4	21.1	4.2	36.3	38.2
2	GS-2	Arusha	Arumeru	Mukulati	Oldonyo Sambu	Losinoni	36.73973	-3.11728	1555	2006/8/1	170.4	2.0	23.8	47.5	76.9	83.6	19.3		
3	GS-3	Arusha	Karatu	Karatu	Daa	Endashangwet	35.55811	-3.42680	1086	2006/8/9	96.5	0.5	37.0	15.6	72.3	35.4	21.2	144.7	166.0
4	GS-4	Arusha	Karatu	Endabash	Endabash	Qaru	35.60586	-3.52685	1497	2006/8/10	27.2	0.4	13.3	3.0	4.0	4.9	62.5	57.9	171.0
5	GS-5	Arusha	Karatu	Eyasi	Mang'ola	Mang'ola Barazani	35.36722	-3.48244	1069	2006/8/9	199.0	1.8	13.6	11.8	36.5	108.2	57.1	146.2	153.2
6	GS-6	Arusha	Monduli	Longido	Engarenaiboro	Mairowa	36.47561	-2.52352	1690	2006/8/2	51.3	0.6	14.3	5.9	33.2	7.5	9.0	19.9	177.3
7	GS-8	Arusha	Monduli	Ketumbeine	Ketumbeine	Orkejuloongishu	36.35007	-2.80400	1090	2006/8/2	7.8	0.4	26.0	3.7	6.1	37.4	3.7	49.0	25.8
8	GS-11	Arusha	Monduli	Kisongo	Lokisale	Meserani Chini	36.43198	-3.53428	1262	2006/8/3	17.1	2.4	2.0	3.0	60.7	15.4	11.1	28.4	22.3
9	GS-12	Arusha	Monduli	Longido	Longido	Longido	36.69217	-2.73155	1337	2006/8/2	180.2	25.0	517.0	3.6	26.6	19.7	5.7	34.2	137.7
10	GS-13	Arusha	Monduli	Makuyuni	Makuyuni	Makuyuni	36.07040	-3.53936	1042	2006/8/6	11.9	1.4	19.4	12.0	7.5	33.6	21.9		
11	GS-14	Arusha	Monduli	Makuyuni	Makuyuni	Naitolia	36.12170	-3.63652	1083	2006/8/10	78.4	0.7	208.0	1.5	277.3	3.0	2.0	7.8	68.6
12	GS-15	Arusha	Monduli	Kisongo	Monduli Juu	Eluway	36.35963	-3.20833	1804	2006/8/4	11.7	3.3	6.8	4.9	28.9	40.9	6.3	64.6	73.3
13	GS-17	Arusha	Monduli	Manyara	Selela	Selela	35.93942	-3.21328	1016	2006/8/6	147.0	1.0	324.5	4.9	189.0	8.7	431.4	9.6	172.7
14	GS-18	Arusha	Monduli	Enduimeti	Tingatinga	Ngereyani	36.85488	-2.97766	1192	2006/8/1	32.0	4.0	33.1	6.7	214.7	18.1	6.1	34.4	203.1
15	GS-19	Arusha	Ngorongoro	Loliondo	Arash	Arash	35.50803	-2.37463	1870	2006/8/8	102.4	0.9	26.2	3.9	7.2	13.3	55.1	17.1	411.4
16	GS-20	Arusha	Ngorongoro	Ngorongoro	Endulen	Endulen	35.26786	-3.21448	1804	2006/8/9	33.3	1.6	13.9	15.9	22.1	20.7	9.6	102.8	52.3
17	GS-22	Arusha	Ngorongoro	Loliondo	Macambo	Piyaya	35.35247	-2.73593	1783	2006/8/8	143.9	0.9	1.1	1.6	6.0	7.9	40.0	14.6	203.7
18	GS-25	Arusha	Ngorongoro	Loliondo	Olgosorock	Loliondo	35.62220	-2.05091	2148	2006/8/7	139.9	0.8	41.3	3.5	428.9	14.3	27.1	39.8	507.0
19	T-24-1	Arusha	Ngorongoro	Pinyinyi	Pinyinyi	Engasero	35.87642	-2.62431	680	2007/6/13	950.2	9.2	73.1	86.2	1422.9				
20	T-24-2	Arusha	Ngorongoro	Pinyinyi	Pinyinyi	Engasero	35.87700	-2.62507	682	2007/6/13	925.2	0.6	433.1	6.4	215.2	18.9	107.0	174.1	234.1
21	GS-29	Dodoma	Dodoma Rural	Mundemu	Lamaiti	Lamaiti	35.53388	-5.79661	1106	2006/8/3	81.8	0.5	13.7	1.3	121.1	2.7	14.3	5.2	537.3
22	GS-30	Dodoma	Bahi	Bahi	Bahi	Bahi Makuru	35.33109	-6.02191	835	2006/7/31	1013.4	1.8	263.5	2.8	5.8	10.3	58.7	18.5	300.9
23	GS-32	Dodoma	Dodoma Rural	Chipanga	Nondwa	Chifutuka	35.33309	-6.57563	934	2006/8/2	112.4	0.8	18.0	1.2	25.8	6.8	83.4	23.2	509.5
24	GS-34	Dodoma	Kondoa	Pahi	Bumbuta	Kisaka	35.96307	-4.56922	1152	2006/8/4	20.1	0.5	3.5	4.0	14.5	5.2	1.9	24.2	43.6
25	GS-35	Dodoma	Kondoa	Kondoa	Changaa	Chololo	35.67970	-5.10505	1334	2006/8/3	711.9	3.2	52.9	5.7	1114.5	17.9	316.0	31.7	2403.8
26	GS-36	Dodoma	Kondoa	Mondo	Dalai	Mtakuja	36.05960	-4.98806	1411	2006/8/4	154.4	0.9	3.0	1.1	20.8	2.7	1.9	4.0	2034.3
27	GS-39	Dodoma	Kondoa	Goima	Kwadelo	Kirere Cang'ombe	36.13820	-4.92853	1277	2006/8/4	269.8	1.7	32.6	26.1	14.2	40.3	458.8	108.7	136.0
28	GS-40	Dodoma	Kondoa	Kwamtoro	Kwamtoro	Kurio	35.40114	-5.26671	1183	2006/8/3	157.0	0.4	349.9	2.8	21.2	6.8	5.8	9.7	714.2
29	GS-41	Dodoma	Kondoa	Kwamtoro	Lalta	Lahoda	35.37257	-5.10040	1205	2006/8/3	11.8	2.2	7.8	10.1	1.5	14.9	29.0	33.7	117.8
30	GS-43	Dodoma	Kondoa	Pahi	Pahi	Ikengwa	36.06035	-4.71221	1207	2006/8/4	197.9	1.0	2.5	1.5	76.5	3.6	1.4	6.2	64.2
31	T-1-1	Dodoma	Kondoa	Kondoa Mjini	Suruke	Kipyuku Hills	35.59283	-5.02087	1406	2006/6/30	1259.3	1.0	324.5	3.2	80.1	17.8	50.0	31.6	9800.0
32	T-2-1	Dodoma	Kondoa	Farkwa	Gwanai	Gwanai	35.81735	-5.31984	1139	2006/7/1	324.3	1.1	59.9	4.7	12.9	41.1	499.9		
33	GS-50	Manyara	Hanang	Endasak	Miashiro	Mara	35.49860	-4.44732	1564	2006/8/7	116.8	0.7	30.2	1.6	56.0	15.3	4.0	26.2	224.5
34	GS-51	Manyara	Kiteto	Kibaya	Partimbo	Olkitikiti	36.75781	-5.52788	1261	2006/8/6	13.6	1.3	5.1	3.0	10.7	5.5	1.9	9.9	302.4
35	GS-54	Manyara	Kiteto	Kibaya	Partimbo	Namelok	36.52820	-5.32376	1530	2006/8/6	22.6	0.9	45.7	1.9	17.0	3.2	96.7	9.4	2217.3
36	T-20-1	Manyara	Kiteto	Kiteto	Partimbo	Mbigili	36.66763	-5.31184	1274	2006/7/2	47.1	3.9	58.4	13.2	203.8	29.6	28.7	46.4	353.4
37	T-20-2	Manyara	Kiteto	Kiteto	Partimbo	Mbigili	36.66632	-5.30515	1266	2006/7/2	54.6	1.3	307.5	2.9	10.6	5.0	51.6	21.2	646.3
38	T-20-3	Manyara	Kiteto	Kiteto	Partimbo	Mbigili	36.66237	-5.31612	1278	2006/7/2	22.6	0.6	49.8	3.9	184.1	10.4	82.4	19.1	457.9
39	T-20-4	Manyara	Kiteto	Kibaya	Partimbo	Mbigili	36.64924	-5.32223	1310	2006/8/6	62.5	1.2	315.8	16.1	93.3	32.0	327.1	43.9	767.5
40	T-20-5	Manyara	Kiteto	Kibaya	Partimbo	Mbigili	36.64136	-5.32375	1310	2006/8/6	153.7	1.0	16.9	1.8	43.7	10.0	128.2	17.8	304.9
41	T-20-6	Manyara	Kiteto	Kibaya	Partimbo	Mbigili	36.66180	-5.31321	1277	2006/9/1	209.0	0.9	17.6	1.6	479.3	2.8	18.4	9.2	196.2
42	T-20-7	Manyara	Kiteto	Kibaya	Partimbo	Mbigili	36.68049	-5.31974	1265	2006/9/1	2520.7	0.8	681.3	3.7	83.8	16.7	19.8	29.5	124.7
43	T-19-1	Manyara	Kiteto	Makami	Ndedo	Ndedo	36.76292	-4.87931	1039	2006/7/11	104.1	0.9	13.5	3.0	4.6	17.5	1.3	64.5	2.8
44	T-19-2	Manyara	Kiteto	Makami	Ndedo	Ndedo	36.80150	-4.86574	1025	2006/7/11	5.9	0.3	24.6	1.2	13.1	12.1	1.0	73.0	18.0
45	T-19-3	Manyara	Kiteto	Makami	Ndedo	Ndedo	36.76422	-4.83279	1035	2006/7/11	101.6	0.7	17.3	2.7	5.9	10.7	2.3	71.4	4.3
46	GS-56	Manyara	Mbulu	Nambis	Kainam	Hareabi	35.58678	-3.91641	1837	2006/8/8	119.7	0.9	22.9	1.7	71.5	2.1	5132.7		
47	GS-57	Manyara	Mbulu	Haidom	Mghang	Laby	35.17236	-4.11301	1873	2006/8/8	71.5	1.3	22.0	14.1	404.3				
48	GS-58	Manyara	Mbulu	Endagikoti	Tlawi	Maskaroda	35.40926	-3.93949	1807	2006/8/8	410.1	0.8	108.3	4.7	9.9	7.3	14.6	24.0	385.7
49	GS-61	Manyara	Simanjoro	Emboret	Loboir Siret	Narakauo	36.49118	-4.22964	1426	2006/8/3	57.1	1.0	24.9	1.8	70.8	3.2	286.5	17.8	918.2
50	GS-62	Manyara	Simanjiro	Terati	Komoro	Sukuro	36.62709	-4.03071	1385	2006/8/3	3.7	0.7	1.4	5.4	5.9	6.6	216.8		

Table 5-6 Location and the Result of Vertical Electrical Sounding (2/4)

No	GS-No	Location					Position			Survey Date	Analysis Result								
		Region	District	Division	Ward	Village	Longitude	Latitude	Altitude		Rho-1 (Ωm)	Depth-1 (m)	Rho-2 (Wm)	Depth-2 (m)	Rho-3 (Wm)	Depth-3 (m)	Rho-4 (Wm)	Depth-4 (m)	Rho-5 (Wm)
51	GS-63	Mareyara	Simanjiro	Orkesmes	Naberera	Namalulu	36.68791	-4.44269	1308	2006/7/2	48.5	0.6	5.4	1.0	88.0	9.7	180.0	21.7	5000.0
52	GS-65	Shinyanga	Kishapu	Mondo	Seke/Bugoro	Dulisi	33.49945	-3.41814	1177	2006/7/25	9.9	0.6	3.0	2.8	31.2	11.9	323.5		
53	GS-66	Shinyanga	Kishapu	Kishapu	Somagedi	Wimate	34.06278	-3.77117	1091	2006/7/26	6.8	1.9	32.9	4.3	5.4	43.8	70.7		
54	GS-67	Shinyanga	Kishapu	Negezi	Ukenyenge	Mwaweja	33.69195	-3.74176	1091	2006/7/25	20.3	2.2	2.9	38.7	1.8	92.1	28.5		
55	GS-68	Shinyanga	Maswa	Mwagala	Lalago	Gula	33.97079	-3.44885	1178	2006/7/27	7.5	1.9	1.4	3.1	5073.2				
56	GS-69	Shinyanga	Maswa	Nunghu	Masela	Mwabomba	33.76414	-3.48014	1160	2006/7/25	3.7	1.8	16.3	3.1	1.4	4.7	318.3	88.0	141.1
57	GS-70	Shinyanga	Maswa	Nunghu/Kigoku	Masela	Masela	33.62253	-3.32304	1214	2006/7/25	2.5	1.5	5.0	2.8	40.0	4.8	20.0	7.8	10229.4
58	GS-71	Shinyanga	Meatu	Kimali	Kimali	Makao	34.83051	-3.39161	1621	2006/7/28	4.5	1.0	17.9	3.1	48.9	12.2	1221.2		
59	GS-72	Shinyanga	Meatu	Kimali	Kimali	Mwangudo	34.49133	-3.50896	1231	2006/7/28	21.5	0.6	0.9	0.9	97.7	2.0	221.9	14.4	2480.9
60	GS-73	Shinyanga	Meatu	Nyalaja	Mwabuzo	Mwabalebi	34.29616	-3.86615	1071	2006/7/27	66.4	0.6	260.9	5.7	0.9	10.0	7.8	30.1	2.7
61	GS-74	Shinyanga	Meatu	Nyalaja	Mwamanongu	Mwanmanongu	34.26200	-3.71838	1100	2006/7/27	100.0	0.1	699.8	2.6	1.9	18.4	4.1	60.8	2.1
62	GS-76	Shinyanga	Meatu	Kimali	Mwanhuzi	Mwagwila	34.22295	-3.43878	1177	2006/7/27	40.0	0.8	7.3	1.4	105.7	5.0	3.1	8.2	251.8
63	GS-77	Shinyanga	Shinyanga Rural	Itwangi	Didia	Bukumbi	33.03036	-3.81605	1187	2006/7/24	67.2	0.9	7.0	1.4	59.1	3.6	7.0	5.7	157.9
64	GS-78	Shinyanga	Kishapu	Negezi	Mwamashele	Buongo	33.85691	-3.75146	1093	2006/7/26	24.5	0.5	205.3	3.2	6.3	34.0	0.9	55.3	47.6
65	GS-79	Shinyanga	Shinyanga Rural	Samuye	Samuye	Masengwa	33.37565	-3.82588	1122	2006/7/24	92.6	0.5	35.5	20.4	11.5	87.4	130.9		
66	GS-80	Shinyanga	Shinyanga Urban	Ibadakuli	Kolandoto	Kolandoto	33.53829	-3.59108	1178	2006/7/24	6.3	0.6	70.4	1.0	21.8	8.9	80.6	23.9	2500.0
67	GS-81	Shinyanga	Shinyanga Urban		Mwawaza	Mwawaza	33.34881	-3.67274	1152	2006/7/24	115.7	0.8	50.4	3.7	20.3	57.2	111.3		
68	GS-82	Singida	Iramba	Nduguti	Gumanga	Gumanga	34.62263	-4.24412	1482	2006/7/18	7.4	0.4	8.9	6.9	50.6	127.0	491.3		
69	GS-83	Singida	Iramba	Nduguti	Ilunda	Kinampundu	34.80495	-4.44672	1534	2006/7/18	380.7	1.0	10.2	1.8	208.3	3.6	14.8	9.1	250.5
70	GS-85	Singida	Iramba	Kisiriri	Kiomboi	Kinambeu	34.36132	-4.29409	1503	2006/7/29	1758.0	1.5	48.6	2.3	12.3	7.7	149.6	11.6	645.7
71	GS-86	Singida	Iramba	Kirumi	Mpambala	Nyahaa	34.55505	-3.97271	1061	2006/7/28	5.1	0.9	0.9	1.4	13.6	4.4	0.6	10.1	47.8
72	GS-87	Singida	Iramba	Nduguti	Mwanga	Malaja	34.81272	-4.22766	1529	2006/7/18	125.9	0.9	32.1	3.5	12.1	9.8	3.4	24.6	150.8
73	GS-89	Singida	Iramba	Ndago	Ndago	Nguvumali	34.37897	-4.57279	1414	2006/7/29	167.6	0.9	39.1	4.0	6.8	12.7	65.5	82.7	197.4
74	GS-90	Singida	Iramba	Shelui	Sherui	Wembere	34.26485	-4.31540	1140	2006/7/22	56.3	0.4	24.8	4.6	32.9	12.6	16.4	47.9	89.1
75	GS-91	Singida	Iramba	Kisiriri	Tulya	Tulya	34.33626	-4.11902	1084	2006/7/29	157.4	0.9	50.2	2.2	7.3	12.1	2.2	22.6	46.9
76	GS-92	Singida	Iramba	Sepuka	Urughu	Mlandala	34.14157	-4.73107	1097	2006/7/20	201.3	1.4	31.6	3.4	5.8	6.4	37.1	14.5	504.3
77	GS-93	Singida	Manyoni	Kintinku	Chikuyu	Chikuyu	35.04503	-5.86942	832	2006/7/31	70.2	1.1	500.7	3.4	7.9	6.2	25.5	8.3	471.2
78	GS-94	Singida	Manyoni	Nkoko	Isseke	Isseke	35.01802	-6.42675	1111	2006/8/1	28.4	1.7	49.0	4.1	21.2	6.8	214.3	8.7	1222.3
79	GS-95	Singida	Manyoni	Itigi	Itigi	Kitaraka	34.37322	-5.64579	1302	2006/7/28	38.8	0.6	14.9	2.4	83.0	4.0	11.1	8.9	223.9
80	GS-98	Singida	Manyoni	Kintinku	Sasajila	Makasusu	34.92019	-6.00629	945	2006/8/1	88.5	3.4	21.2	19.0	7.7	28.3	371.0		
81	GS-99	Singida	Singida Rural	Ikungi	Issuna	Nkuhi	34.77265	-5.35130	1381	2006/7/18	321.9	1.4	16.7	6.1	7.7	22.7	3.3	35.6	81.9
82	GS-100	Singida	Singida Rural	Ilongero	Kinyeto	Igauri	34.79882	-4.66529	1549	2006/7/16	4.3	1.3	5.5	4.2	3320.8				
83	GS-101	Singida	Singida Rural	Ikungi	Mang'onyi	Sambaru	35.06622	-5.25707	1210	2006/7/29	17.9	2.1	6.1	3.1	14.5	27.8	1.6	40.1	74.1
84	GS-102	Singida	Singida Rural	Mgori	Mgori	Mgori	34.95876	-4.84885	1320	2006/7/16	87.5	3.3	2.1	5.3	63.5	9.4	2.5	17.3	226.6
85	GS-103	Singida	Singida Rural	Sepuka	Mgungira	Iyumbu	34.03919	-5.14585	1057	2006/7/20	17.7	2.7	0.9	3.1	8.6	45.7	41.0	105.8	6.0
86	GS-105	Singida	Singida Rural	Ihanja	Muhinteri	Iglansoni part 2	34.48139	-5.32769	1253	2005/7/21	9.7	0.5	0.6	0.8	321.2				
87	GS-106	Singida	Singida Rural	Sepuka	Mwaru	Msosa	34.15391	-4.94711	1091	2006/7/20	200.7	0.9	7.2	5.8	50.0	7.4	2.1	14.2	205.8
88	GS-107	Singida	Singida Rural	Sepuka	Mwaru	Ighombwe	34.33716	-4.96077	1167	2006/7/21	299.9	0.8	777.9	2.8	48.1	18.1	11.4	27.7	387.1
89	T-13-1	Singida	Singida Rural	Sepuka	Sepuka	Mtunduru	34.54601	-4.84128	1477	2006/7/12	5817.5	0.5	9000.0	3.4	164.8	10.8	250.3		
90	T-13-2	Singida	Singida Rural	Sepuka	Sepuka	Mtunduru	34.53260	-4.85709	1469	2006/7/12	1724.0	3.2	98.4	7.4	1618.7	15.5	254.7	28.9	4440.8
91	T-13-3	Singida	Singida Rural	Sepuka	Sepuka	Mtunduru	34.52757	-4.83370	1461	2006/7/12	22.9	0.9	8.7	8.4	115.9	17.4	21.1	41.2	223.5
92	GS-108	Singida	Singida Rural	Mgori	Ngimu	Pohama	35.13755	-4.75028	1450	2006/7/16	37.0	4.5	10.0	508.1					
93	GS-109	Singida	Singida Rural	Mungaa	Ntuntu	Ntuntu	34.99435	-5.13445	1510	2006/7/18	257.0	3.6	2.6	4.9	754.4				
94	GS-110	Singida	Singida Urban	Madewa	Mwankoko	Mwankoko A	34.62996	-4.84887	1485	2006/7/20	40.5	0.8	5.0	1.3	15.9	17.2	422.2	35.2	2553.8
95	GS-112	Tabora	Igunga	Simbo	Chabutwa	Majengo	33.43701	-4.61803	1209	2006/7/26	30.8	3.0	11.5	4.4	38.3	27.4	95.8	97.9	210.5
96	GS-113	Tabora	Igunga	Choma	Choma	Choma	33.36647	-4.00402	1108	2006/7/24	21.0	0.3	6.8	3.3	24.2	48.7	199.3		
97	GS-114	Tabora	Igunga	Igunga	Itumba	Buhekela	33.74387	-4.79996	1055	2006/7/23	45.2	0.5	27.2	5.9	84.5	9.9	18.5	18.6	232.6
98	GS-115	Tabora	Igunga	Igunga	Igunga	Mgongoro	34.04684	-4.39261	1036	2006/7/22	1.6	0.2	3.2	7.3	3.0	38.6	7.6		
99	GS-116	Tabora	Igunga	Igunga	Mwanzugi	Mwanzugi	33.89657	-4.36617	1083	2006/7/23	10.6	2.8	2.8	9.4	9.1	46.4	76.7		
100	GS-117	Tabora	Igunga	Igulubi	Igulubi	Kalangale	33.65567	-3.96046	1065	2006/7/24	19.0	1.4	9.1	45.5	157.2				

Table 5-6 Location and the Result of Vertical Electrical Sounding (3/4)

No	GS-No	Location					Position			Survey Date	Analysis Result								
		Region	District	Division	Ward	Village	Longitude	Latitude	Altitude		Rho-1 (Ωm)	Depth-1 (m)	Rho-2 (Wm)	Depth-2 (m)	Rho-3 (Wm)	Depth-3 (m)	Rho-4 (Wm)	Depth-4 (m)	Rho-5 (Wm)
101	GS-118	Tabora	Igunga	Igulubi	Isakamaliwa	Hindishi	33.97948	-4.13970	1083	2006/7/23	6.8	1.0	0.4	1.7	3.1	27.5	0.5	51.7	14.4
102	GS-120	Tabora	Igunga	Igunga	Itumba	Chagana	34.91372	-4.56739	1043	2006/7/22	35.2	1.2	7.4	18.7	0.9	32.3	43.4		
103	GS-121	Tabora	Igunga	Igulubi	Mwamashimba	Imalanguzu	33.80265	-4.11595	1122	2006/7/24	112.6	2.5	8.6	12.8	0.8	25.9	6.9	121.2	3.6
104	GS-122	Tabora	Igunga	Nkinga	Nkinga	Ulaya	33.43102	-4.38678	1265	2006/7/25	2520.7	1.0	223.6	3.6	29.5	8.3	162.9	88.9	2250.2
105	GS-123	Tabora	Igunga	Simbo	Sunguzwi	Nguriti	33.56159	-4.43943	1202	2006/7/25	63.2	0.7	11.8	1.2	121.8	4.8	19.8	7.7	624.8
106	Gs-124	Tabora	Nzega		Lusu	Lusu	33.22118	-4.02908	1105	2006/7/25	18.5	0.6	40.2	7.2	21.2	32.5	34.0	52.6	173.8
107	GS-126	Tabora	Nzega	Itobo	Mwamala	Nawa	32.89010	-4.01083	1147	2006/7/26	17.2	1.1	2.5	1.3	8.5	18.5	1.6	27.9	82.7
108	GS-127	Tabora	Nzega	Puge	Ndala	Wita	33.28093	-4.74312	1219	2006/7/26	25.0	1.6	3.0	1.9	35.0	22.6	80.0	40.6	3236.8
109	GS-128	Tabora	Igunga	Mwakarundi	Shigamba	Kagungwa	33.10327	-4.19761	1192	2006/7/25	21.3	0.5	2.2	1.0	40.3	5.8	79.5	14.0	839.6
110	GS-130	Tabora	Sikonge	Sikonge	Igigwa	Nyahua	33.33403	-5.37905	1167	2006/7/27	1190.6	1.8	198.5	2.5	15.5	37.5	125.7	82.9	876.2
111	GS-131	Tabora	Uyui	Igalula	Kizengi	Kizengi	33.58269	-5.34718	1172	2006/7/27	42.4	0.6	11.9	1.4	29.2	18.1	248.8		
112	GS-133	Tabora	Uyui	Utende	Igulula	Mwakadala	33.65466	-4.90020	1186	2006/7/23	127.0	0.8	5.2	1.3	147.3	1.9	32.0	22.4	382.4
113	T-16-1	Tabora	Uyui	Igulala	Igulala	Seniki	33.27674	-5.17534	1264	2006/7/8	13.0	0.4	5.8	2.3	261.0	4.3	163.3	9.3	1255.1
114	T-16-2	Tabora	Uyui	Igulala	Igulala	Seniki	33.27106	-5.17309	1264	2006/7/8	13.1	0.8	4.4	1.3	20.7	3.1	89.7	15.7	1203.3
115	T-1-2	Dodoma	Bahi	Bahi	Pamantwa	Mkakatika	35.35014	-5.91408	896	2006/7/31	293.0	2.0	77.3	5.3	38.3	23.3	1222.3		
116	T-1-3	Dodoma	Bahi	Bahi	Pamantwa	Mkakatika	35.34882	-5.91335	895	2006/7/31	23.3	0.8	118.1	2.8	43.5	22.6	292.9	30.5	844.1
117	T-2-2	Dodoma	Dodoma Rural	Munoemu	Babayu	Kongogo	35.62640	-5.65422	1050	2006/7/12	41.7	0.4	25.0	5.8	4.1	8.1	30.0	76.0	116.9
118	T-3-1	Dodoma	Kondoa	Farkwa	Farkwa	Bubutole	35.55725	-5.31521	1099	2006/6/30	18.2	1.1	29.8	1.4	77.9	6.3	25.3	57.7	96.4
119	T-3-2	Dodoma	Kondoa	Farkwa	Farkwa	Bubutole	35.55470	-5.31322	1095	2006/6/30	21.8	0.7	74.7	7.2	12.9	35.8	96.1		
120	T-3-3	Dodoma	Kondoa	Farkwa	Farkwa	Bubutole	35.55382	-5.31303	1094	2006/6/30	22.0	1.4	44.9	3.5	16.7	60.0	108.6		
121	T-4-1	Dodoma	Kondoa	Pahi	Kalamba	Loo	35.88363	-4.87931	1509	2006/7/1	911.4	3.0	3.9	5.4	55.9	7.6	138.0	14.4	263.4
122	T-4-2	Dodoma	Kondoa	Pahi	Kalamba	Loo	35.87705	-4.88251	1494	2006/7/1	10.0	2.7	29.2	5.9	2.6	10.4	550.3	20.1	864.1
123	T-4-3	Dodoma	Kondoa	Pahi	Kalamba	Loo	35.86756	-4.89000	1506	2006/7/1	426.9	0.9	245.5	1.7	201.9	8.1	124.3	22.1	637.8
124	T-4-4	Dodoma	Kondoa	Pahi	Kalamba	Loo	35.86611	-4.88766	1485	2006/8/31	562.5	0.7	9.7	1.3	209.6	4.1	48.7	12.5	584.4
125	T-4-5	Dodoma	Kondoa	Pahi	Kalamba	Loo	35.86891	-4.88896	1489	2006/8/31	62.5	0.6	10.1	4.8	25.9	6.1	6.5	16.5	62.2
126	T-4-6	Dodoma	Kondoa	Pahi	Kalamba	Loo	35.87260	-4.88711	1484	2006/8/31	15.4	2.7	6.4	5.2	22.4	8.1	9.7	27.5	120.3
127	T-5-1	Dodoma	Dodoma Rural	Chipalamga	Mpalanga	Nholi	35.48404	-6.29414	1004	2006/7/10	1105.7	1.5	64.7	11.3	192.2	60.8	1092.1	127.1	518.7
128	T-5-2	Dodoma	Dodoma Rural	Chipanga	Mpalanga	Mpalanga	35.47862	-6.33644	955	2006/8/2	92.6	1.9	7.5	2.9	40.7	5.6	8.3	8.2	390.9
129	T-5-3	Dodoma	Dodoma Rural	Chipanga	Mpalanga	Mpalanga	35.47188	-6.34680	946	2006/8/2	189.0	0.9	13.1	1.5	203.5	2.9	2.1	7.3	135.7
130	T-6-1	Manyana	Hanang	Katesh	Balangidalalu	Dumbeta	35.36692	-4.58669	1546	2006/7/5	28.1	12.5	112.4	24.6	5.0	32.9	194.2		
131	T-6-2	Manyana	Hanang	Katesh	Balangidalalu	Dumbeta	35.36895	-4.58404	1549	2006/7/5	14.5	0.4	94.7	3.6	62.4	25.9	32.1	77.0	77.6
132	T-6-3	Manyana	Hanang	Katesh	Balangidalalu	Dumbeta	35.35964	-4.59342	1518	2006/7/5	10.5	2.9	3.1	4.9	96.2	17.1	47.0	29.9	210.7
133	T-7-1	Manyara	Babati	Bashanet	Dareda	Bermi/Seloto	35.50853	-4.23540	1599	2006/7/4	2.2	0.3	6.3	2.6	19.9	5.2	2.5	12.2	190.3
134	T-7-2	Manyara	Babati	Bashanet	Dareda	Seloto	35.48875	-4.24282	1675	2006/7/4	101.4	4.5	52.4	36.1	1636.0				
135	T-8-1	Singida	Manyoni	Nkonko	Sanza	Ikasi	35.15852	-6.24101	833	2006/7/9	95.4	3.2	12.7	3.3	40.1	4.9	122.2	4.5	
136	T-8-2	Singida	Manyoni	Nkonko	Sanza	Ikasi	35.16049	-6.24609	838	2006/7/9	243.2	1.0	120.1	6.7	18.5	20.7	4.9	66.2	35.8
137	T-9-1	Singida	Manyoni	Kilimatinde	Makuru	Ilalo	35.00445	-5.65725	1082	2006/7/9	9.4	6.8	4.0	11.1	22.9	15.8	7.0	76.6	74.6
138	T-9-2	Singida	Manyoni	Kilimatinde	Makuru	Hika	34.98556	-5.61932	1178	2006/7/9	339.3	1.9	6.1	2.6	250.2	47.0	823.7	81.4	1434.2
139	T-10-1	Manyara	Hanang	Bassuto	Hirbadaw	Hirbadaw	34.90223	-4.33915	1625	2006/7/5	201.9	0.7	65.6	5.4	86.7	17.6	40.1	25.0	1274.4
140	T-10-2	Manyara	Hanang	Bassuto	Hirbadaw	Hirbadaw	34.92006	-4.33772	1585	2006/7/5	45.9	0.7	7.6	7.5	18.8	8.1	4.8	24.8	68.1
141	T-10-3	Manyara	Hanang	Bassuto	Hirbadaw	Hirbadaw	34.90277	-4.35319	1602	2006/7/5	225.7	2.7	87.9	12.9	96.5	16.8	47.0	198.3	240.8
142	T-11-1	Manyara	Mbulu	Endagikot	Tlawi	Tlawi	35.46530	-3.91082	1940	2006/7/4	13.9	0.4	1.9	2.0	9.7	14.7	334.2		
143	T-11-2	Manyara	Mbulu	Endagikot	Tlawi	Tlawi	35.46475	-3.90875	1943	2006/7/4	15.0	3.2	23.3	6.0	1.1	9.4	28.6	13.4	379.6
144	T-11-3	Manyara	Mbulu	Endagikot	Tlawi	Tlawi	35.44907	-3.90797	1952	2006/7/4	286.1	1.1	37.1	6.4	355.8	18.3	20.4	32.5	357.9
145	T-11-4	Manyara	Mbulu	Endagikot	Tlawi	Tlawi	35.47646	-3.88903	1951	2006/7/5	19.5	0.6	6.3	9.9	31.6	43.9	192.6		
146	T-12-1	Singida	Iramba	Kinyangiri	Msingi	Msingi	34.55103	-4.33522	1243	2006/7/7	28.4	0.7	8.9	2.9	34.3	7.9	597.5		
147	T-12-2	Singida	Iramba	Kinyangiri	Msingi	Msingi	34.56765	-4.37563	1283	2006/7/7	378.5	1.8	18.3	18.0	3.9				
148	T-12-3	Singida	Iramba	Kinyangiri	Msingi	Msingi	34.57826	-4.38189	1266	2006/7/7	9.3	0.5	3.7	7.8	10.4	44.9	2.7	161.0	35.8
149	T-13-4	Singida	Singida Rural	Sepuka	Sepuka	Munangana	34.56569	-4.75194	1499	2006/7/20	8.7	0.8	22.4	6.2	914.7				
150	T-13-5	Singida	Singida Rural	Sepuka	Sepuka	Iporio	34.56226	-4.75001	1505	2006/7/20	166.6	0.9	1.4	1.5	32.9	4.8	67.7	12.8	1209.1

Table 5-6 Location and the Result of Vertical Electrical Sounding (4/4)

No	GS-No	Location					Position			Survey Date	Analysis Result								
		Region	District	Division	Ward	Village	Longitude	Latitude	Altitude		Rho-1 (Ωm)	Depth-1 (m)	Rho-2 (Wm)	Depth-2 (m)	Rho-3 (Wm)	Depth-3 (m)	Rho-4 (Wm)	Depth-4 (m)	Rho-5 (Wm)
151	T-13-6	Singida	Singida Rural	Sepuka	Sepuka	Iporio	34.55638	-4.75039	1509	2006/7/20	1480.4	2.7	82.2	7.6	2000.2	43.7	536.0	73.9	3069.6
152	T-14-1	Tabora	Igunga	Nanga	Nanga	Igogo	33.77901	-4.29066	1104	2006/7/7	47.7	0.5	10.7	2.8	2.1	4.1	25.5	58.4	29.8
153	T-14-2	Tabora	Igunga	Nanga	Nanga	Igogo	33.76144	-4.29724	1109	2006/7/7	18.3	0.4	9.0	10.0	0.8	15.6	2.2	53.6	43.7
154	T-15-1	Tabora	Uyui	Igalula	Kizengi	Nkongwa	33.99472	-5.36837	1243	2006/7/8	33.4	1.0	400.1	1.8	10.5	40.2	273.4		
155	T-15-2	Tabora	Uyui	Igalula	Kizengi	Nkongwa	33.99646	-5.36013	1283	2006/7/8	23.7	0.3	60.0	3.0	7.5	31.0	355.4		
156	T-15-3	Tabora	Uyui	Igalula	Kizengi	Nkongwa	33.99235	-5.37014	1266	2006/7/8	27.4	1.0	81.1	2.8	9.5	34.9	301.6		
157	T-16-3	Tabora	Igunga	Igulubi	Mwamashima	Kininginila	33.91155	-4.03112	1086	2006/7/24	108.1	2.2	33.7	4.7	4.7	29.6	2.5	112.2	8.5
158	T-17-1	Manyara	Babati	Mbugwe	Mwada	Mwada	35.83190	-3.94191	979	2006/7/11	1.5	1.2	5.3	1.9	1.6	13.9	4.4	52.3	27.1
159	T-17-2	Manyara	Babati	Mbugwe	Mwada	Mwada	35.84195	-3.92033	976	2006/7/11	3.1	1.8	11.6	3.0	2.8	11.2	5.0	84.2	24.4
160	T-17-3	Manyara	Babati	Mbugwe	Mwada	Mwada	35.82591	-3.91744	992	2006/7/11	81.4	0.5	8.8	3.2	23.8	5.1	6.2	48.4	16.3
161	T-17-4 (GS-44)	Manyara	Babati	Mbugwe	Magugu	Mapea	35.75789	-4.00821	1006	2006/7/30	43.1	0.5	138.0	5.9	11.3	14.0	1.0	28.6	27.0
162	T-18-1	Dodoma	Kondoa	Bereko	Masange	Masange	35.81546	-4.59137	1199	2006/7/10	261.2	1.5	84.1	2.8	8.2	46.2	71.0	84.6	500.1
163	T-18-2	Dodoma	Kondoa	Bereko	Masange	Masange	35.81753	-4.59369	1197	2006/7/10	27.6	0.3	10.5	4.5	4.1	13.9	15.2	36.1	185.1
164	T-18-3	Dodoma	Kondoa	Bereko	Masange	Masange	35.80318	-4.60344	1245	2006/7/10	360.9	1.1	167.7	2.6	30.3	14.6	8.4	25.2	5000.0
165	GS-52-1 (T-19-4)	Manyara	Kiteto	Ndedo	Makame	Makame	36.66566	-4.66290	1205	2006/8/5	105.2	1.0	445.4	3.0	147.6	11.8	39.3	21.3	2023.8
166	GS-52-2 (T-19-5)	Manyara	Kiteto	Ndedo	Makame	Makame	36.70853	-4.63162	1049	2006/8/5	106.5	2.9	27.9	27.3	2.3	39.6	10.0	124.6	0.1
167	GS-64 (T-20-8)	Shinyanga	Kishapu	Negezi	Ngofila	Ngofila	33.78181	-3.93537	1057	2006/7/26	4.3	0.8	1.2	18.2	2.7	121.1	31.6		
168	T-21-1	Shinyanga	Maswa	Nughu/Kigoku	Masela	Mwasayi	33.68623	-3.34085	1216	2007/6/9	156.4	1.0	5.3	1.8	36.4	3.2	7.9	5.7	346.3
169	T-21-2	Shinyanga	Maswa	Mwagara	Busilili	Bugalama	33.68608	-3.33857	1217	2007/6/9	6.2	0.3	4.8	1.1	12.3	7.1	805.6		
170	T-21-3	Shinyanga	Maswa	Nughu/Kigoku	Masela	Mwasayi	33.68677	-3.34095	1217	2007/6/9	52.0	0.7	1.7	0.9	13.8	15.5	350.1	65.0	800.1
171	T-22-1	Shinyanga	Meatu	Kimari	Kimari	Mwangudo	34.50555	-3.50322	1247	2007/6/10	13.0	0.5	0.4	0.7	10.3	5.3	48.6	9.1	1285.2
172	T-22-2	Shinyanga	Meatu	Kimari	Kimari	Mwangudo	34.50412	-3.50413	1247	2007/6/10	8.5	0.4	6.5	1.8	11.8	6.5	83.9	21.4	568.8
173	T-23-1	Arusha	Ngorongoro	Loliondo	Orgosorok	Loliondo	35.62104	-2.05118	2143	2007/6/12	37.1	1.8	73.1	7.0	231.5	18.1	23.2	45.3	309.1
174	T-23-2	Arusha	Ngorongoro	Loliondo	Orgosorok	Loliondo	35.61991	-2.05134	2138	2007/6/12	168.8	4.0	68.0	11.1	22.4	49.0	1165.4		
175	T-23-3	Arusha	Ngorongoro	Loliondo	Orgosorok	Sakala	35.60753	-2.05166	2106	2007/6/12	83.2	1.2	6.6	5.7	4.3	11.4	113.1	18.6	1279.8
176	GS-47 (T-24-3)	Manyara	Hanang	Basotu	Basotu	Basotu	35.06890	-4.41442	1613	2006/8/7	39.1	0.6	2.9	0.8	37.1	3.8	1.5	7.2	175.9
177	T-25-1	Arusha	Longido	Kitumbein	Kitumbein	Orkejuloongishu	36.33042	-2.81587	1136	2007/6/17	43.5	3.0	74.4	6.2	5.2	7.0	39.2	72.0	183.5
178	T-25-2	Arusha	Longido	Kitumbein	Kitumbein	Orkejuloongishu	36.32236	-2.82154	1159	2007/6/17	36.2	0.9	100.1	3.3	10.0	3.7	44.4	82.6	179.6
179	T-25-3	Arusha	Longido	Kitumbein	Kitumbein	Orkejuloongishu	36.30562	-2.82635	1225	2007/6/17	379.6	0.7	180.9	4.3	27.5	35.3	539.0		
180	T-26-1	Arusha	Monduli	Manyara	Engaruka	Engaruka Chini	35.99940	-2.99348	844	2007/6/14	155.9	0.7	6.0	3.7	45.7	19.5	105.2		
181	T-26-2	Arusha	Monduli	Manyara	Engaruka	Engaruka Chini	35.99945	-2.99352	844	2007/6/14	108.2	0.6	5.2	3.6	64.9	36.2	137.3		
182	T-27-1	Arusha	Monduli	Kisongo	Monduli Juu	Mfereji	36.44564	-3.17310	1332	2007/6/16	127.1	0.4	54.5	6.2	21.3	61.7	209.3		
183	T-27-2	Arusha	Monduli	Kisongo	Monduli Juu	Mfereji	36.44435	-3.17389	1318	2007/6/16	92.8	0.4	43.3	3.3	16.2	37.9	253.2		
184	T-27-3	Arusha	Monduli	Kisongo	Monduli Juu	Mfereji	36.44655	-3.17237	1333	2007/6/16	231.0	0.9	41.0	12.3	83.3	18.1	31.7	69.2	126.8
185	T-28-1	Arusha	Longido	Enduimet	Olmolog	Olmolog	37.12268	-2.86366	1675	2007/6/18	31.3	7.1	141.1	15.0	13.5	18.5	677.1		
186	T-28-2	Arusha	Longido	Enduimet	Olmolog	Olmolog	37.12337	-2.86117	1668	2007/6/18	32.6	3.3	67.1	13.1	170.2	52.5	445.8		
187	T-29-1	Arusha	Arumeru	Kingori	Ngarenanyuki	Uwiro	36.84868	-3.14596	1416	2007/6/20	63.3	3.2	3.1	5.7	110.5	17.9	19.9	31.7	147.3
188	T-29-2	Arusha	Arumeru	Kingori	Ngarenanyuki	Uwiro	36.84893	-3.14634	1450	2007/6/20	98.7	1.5	1.2	2.4	19.0	5.3	50.5	10.5	90.6
189	T-30-1	Arusha	Longido	Sinya	Sinya	Tingatinga	36.95004	-2.95344	1207	2007/6/19	193.0	0.6	83.9	1.4	215.9	4.0	54.4	8.0	828.9
190	T-30-2	Arusha	Longido	Sinya	Sinya	Tingatinga	36.96155	-2.96533	1223	2007/6/19	18.0	1.0	9.8	1.9	42.8	18.0	147.5	31.5	355.2

(1) Relationship between Resistivity and Geology

The resistivity values resulted from VES were compared with the geology confirmed by the test borehole drilling as shown in **Table 5-7**.

Fresh igneous and metamorphic rock showed high resistivity more than 400 ohm-m. Resistivity value of gneiss is higher than granite. If they were weathered, the resistivity value deceased to 100 to 200 ohm-m. Strongly weathered granite or gneiss showed very low resistivity less than 10 ohm-m because they contain much clay mineral. In the granite and the metamorphic rock area, their resistivity values vary widely depending on the degree of weathering. Since aquifer in these areas is presumed the weathered layer or fracture zone, low resistivity layers have high possibility of aquifer.

As for sedimentary rocks, banded iron-rock and tuff were found in IDB. Banded iron-rock has low resistivity (44 ohm-m) because it contains much iron.

In general, clay showed very low resistivity (less than 10 ohm-m) and other soft-sediments: sand and gravel, also showed very low resistivtiy (10 to 43 ohm-m). It is considered that the soft-sedimentary layer is saturated with the groundwater containing many minerals. Besides, saline water with very low resistivity is accumulated in the soft-sediment area.

Table 5-7 Comparison between Geology and Resistivity Value by VES

Geology		Range	Average (Ωm)
Igneous Rock	Granite	35.8 - 2000	472
	Weathered Granite	87.9 - 355.4	189
	Strongly weathered granite	7.5 - 7.5	8
Metamorphic Rock	Gneiss	357.9 - 5000	2331
	Weathered Gneiss	10.5 - 864.1	212
	Strongly weathered gneiss	8.4 - 8.4	8
	Schist	357.9 - 357.9	358
Volcanic Rock	Basalt (Lava)	83.3 539.0	311.2
	Pyroclastic Deposit	105.2 180.9	143.1
	Tuff Breccia	13.5 141.1	60.7
	Agglomerate	19.9 677.1	245.3
Sedimentary Rock	Banded Iron-rock	43.7 - 43.7	44
	Tuff	12.4 - 147.5	92.1
Soft-sediment	Gravel with sand	34.2 - 52.4	43
	Sand with gravel	12.9 - 12.9	13
	Medium sand with gravel	4.0 - 22.9	11
	sand	2.1 - 82.2	31
	Clayey sand	18.5 - 27.9	23
	Sandy Clay	2.6 - 12.9	8
	Clay	1.2 - 4.7	3

(2) Resistivity Analysis Pattern and Aquifer

Typical resistivity analysis pattern is categorized by following three patterns. Note that the resistivity of the shallow layer is depending on the soil conditions which correspond to the weather at the survey date.

Pattern 1: High (Middle) - Low – High

This pattern is typical for igneous rock and metamorphic rock area. Since the survey was conducted in dry season, first layer from the surface had relatively higher resistivity. Low resistivity of the middle layer is estimated as weathered layer or fracture zone. If there is no low resistivity in the middle layer or the low resistivity layer is very thin, it means that groundwater potentiality is very low. On the other hand, if the resistivity is less than 10 ohm-m, the layer may be clay or the groundwater may be salty water. The deepest layer shown high resistivity is presumed to be bedrock. Although the possibility of water struck is low in the bedrock, fissure water can be expected in granite area.

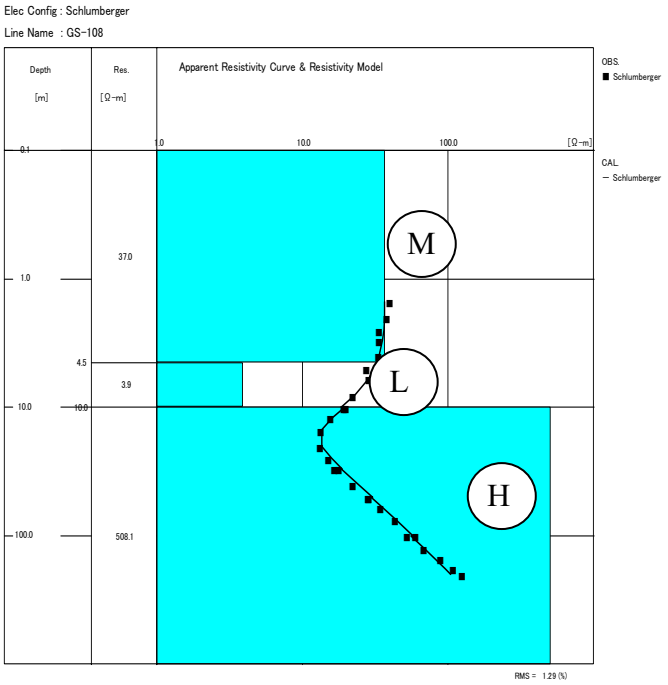

Figure 5-17 Typical Resistivity Structure -Pattern 1-

Pattern 2: Middle (High) – Low

This pattern is typical for soft-sediment area. If the value of low resistivity layer is less than 10 Ωm, it can be regarded to be clay layer or contained salty groundwater. It is difficult to get freshwater in this very low resistivity site. In the soft-sediment area, there is no high resistivity layer up to 200 m which is exploration depth in this VES.

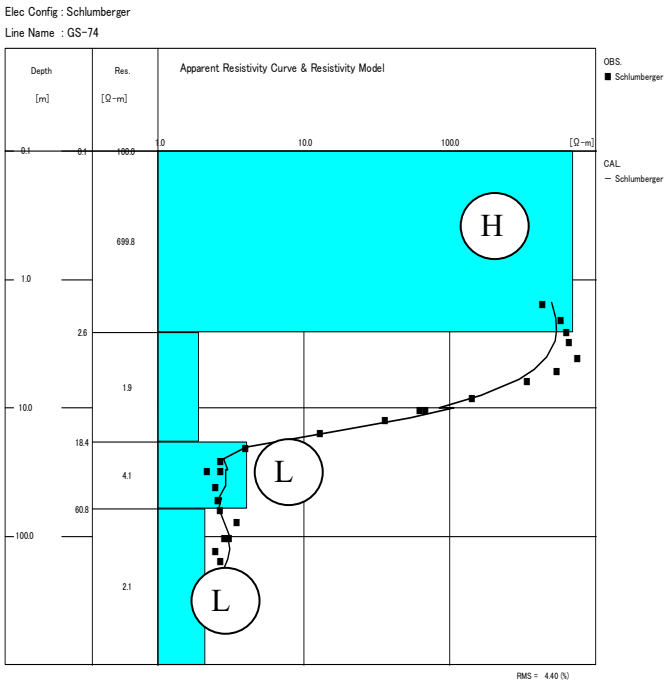

Figure 5-18 Typical Resistivity Structure -Pattern 2-

Pattern 3: Low(Middle) – High

This pattern is typical for granite area with shallow weathered zone. Weathered layer which shows low resistivity is very thin. And very high resistivity (over 500 Ωm) appears immediately. The high resistivity shows intact rock. Possibility of groundwater is very low.

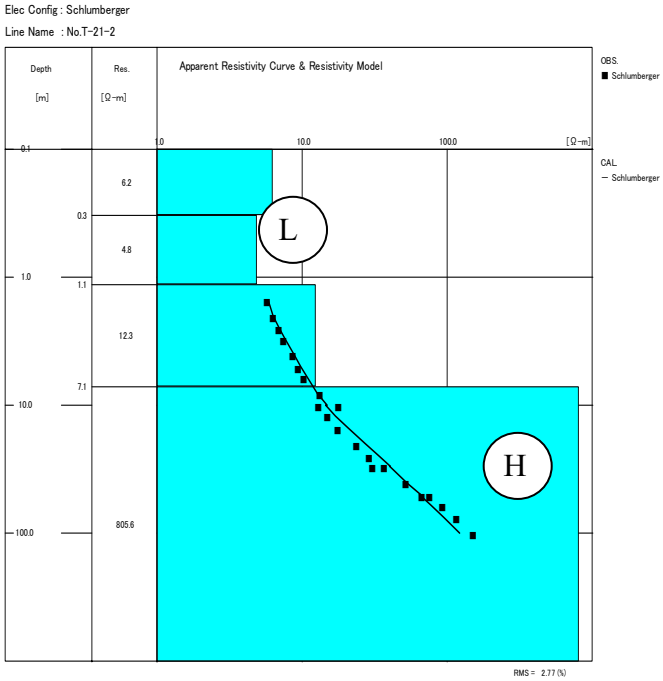

Figure 5-19 Typical Resistivity Structure
-Pattern 3-

(3) Resistivity Distribution by VES

Based on the geophysical survey, resistivity distribution is illustrated focusing on the bedrock as shown in **Figure 5-19**. The distribution of resistivity is well-corresponded to geology which has resistivity as shown in **Table 5-8**.

Table 5-8 Resistivity Range and Geology in IDB

Resistivity (Ωm)	Area	Bedrock geology	Remark
Very High (800-2000)	Kondoa, Shinyanga, Kishapu Meatu, Maswa,,	Granite	Few fault and lineament
	South of Babati	Metamorphic rock	-
High (500-800)	Singida, Iramba, Hanang, West of Uyui, Sikonge	Granite	-
	Mbulu, Kiteto, Karatu,	Metamorphic rock	-
Middle (200-500)	Bahi, Manyoni, East of Uyui	Granite	-
	Simanjiro	Metamorphic rock	-
Low (100 – 200)	Monduli, Ngorongoro, Arumeru	Volcanic rock	-
Very Low (10 – 100)	South of Shinyanga, South of Kisyapu, Igunga, Nzega	Soft-sediment	Not encountered bedrock until 200m

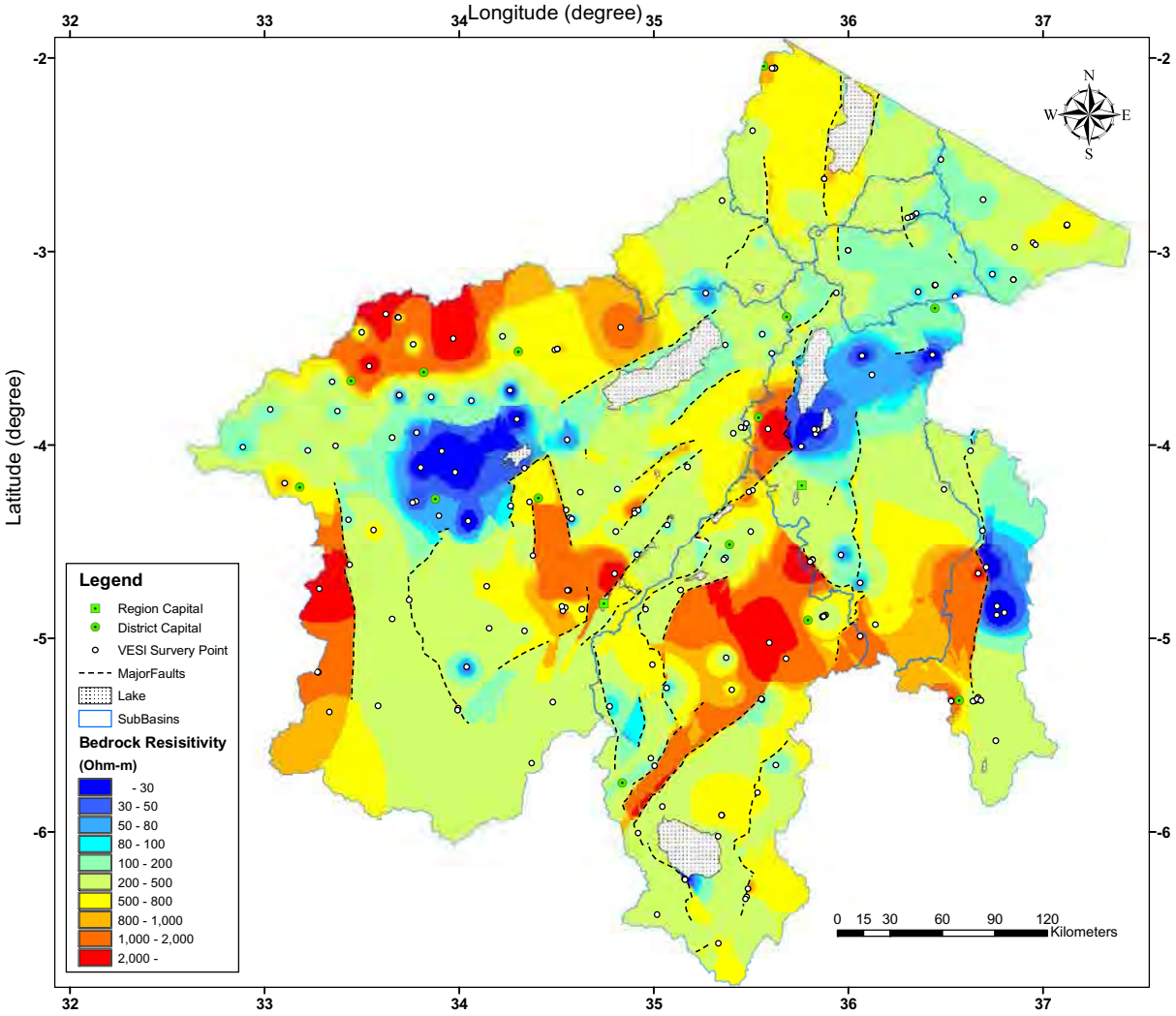

Figure 5-20 Distribution of Bedrock Resistivity Based on Geophysical Survey

On the other hand, a distribution of the bedrock depth based on VES results is shown in **Figure 5-21**. The feature of the distribution is described below.

- Very shallow area: Singida and Kondoa, Mbulu
- Very deep area: Manonga river and Wembele river area,
  Magugu (Babati district),
  Ndedo and Makame (Kiteto district).

These are also well-corresponding to the geological distribution.

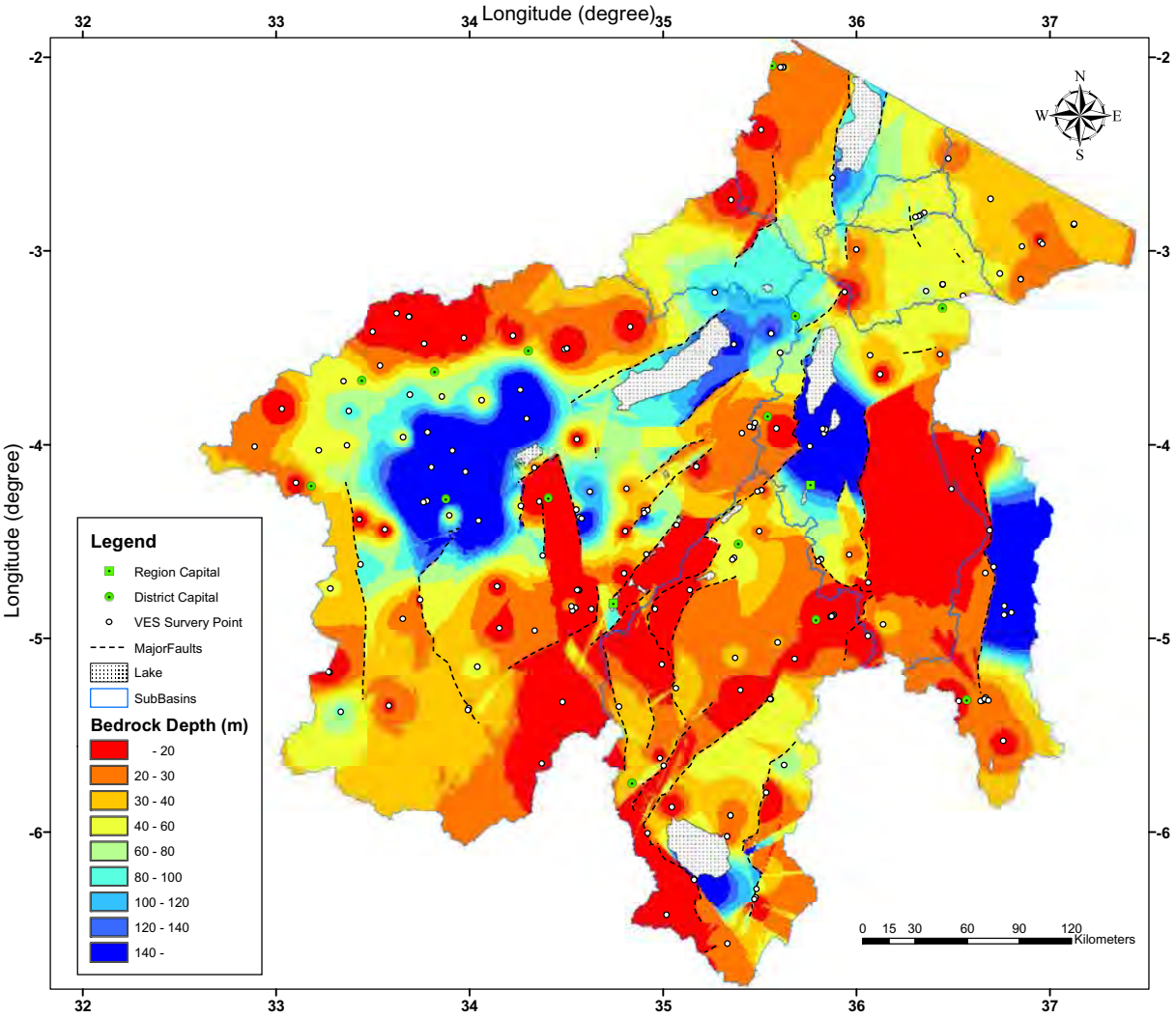

Figure 5-21 Distribution of Bedrock Depth Based on Geophysical Survey

5.3.2 Geophysical Survey for Test Borehole Drilling

Three kinds of geophysical survey method were conducted to select test borehole drilling sites. The Vertical Electrical Sounding (VES) was carried out to figure out the outline of geological structure. When the site wasn't horizontal layered structure, two-dimensional resistivity survey or Magnetic survey was carried out at appropriate line in the candidate areas. Finally, the drilling points were determined on the basis of geophysical survey result, accessibility and topographic feature. The candidate areas for test borehole drilling were selected in the whole IDB. Criteria for selection were explained in Chapter 6. Quantity for survey is shown in **Table 5-9**. The location map of the test borehole drilling sites is shown in **Figure 6-1** of Chapter 6.

VES was conducted 76 points in total, Two-dimensional resistivity survey was carried out in 2 villages, and Magnetic survey was carried out in 11 villages.

Table 5-9 Quantity of Survey in each Test Borehole Drilling Site

Drilling No.	Region	District	Ward	Village	Survey	No. of Survey
TD-1	Singida	Manyoni	Kintinku	Lusilile	VES	2
TD-2	Dodoma	Bahi	Babayu	Kongogo	VES	1
TD-3	Dodoma	Kondoa	Farkwa	Bubutole	VES	3
TD-4	Dodoma	Kondoa	Kalamba	Loo	VES	6
TD-5	Dodoma	Bahi	Mpalanga	Nholi	VES	3
TD-6	Manyana	Hanang	Balangi Dalalu	Numbeta	VES	3
					Magnetic	1
TD-7	Manyara	Babati	Dareda	Bermi/Seloto	VES	2
					Magnetic	1
TD-8	Singida	Manyoni	Sanza	Ikasi	VES	2
TD-9	Singida	Manyoni	Makuru	Ilalo	VES	2
TD-10	Manyara	Hanang	Hirbadaw	Hirbadaw	VES	3
					2-D Res	1
TD-11	Manyara	Mbulu	Tlawi	Tlawi	VES	4
					Magnetic	1
TD-12	Singida	Iramba	Msingi	Misingi	VES	3
					2-D Res	1
Td-13	Singida	Singida Rural	Sepuka	Sepuka	VES	3
					Magnetic	1
TD-14	Tabora	Igunga	Nanga	Igogo	VES	2
TD-15	Tabora	Uyui	Kizengi	Nkongwa	VES	3
TD-16	Tabora	Igunga	Mwamashima	Kininginila	VES	1
TD-17	Manyara	Babati	Magugu	Mapea	VES	4
					Magnetic	1
TD-18	Dodoma	Kondoa	Masange	Masange	VES	3
					Magnetic	1
TD-19	Manyara	Kiteto	Makame	Makeme	VES	2
TD-20	Shinyanga	Kishapu	Ngofila	Ngofila	VES	1
TD-21	Shinyanga	Maswa	Nughu/Kigoku	Mwasayi	VES	3
					Magnetic	1
TD-22	Shinyanga	Meatu	Kimari	Mwangudo	VES	2
					Magnetic	1
TD-23	Arusha	Ngorongoro	Orgosorok	Loliondo	VES	3
TD-24	Manyara	Hanang	Bassotu	Bassotu	VES	1
TD-25	Arusha	Longido	Kitumbein	Orkejuloongishu	VES	3
TD-26	Arusha	Monduli	Manyara	Engaruka Chini	VES	2
TD-27	Arusha	Monduli	Monduli Juu	Mfereji	VES	3
					Magnetic	1
TD-28	Arusha	Longido	Olmolog	Olmolog	VES	2
					Magnetic	1
TD-29	Arusha	Arumeru	Ngarenanyuki	Uwiro	VES	2
					Magnetic	1
TD-30	Arusha	Longido	Sinya	Tingatinga	VES	2

(1) Test Drilling No. 1 (Lusilile Village, Manyoni District, Singida Region)

At first, the site No.1 area was selected in Bahi district in Dodoma region. But the survey result was not fitted in our purpose. Because the results indicated that the bedrock depth too shallow. This site was expected to drill in soft-sediment area. Therefore the site was shifted to Manyoni district near previous site beyond the regional boundary.

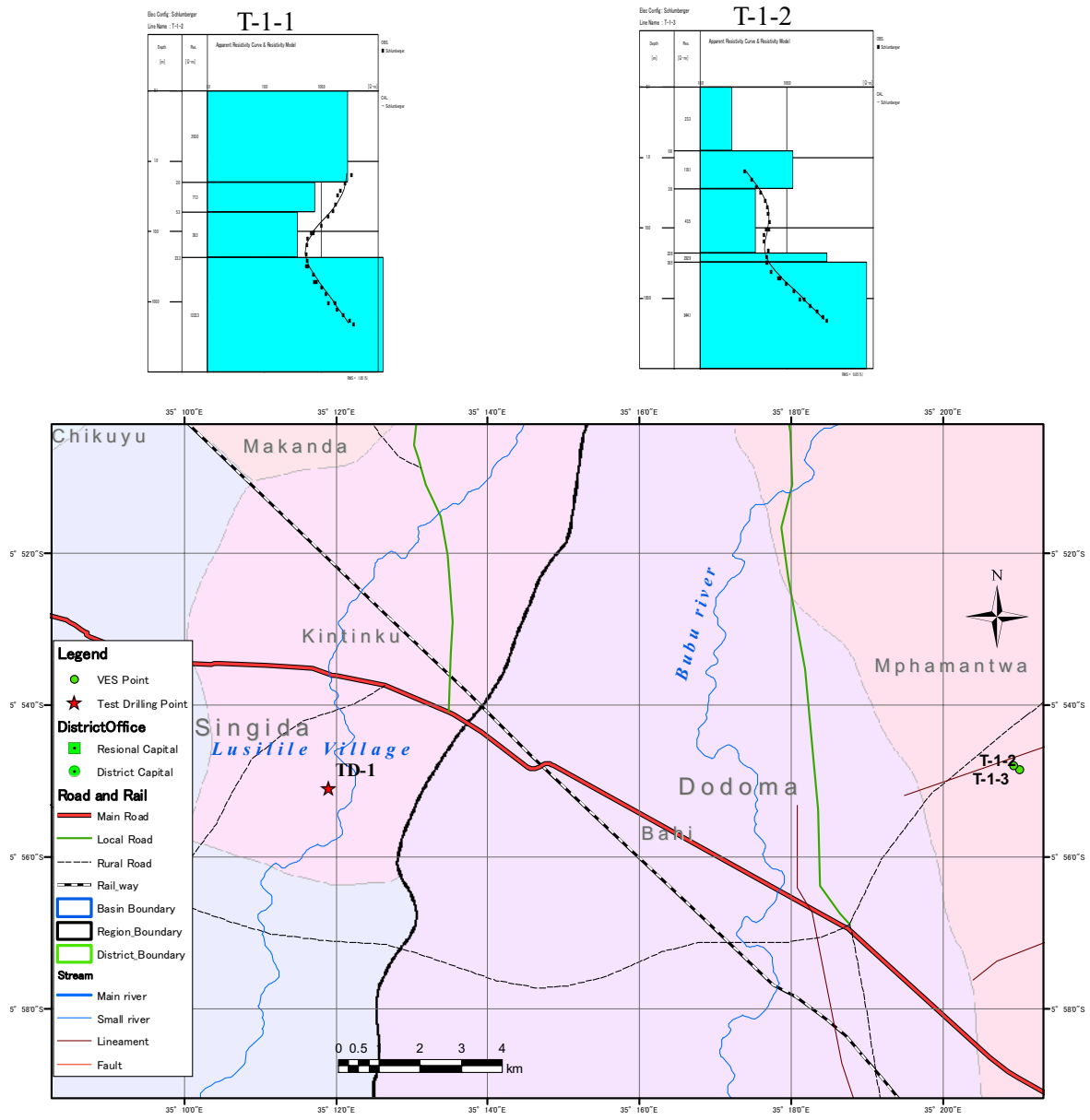

Figure 5-22 Location of Test Borehole Drilling No.1 and Survey Result

(2) Test drilling No. 2 (Kongogo Village, Bahi District, Dodoma Region)

The site No.2 area was planned in the middle of the G sub- basin. This area is a granite area in existing geological information and the remote sensing analysis showed many faults and lineaments in this area. In the VES result, this area is typical granite area. The bedrock would expect to get at 76 m depth. The weathered layer was expected as an aquifer.

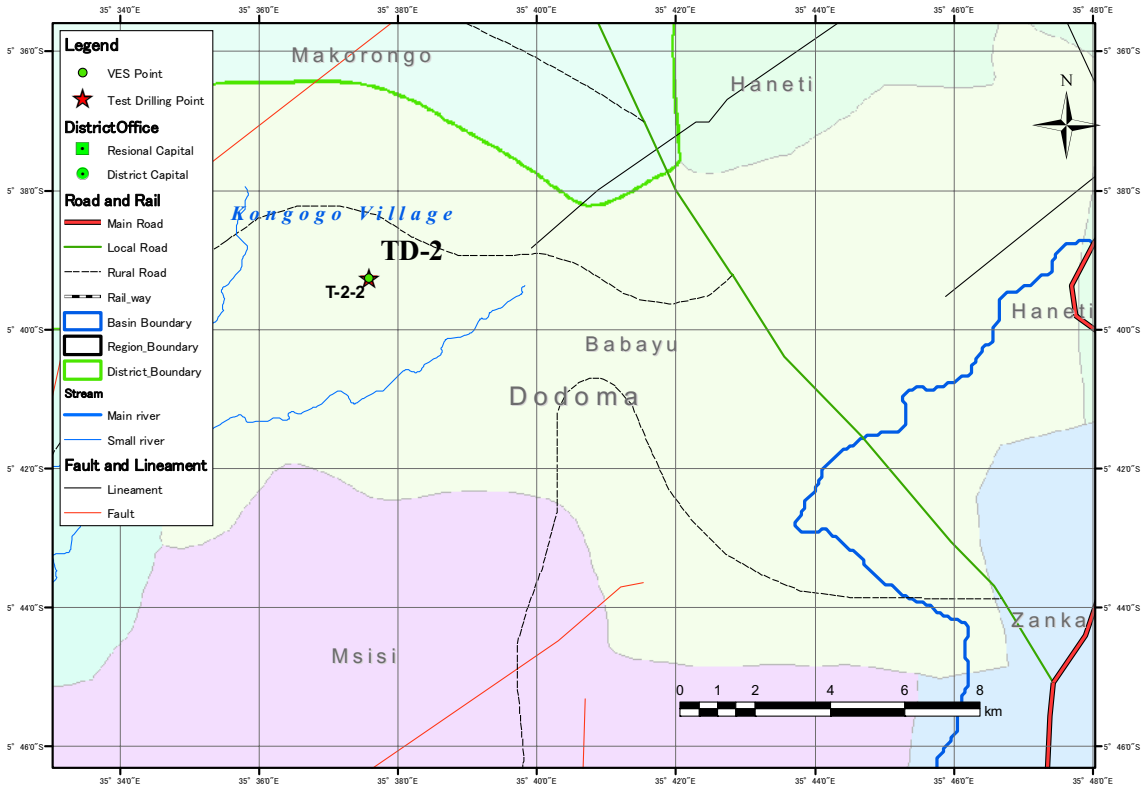

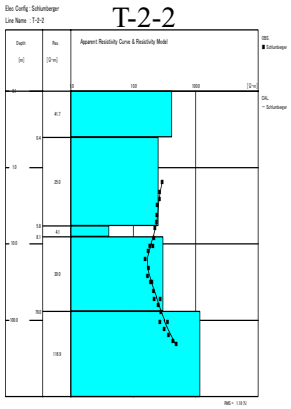

Figure 5-23 Location of Test Borehole Drilling No.2 and Survey Result

(3) Test Drilling No. 3 (Bubutole Village, Kondoa District, Dodoma Region)

This site was planned in the middle of Bubu river in the G sub-basin. This place is the bottleneck of Bubu river system which the river water gathered from upper stream is flowing through this place to the down stream. Three points of VES were conducted in this area. The results of them are almost the same. T-3-3 point was finally selected for the drilling site.

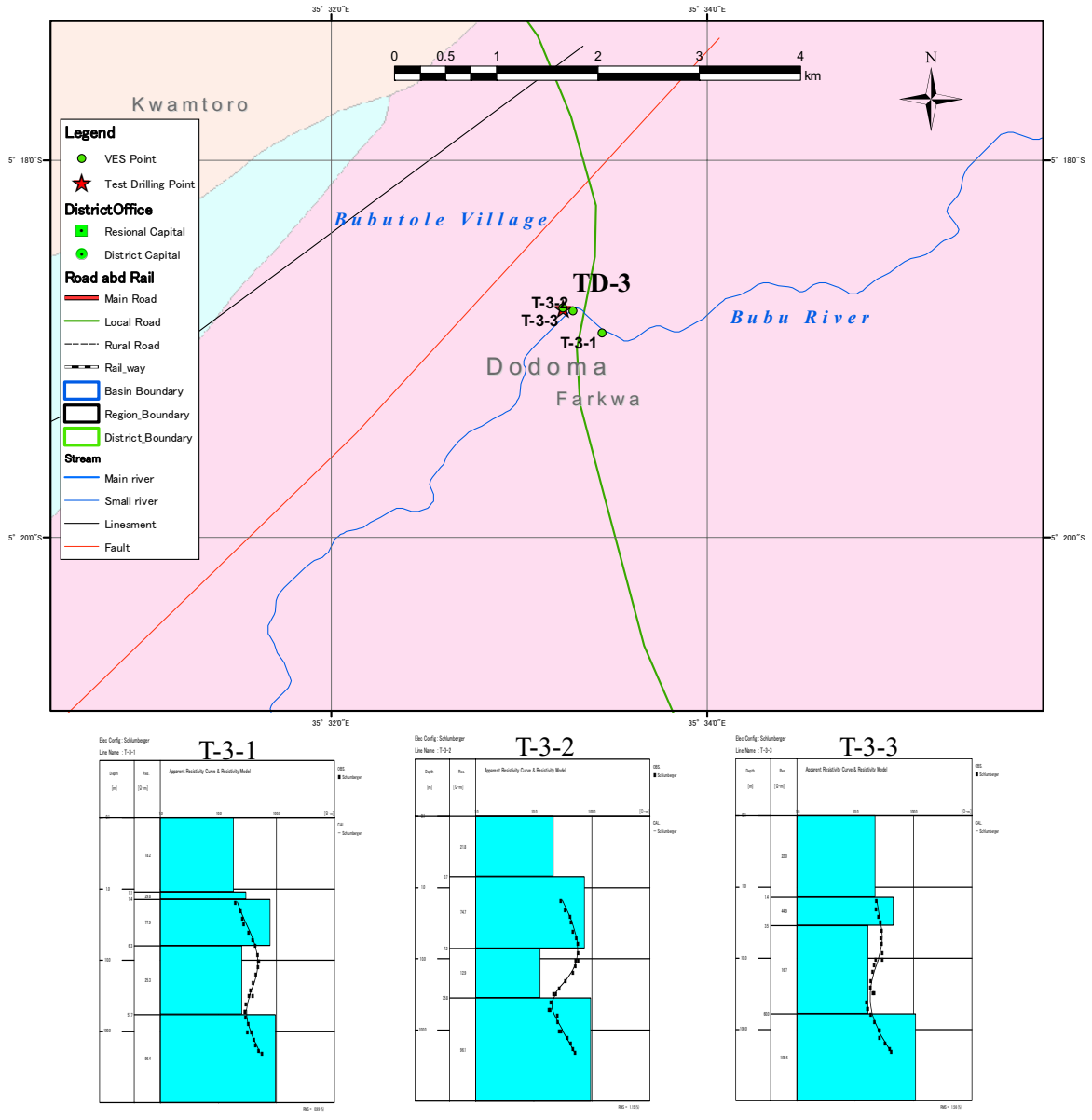

Figure 5-24 Location of Test Borehole Drilling No.3 and Survey Result

(4) Test Drilling No. 4 (Loo Village, Kondoa District, Dodoma Region)

This site was planned in the upper part in the G sub-basin. The geology of this area was assumed as metamorphic rocks. Satellite image analysis indicated existence of a fault around this area. Geophysical survey was conducted to find the fault. The results of VES show some difference among T-4-1, T-4-2 and T-4-3. The location of the fault was estimated between T-4-2 and T-4-3. After the analysis, VES were conducted additionally at T-4-4, T-4-5 and T-4-6. The location of the fault was assumed between T-4-4 and T-4-5. The drilling site was finally selected at T-4-5 based on the fault dip.

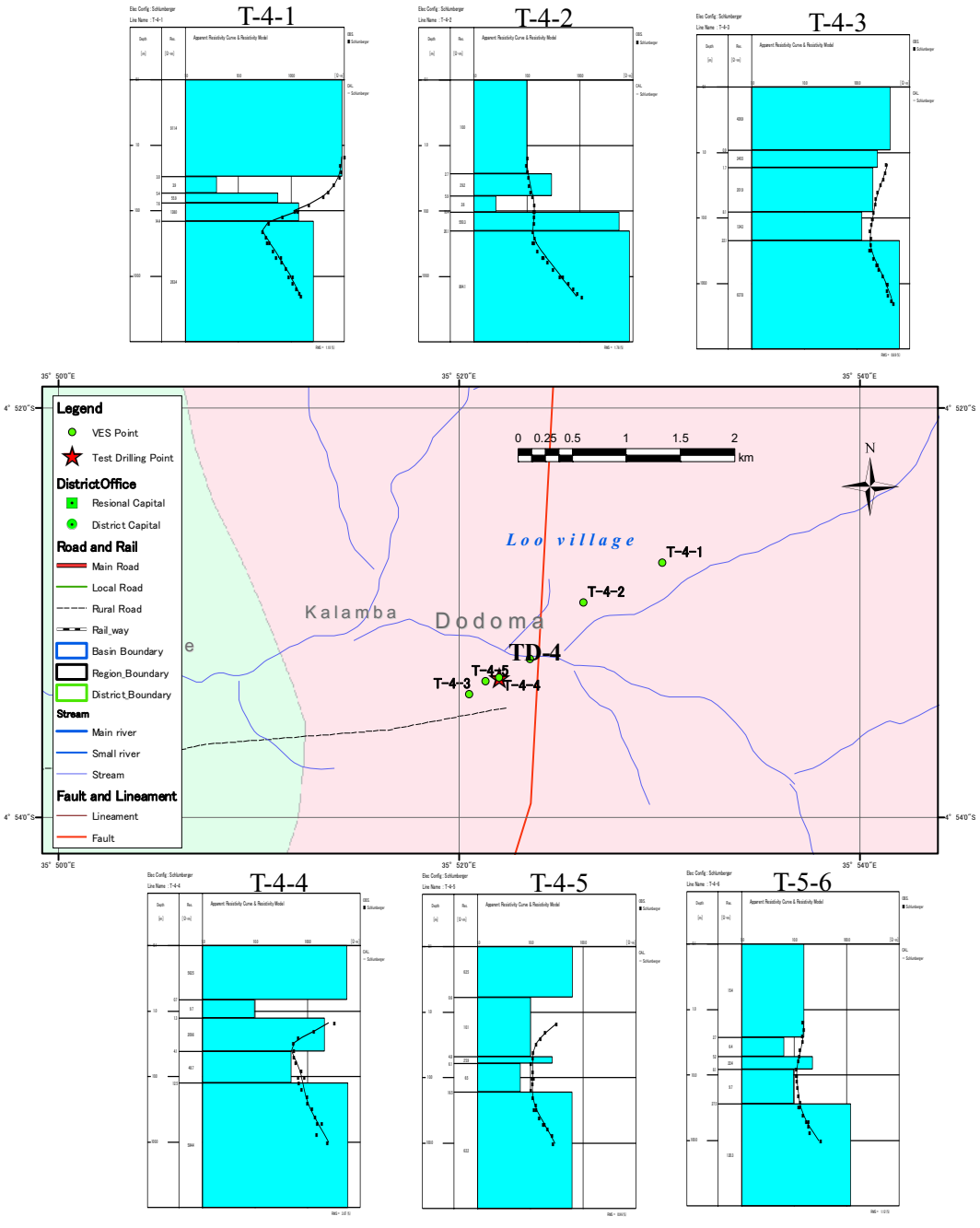

Figure 5-25 Location of the Test Borehole Drilling Site No.4 and Survey Results

(5) Test Drilling No. 5 (Nholi Village, Bahi District, Dodoma Region)

This site was planned in the Dodoman System which was the oldest formation in Tanzania. T-5-1 was located at hilly site of the Dodoman System; however, the result of VES indicated no aquifer there. Besides, the access road was very bad. T-5-2 and T-5-3 were located at the foot of the hill. Since T-5-3 has lower resistivity value in the bedrock based on the comparison between T-5-2 and T-5-3, T-5-3 was selected for the drilling site.

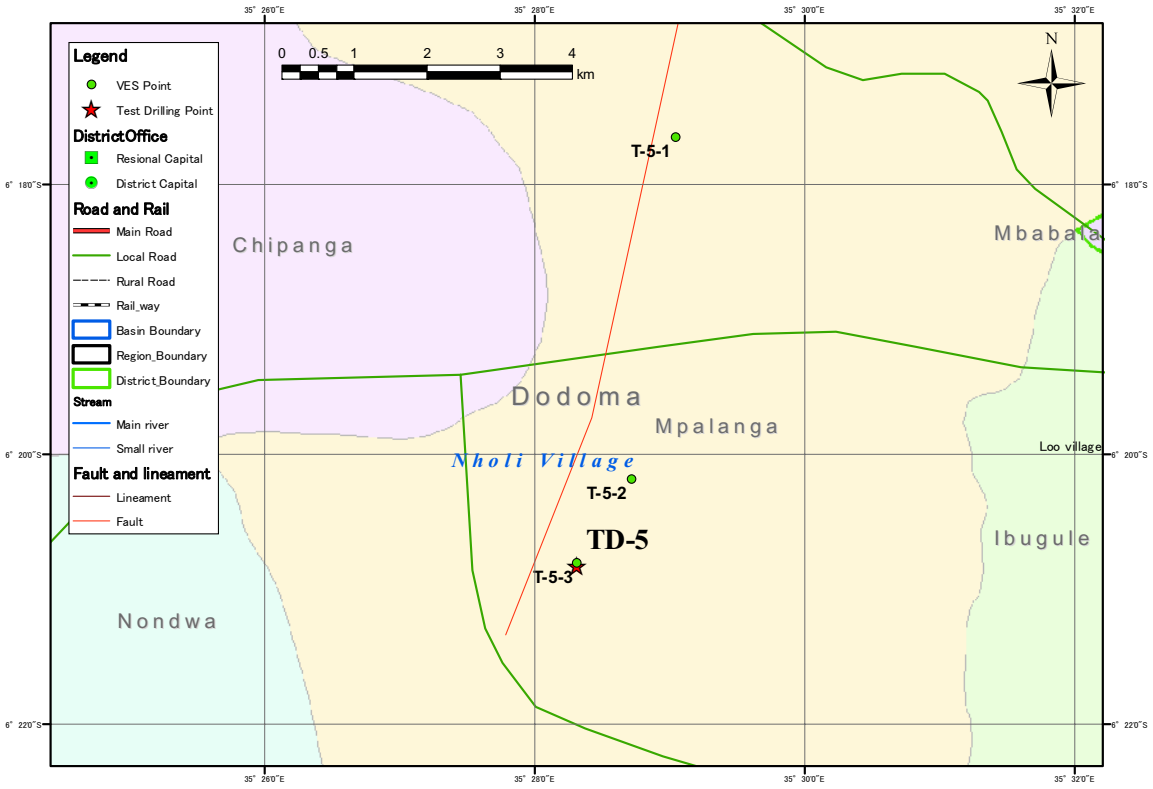

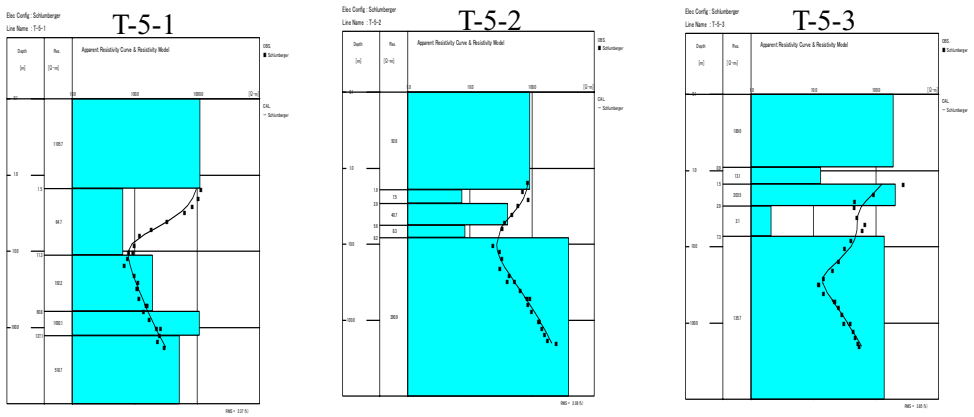

Figure 5-26 Location of Test Borehole Drilling No.5 and Survey Result

(6) Test Drilling No. 6 (Numbeta Village, Hanang District, Manyara Region)

This site was selected as volcanic rock or pyroclastic sediment area from Mt. Hanang. This area is also located upstream of the G sub-basin. T-6-1 and T-6-3 have almost the similar resistivity structure and the resistivity value of T-6-2 shows lower than other two points. Magnetic survey was conducted to determine the drilling point. Since T-6-2 has more clear magnetic anomaly which means some different type of rocks is contacted below ground, T-6-2 was selected for the drilling site.

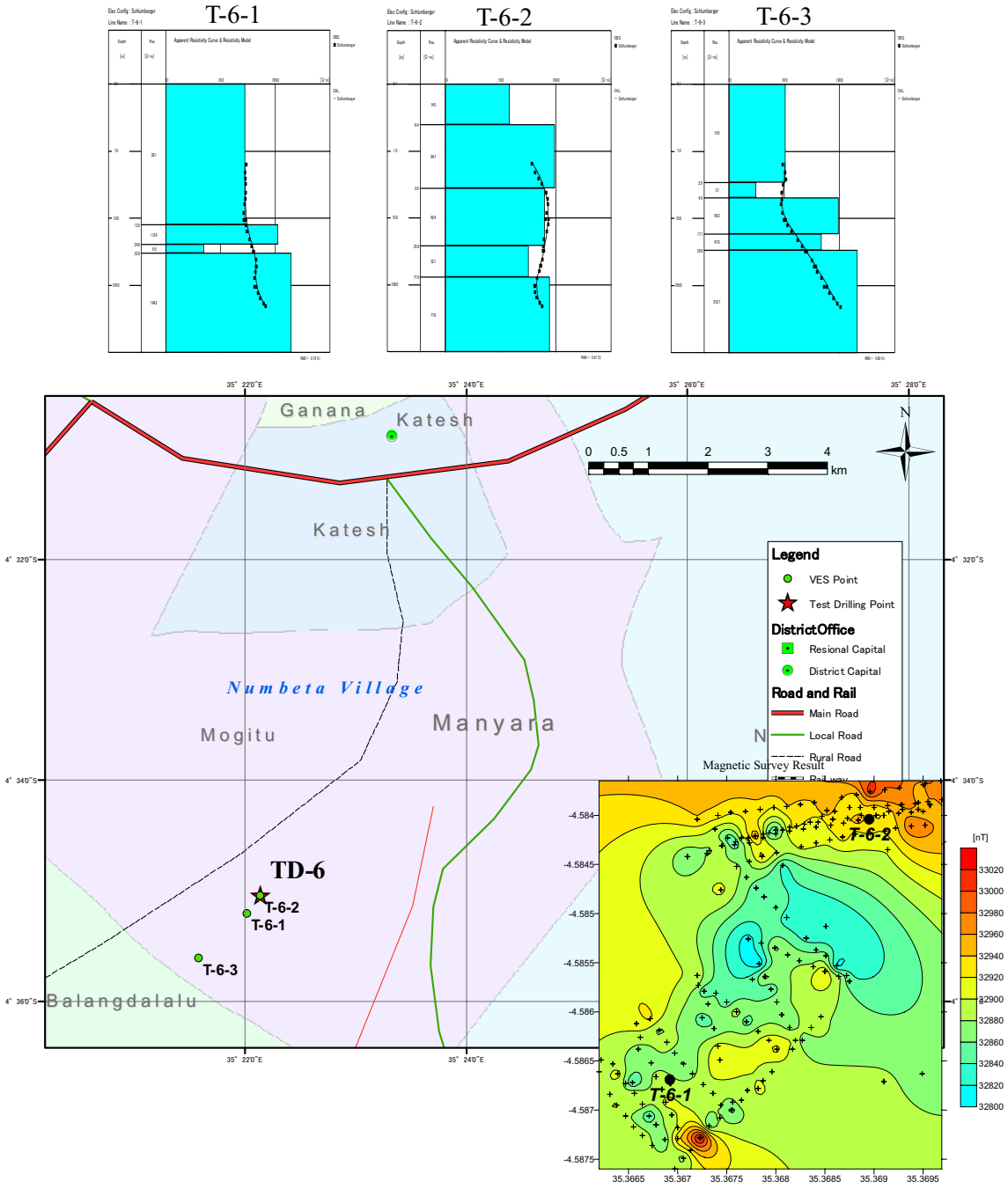

Figure 5-27 Location of Test Borehole Drilling No.6 and Survey Result

(7) Test Drilling No. 7 (Bermi/Seloto Village, Babati District, Manyara Region)

This area is located at the foot of the escarpment of the Great Rift Valley. This site was selected not only as the upstream of the G sub-basin but expected much groundwater in the fracture zone by tectonic movement. As the result of comparison between T-7-1 and T-7-2, the bedrock depth at T-7-1 is shallower than T-7-2. Since magnetic anomaly was found around T-7-2 by the magnetic survey, T-7-2 was selected for the test borehole drilling site.

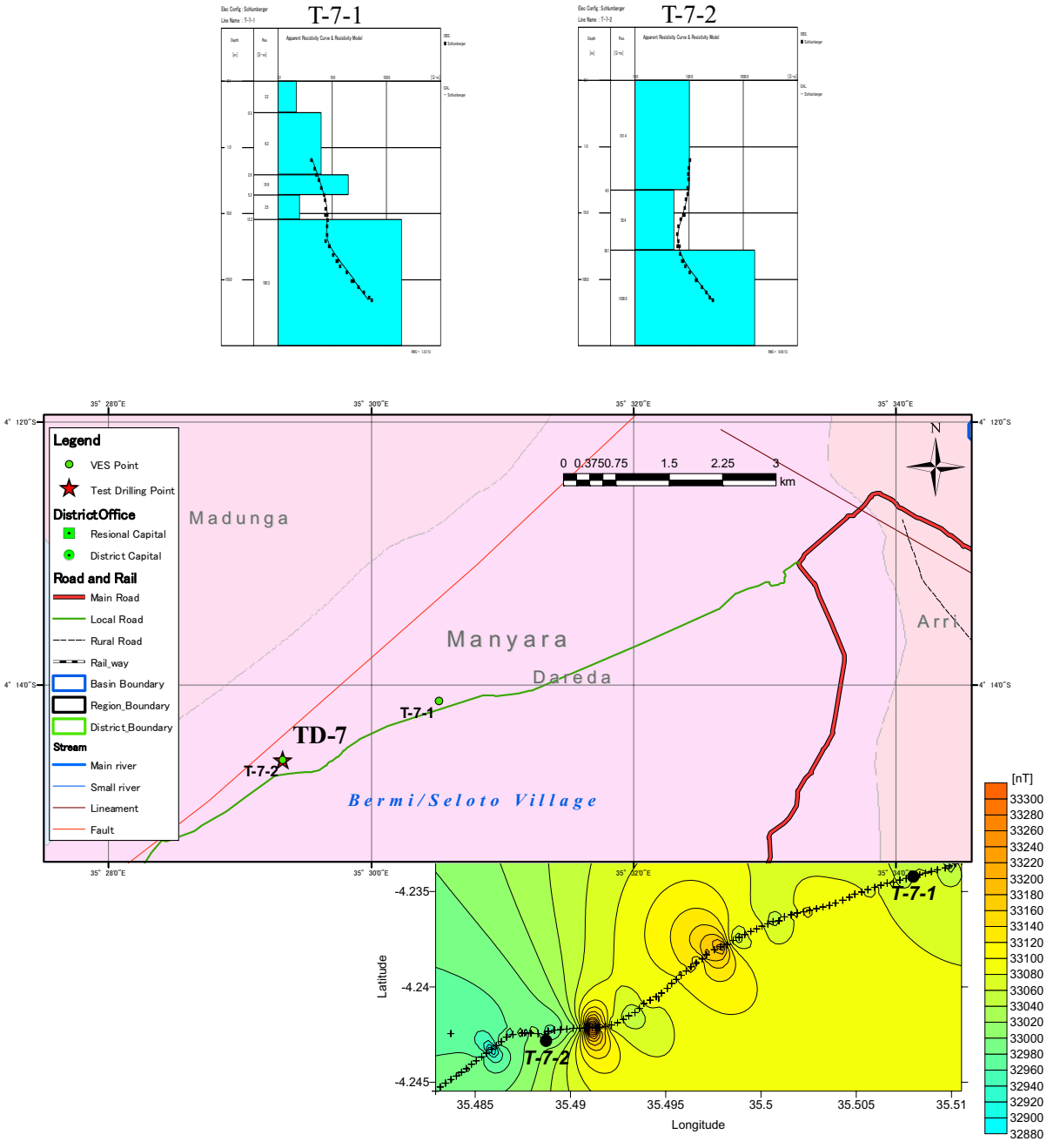

Figure 5-28 Location of Test Borehole Drilling No.7 and Survey Result

(8) Test Drilling No. 8 (Ikasi Village, Manyoni District, Singida Region)

This site is located in the downmost area of the G sub-basin. The Bahi swamp whose water is much salty is lying beside the site. The southwest of the area is facing to the escarpment of the Rift Valley. The result of VES of T-8-1 shows very low resistivity from Gl-10m to the deeper part. As for T-8-2, the resistivity structure has slightly high resistivity layer in the deeper part. They were expected that the fresh water would be gotten; however, the drilling site was shifted to the site 2 km apart from T-8-2 because of accessibility problem. The drilling site was finally selected by topographic feature etc.

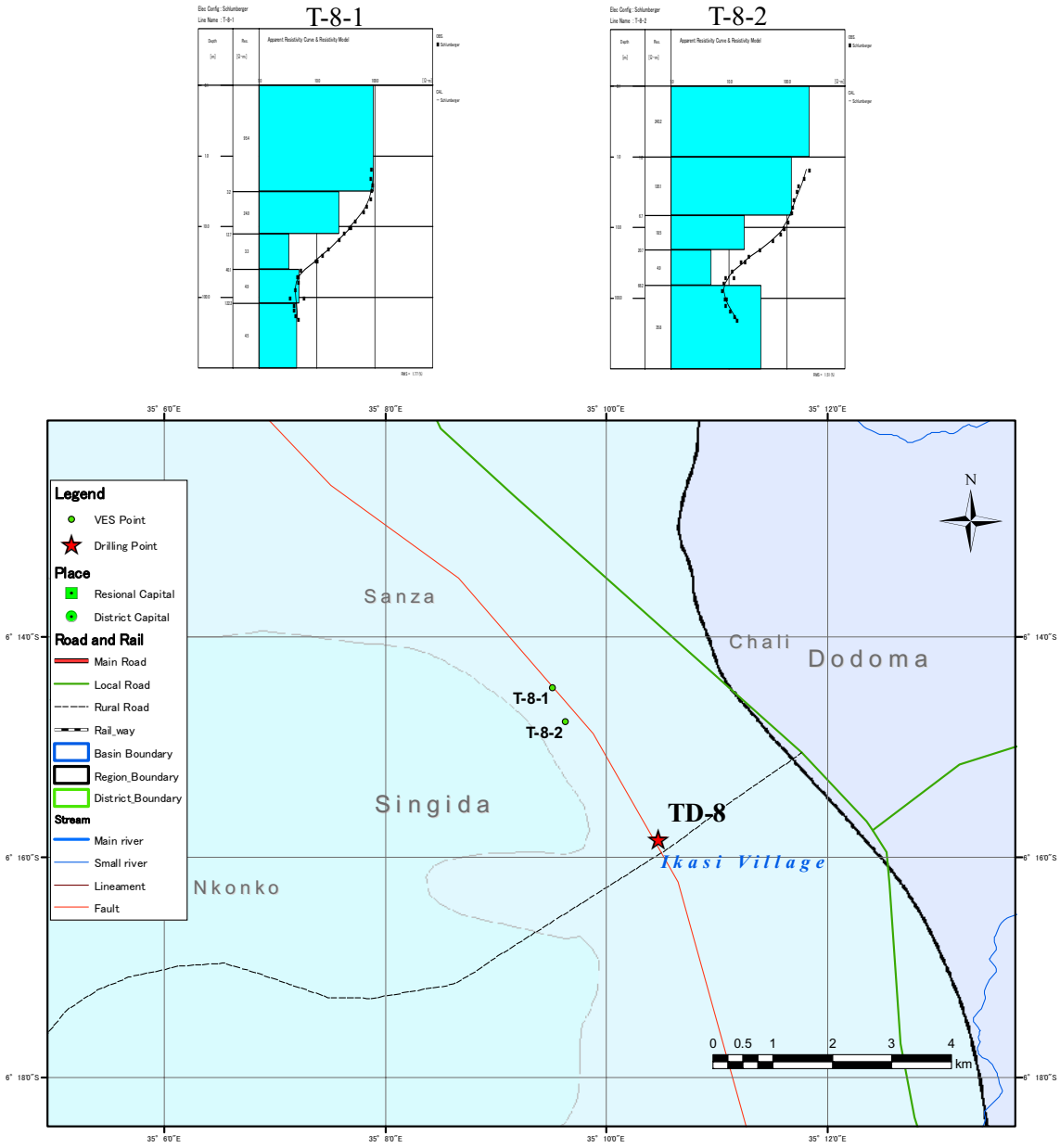

Figure 5-29 Location of Test Borehole Drilling No.8 and Survey Result

(9) Test Drilling No. 9 (Ilalo Village, Manyoni District, Singida Region)

The western escarpment of the Gregory Rift Valley is running through the eastern side of this area; however, the topographic feature of this is unclear than the eastern escarpment. Test drilling site No.9 was selected around the western escarpment to check the possibility of groundwater development near the rift fault. The result of VES at T-9-2 shows very high resistivity. This high resistivtiy was assumed as granite which had no fissure. T-9-1 was expected as the place where was located near the fault zone because of the low resistivity. Finally, the drilling site was shifted to the south of T-9-1 because of accessibility for drilling rig, where has the same topographic feature of T-9-1.

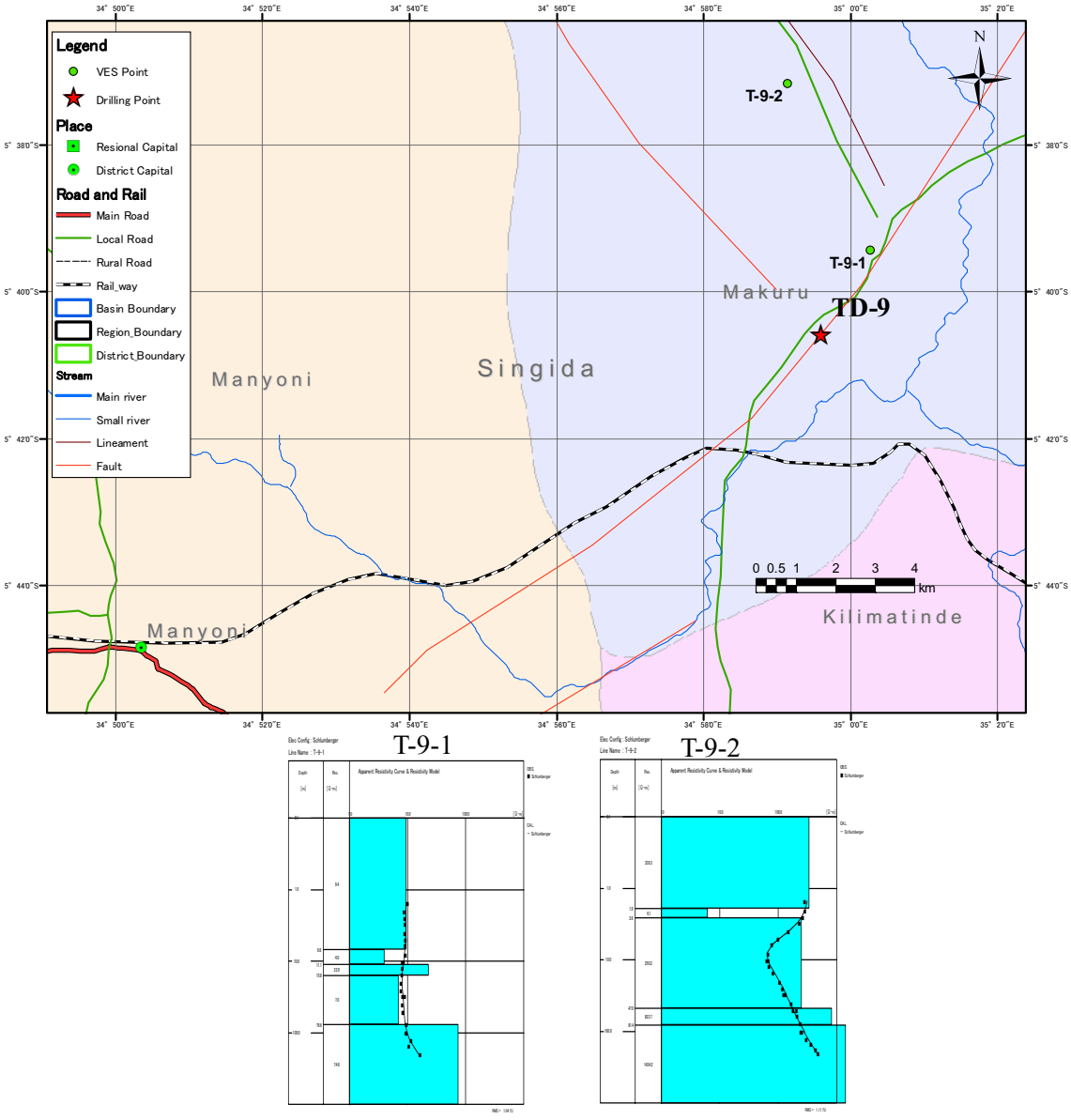

Figure 5-30 Location of Test Borehole Drilling No.9 and Survey Result

(10) Test Drilling No. 10 (Hirbadaw Village, Hanang District, Manyara Region)

This area is located in the middle of the A sub-basin. The geology of the area was expected to be the Nyanzian System and an existence of fault was presumed in the area base on the satellite image analysis. T-10-1 and T-10-2 belong to the Nyanzian System with high resistivity and the soft-sediment area with low resistivity respectively. On the other hand, a fracture zone caused by the fault was expected at T-10-3. Two-dimensional resistivity survey was conducted along the measurement line which cut across this fault. The fault could be apparently detected around T-10-3 by the survey as shown in Figure 2-30. Therefore, T-10-3 was selected for the drilling site.

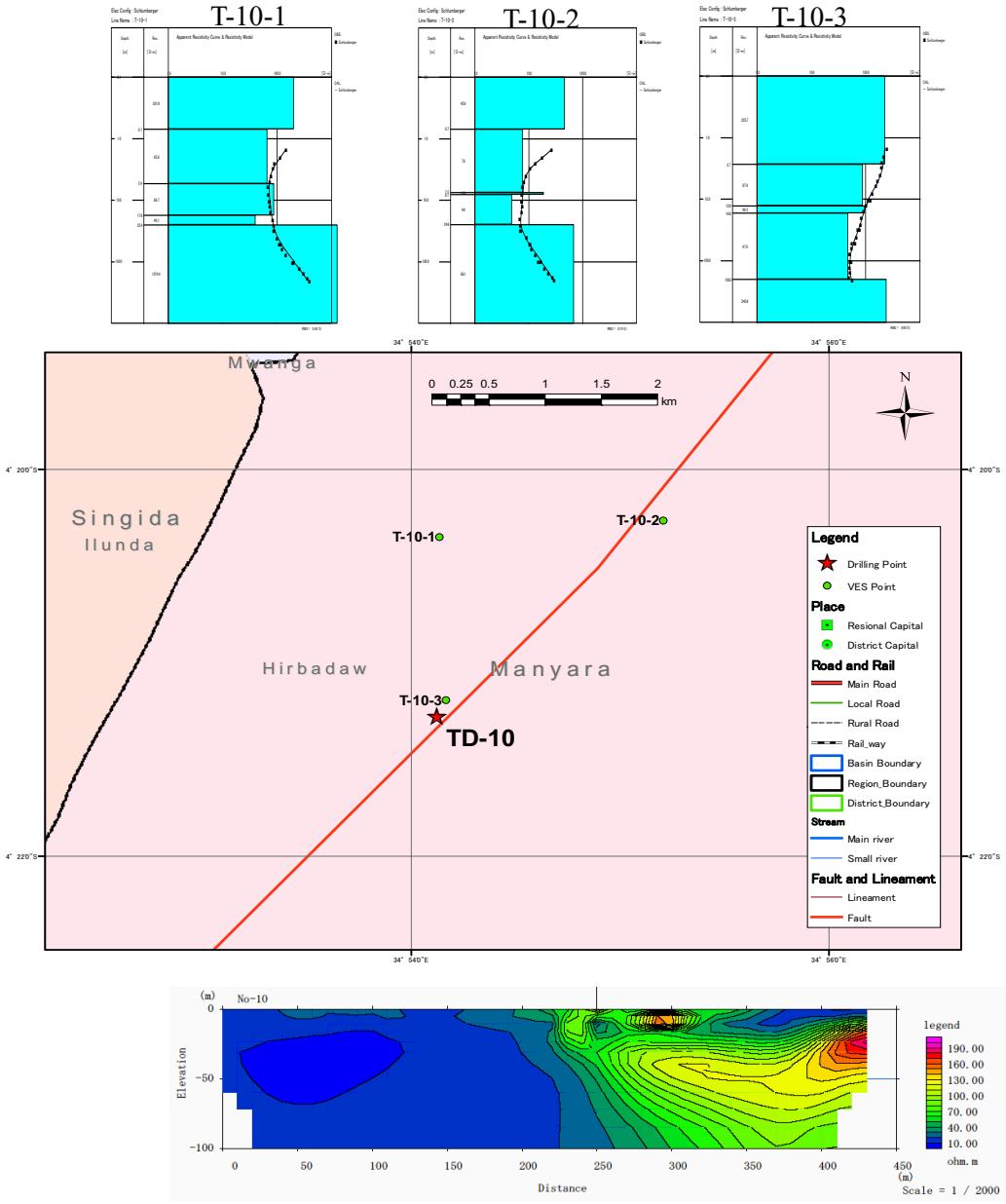

Figure 5-31 Location of Test Borehole Drilling No.10 and Survey

(11) Test Drilling No. 11 (Tlawi Village, Mbulu District, Manyara Region)

This area was selected as an upstream of the A sub-basin. The geology of the area is regarded as metamorphic rock area. Each VES could detect the bedrock with high resistivity. The bedrock of T-11-1 and T-11-2 sites was shallow around 10 m depth. T-11-3 and T-11-4 showed almost the same resistivity structure. T-11-3 had a low resistivity layer in the range from 20 m to 30 m which was probably a fracture zone. Based on magnetic survey results around T-11-3, the result some anomaly was detected in the northern side of T-11-3. Since this anomaly was assumed to be fault, T-11-3 was finally selected as the drilling site.

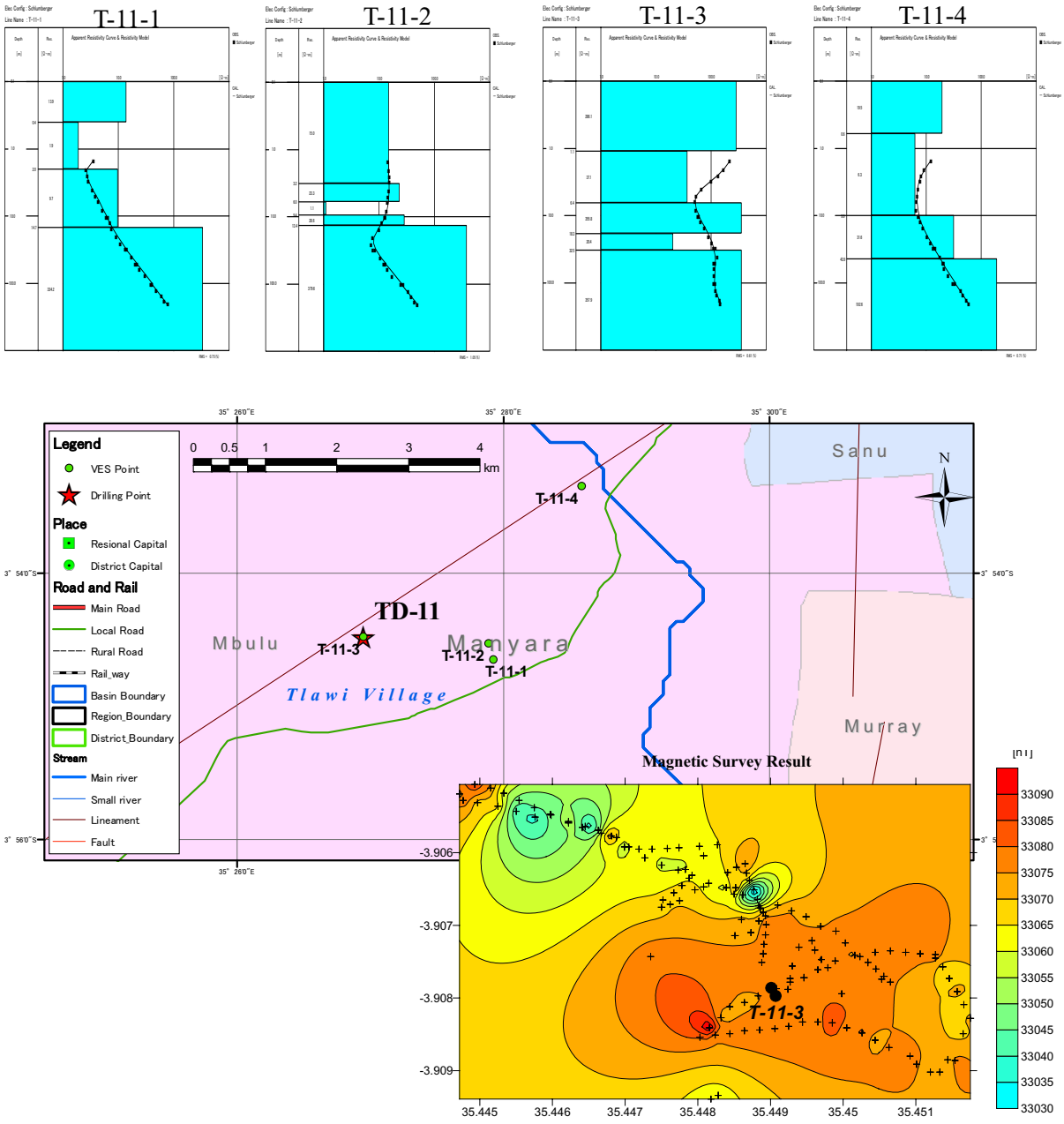

Figure 5-32 Location of Test Borehole Drilling No.11 and Survey Results

(12) Test Drilling No. 12 (Misingi Village, Iramba District, Singida Region)

This area was selected as the middle part of the A sub-basin. The geology of the area belongs to Nyanzian System. The existence of faults was presumed in the area based on the satellite image analysis. The result of VES at T-12-1 showed higher resistivity than T-12-2 and T-12-3. T-12-1 was regarded as Nyanzian bedrock area. On the other hand, T-12-2 and T-12-3 was regarded as soft-sediment area. Two-dimensional resistivity survey was conducted around T-12-1 area and detected a low resistivity zone on the end of the measurement line. The drilling site was finally determined in the low resistivity zone in consideration of the topographic feature and accessibility.

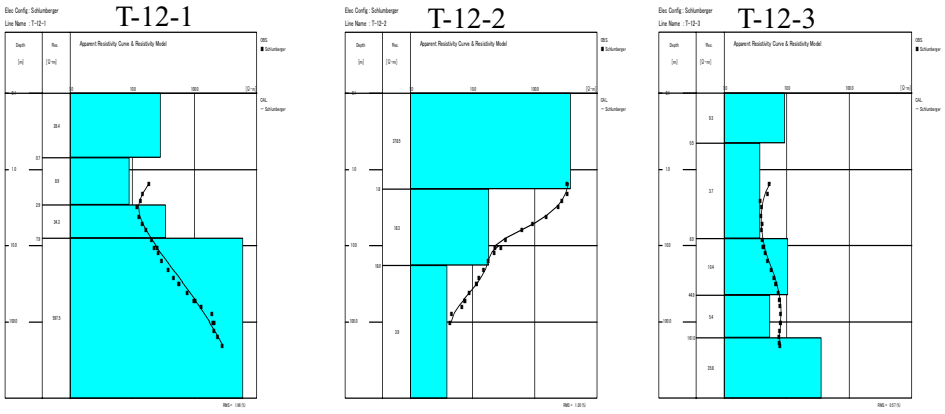

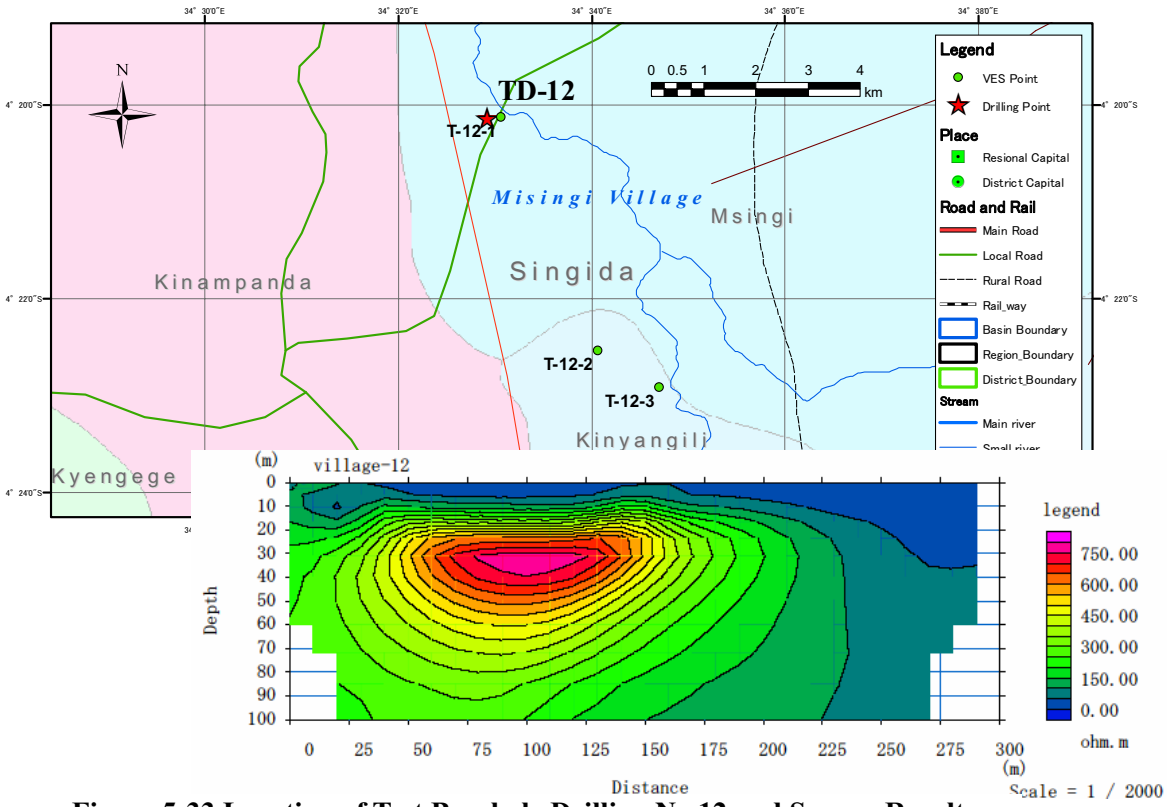

Figure 5-33 Location of Test Borehole Drilling No.12 and Survey Result

(13) Test Drilling No. 13 (Sepuka Village, Singida Rural District, Singida Region)

This area was selected as the typical granite area. Each result of VES showed very high resistivity from shallow to deep part. Magnetic survey was conducted along the road in this area. Although magnetic anomaly was detected slight near the start point of the measurement line, the point was selected as the drilling point.

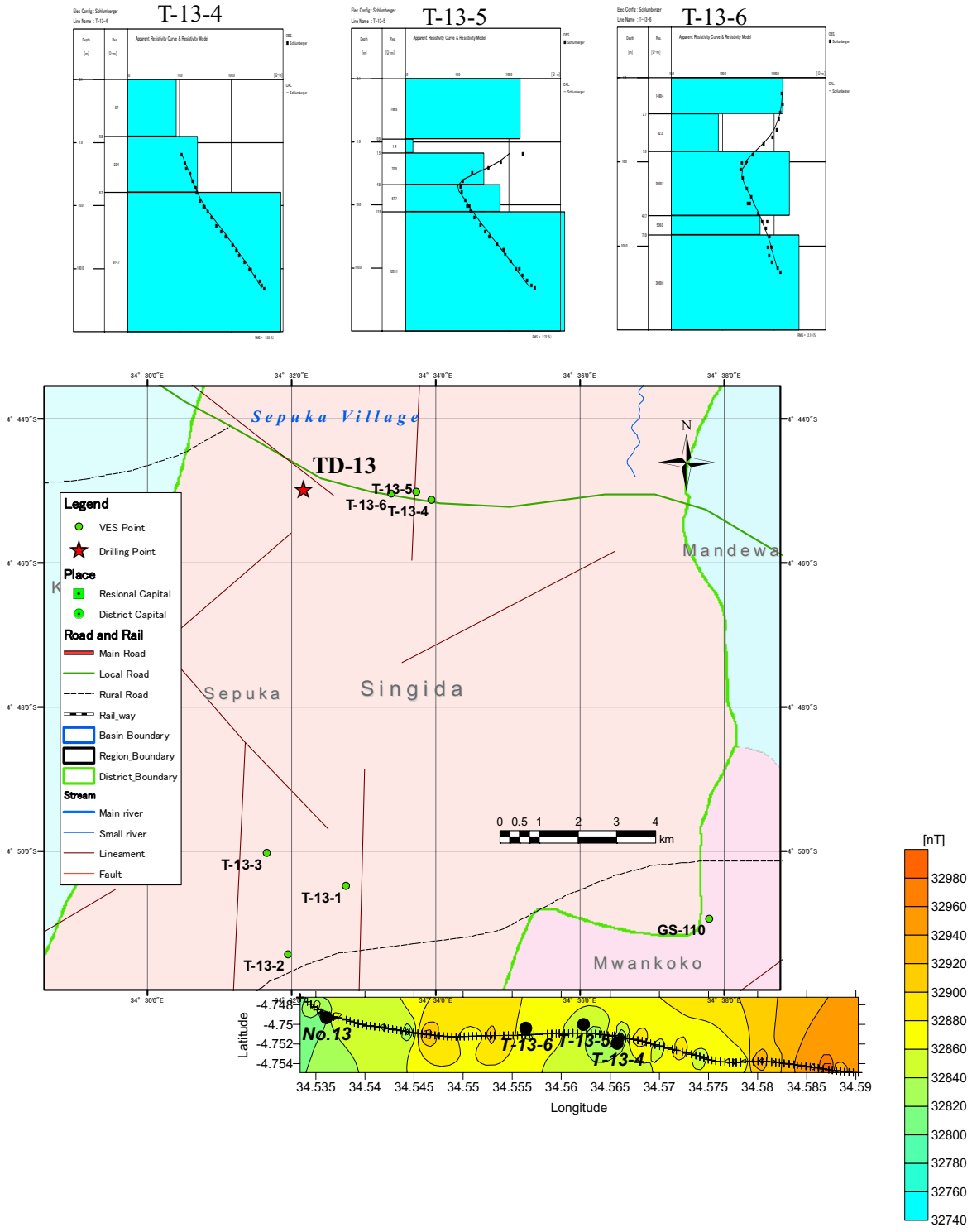

Figure 5-34 Location of Test Borehole Drilling No.13 and Survey Results

(14) Test Drilling No. 14 (Igogo Village, Igunga District, Tabora Region)

This area is located in the soft-sediment area in the A sub-basin. Hill of banded iron-rock of Nyanzian System is distributed around the area. T-14-1 was just located in the foot of the hill of banded iron-rock and T-14-2 was located in the soft-sediment area about 500m apart from the hill. T-14-2 was selected to confirm the dip angle of the hill into underground. Based on the result of VES, the angle was approximately 6 degree.

It was presumed that the soft-sediment area had very low resistivity and the banded Iron-rock had slightly higher resistivity than it. T-12-2 was selected for the test borehole drilling site whose weathered zone over the bedrock or sandy layer in the soft-sediment was expected as aquifer.

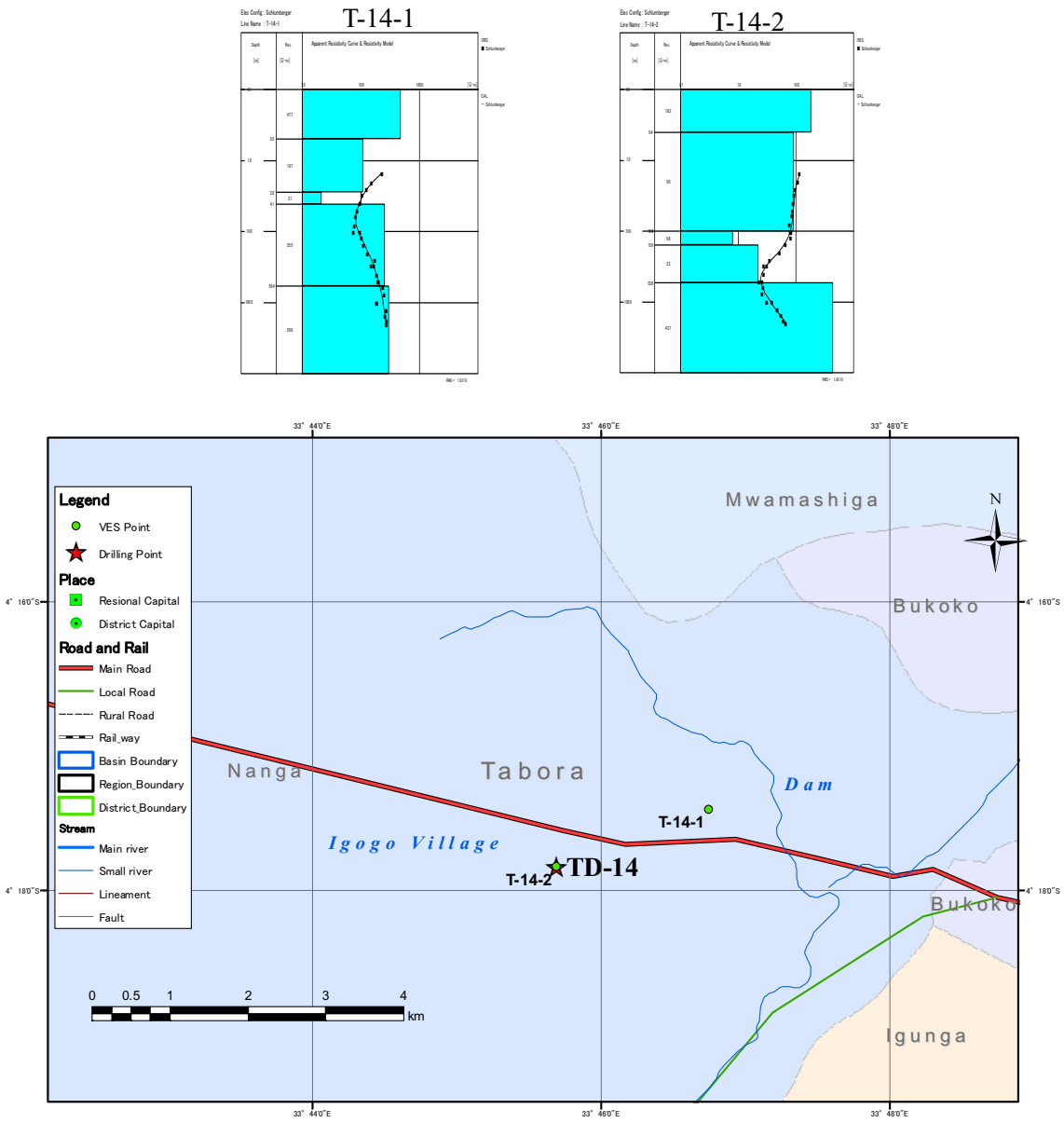

Figure 5-35 Location of Test Borehole Drilling Site No.14 and Survey Results

(15) Test Drilling No. 15 (Nkongwa Village, Uyui District, Tabora Region)

This area was probably located in the boundary zone between granite area and soft-sediment area. Based on the VES, three survey points have almost the same resistivity structure. The weathered zone over the bedrock was expected as an aquifer. Since the resistivity of weathered zone at T-15-2 showed the lowest value of them, T-15-2 was selected as the drilling point.

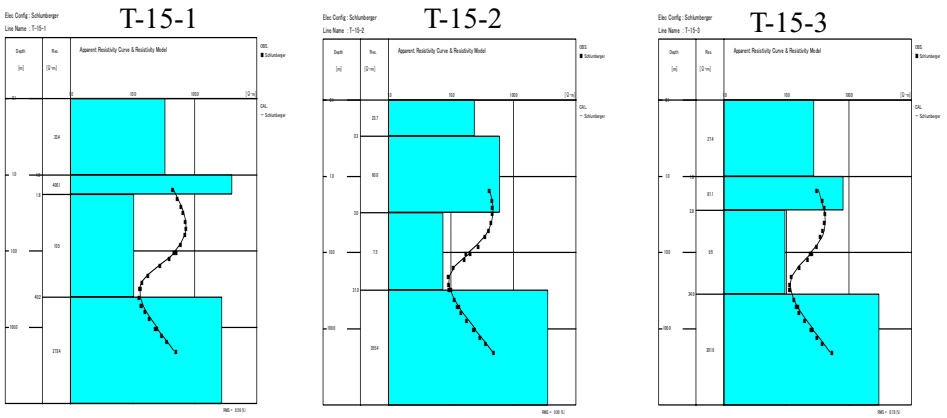

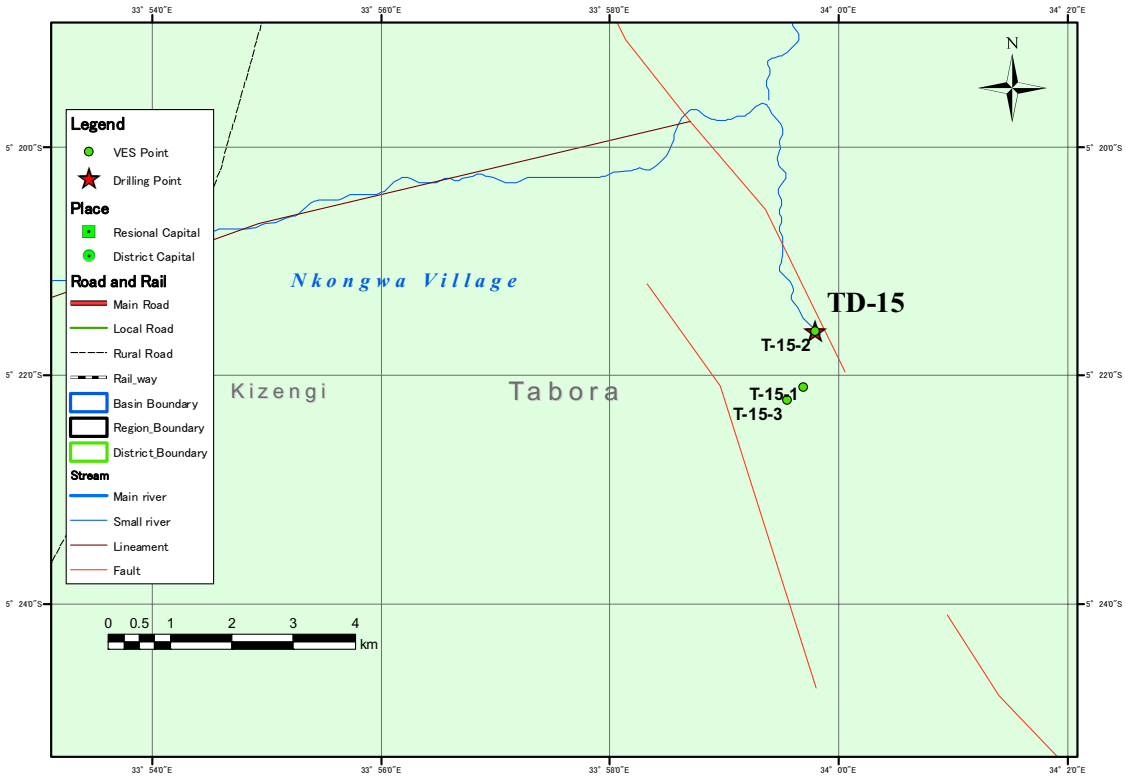

Figure 5-36 Location of Test Borehole Drilling No.15 and Survey Results

(16) Test Drilling No. 16 (Kininginila Village, Igunga District, Tabora Region)

This area was selected as the downmost of the A sub-basin. It was estimated that the very thick soft-sedimentary layer was distributed in this area. The result of VES showed that the low resistivity layer continued to 200 m depth (exploration depth). This implies that the bedrock is lying deeper than 200m.

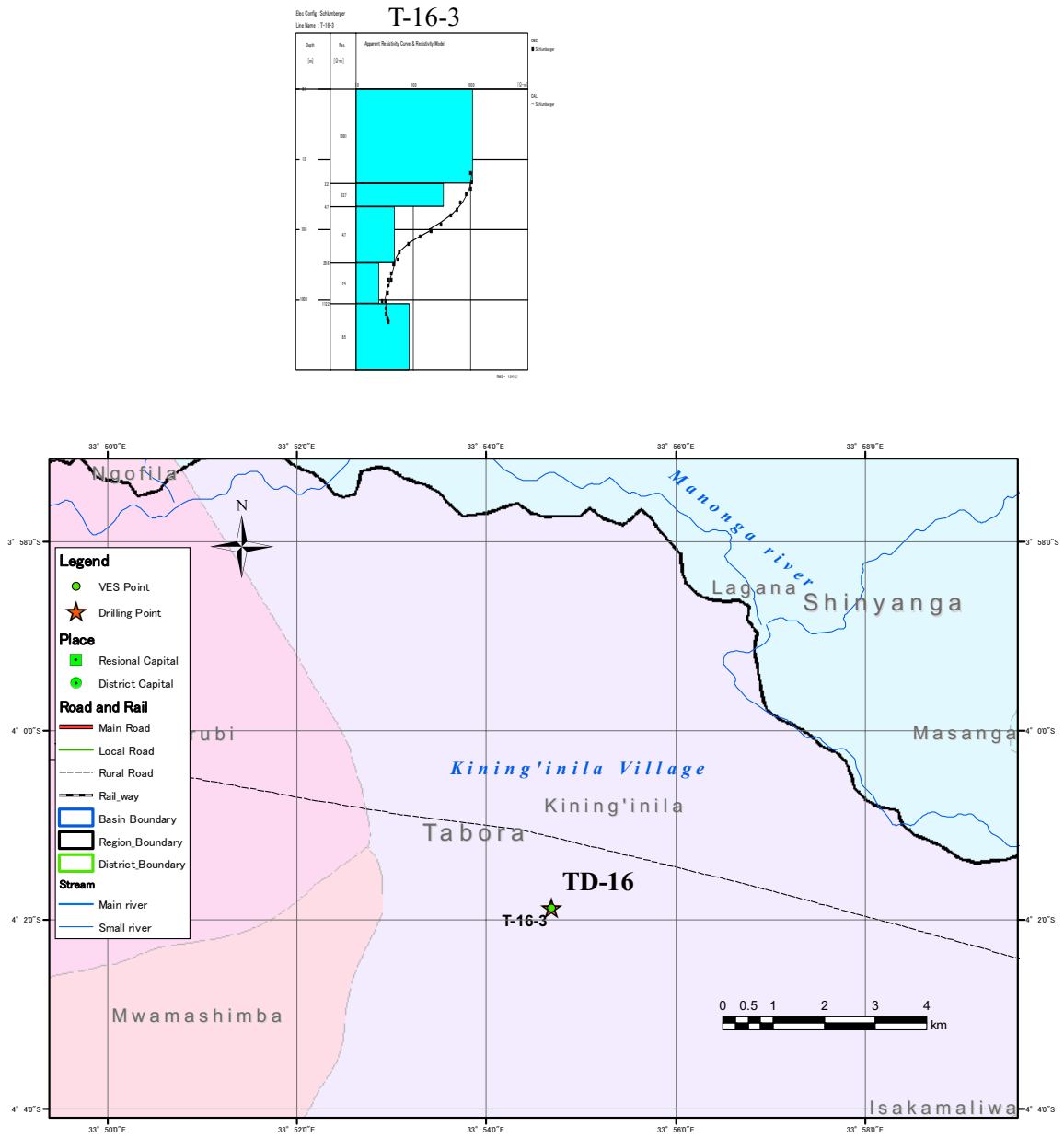

Figure 5-37 Location of Test Borehole Drilling No.16 and Survey Results

(17) Test Drilling No. 17 (Mapea Village, Babati District, Manyara Region)

This area was selected as downstream of the D sub-basin. Soft-sedimentary layer is distributed widely in this area. Since the results of VES showed very low resistivity, it was assumed that the groundwater was much salty. T-17-4 was located the upper than T-17-1, T-17-2 and T-17-3 in order to avoid very thick sedimentary layer. Although the result of the magnetic survey around T-17-4 could not detect clear anomaly, T-17-4 was finally selected as the drilling point.

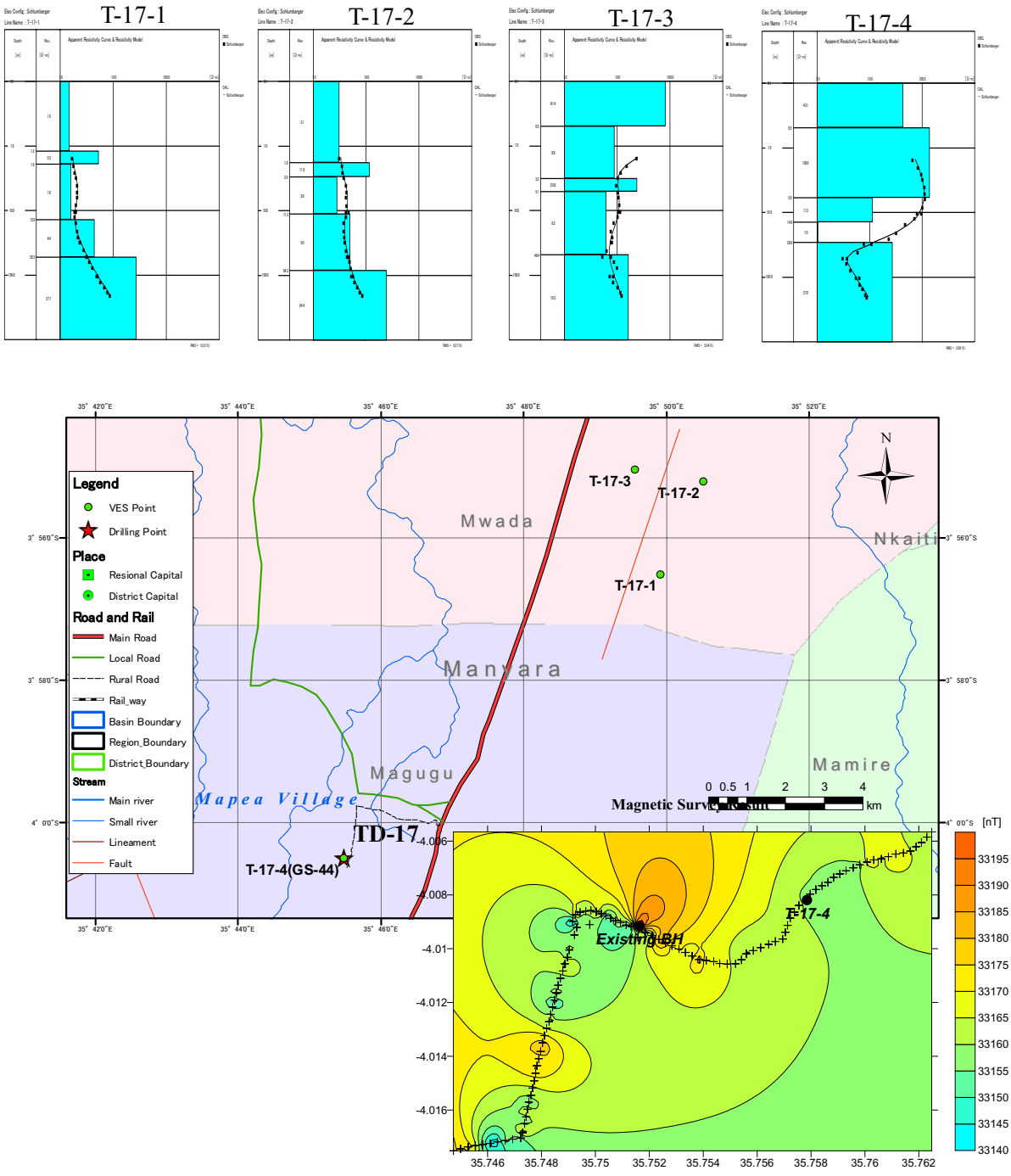

Figure 5-38 Location of Test Borehole Drilling No.17 and Survey Result

(18) Test Drilling No. 18 (Masange Village, Kondoa District, Dodoma Region)

This area was selected as the upstream of the D sub-basin. Gneiss of the Mozambique Metamorphic Belt is distributed as bedrock in the area. Bedrock depth of T-18-1 was estimated deeper than which was estimated by the others based on the result of VES. Since magnetic anomaly was detected around T-18-3, it was determined finally as the drilling point.

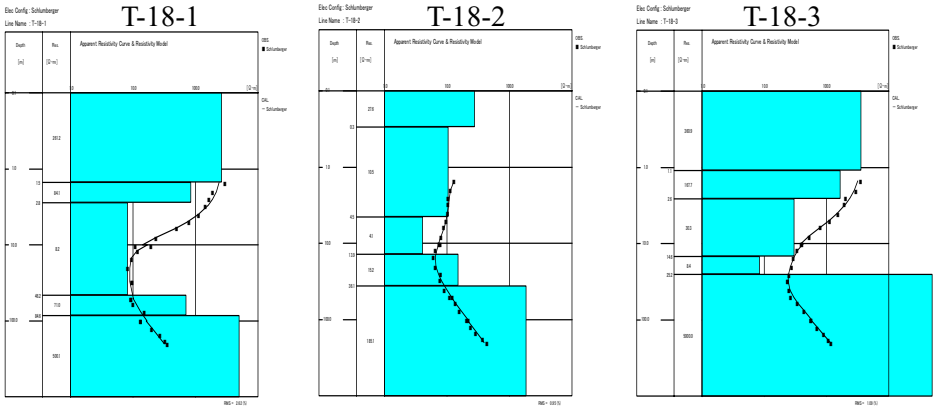

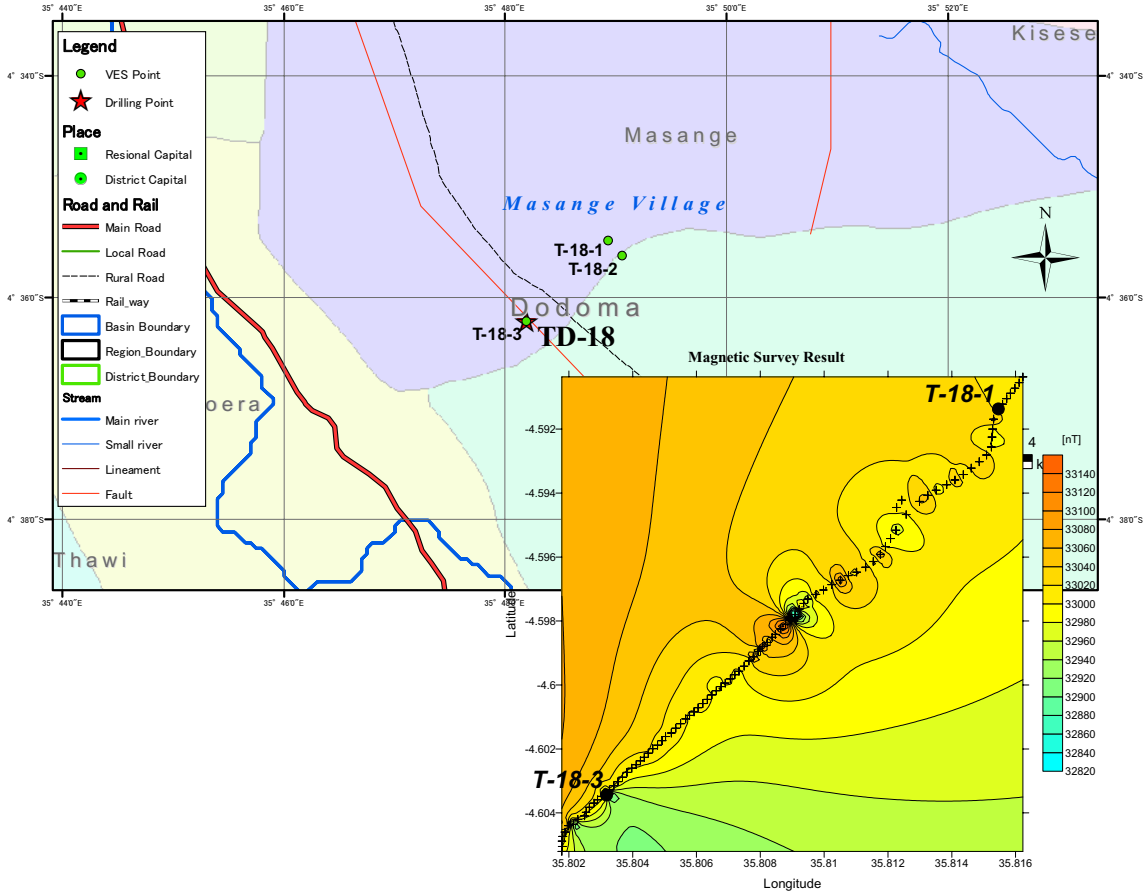

Figure 5-39 Location of Test Borehole Drilling No.18 and Survey Result

(19) Test Drilling No. 19 (Makame Village, Kiteto District, Manyara Region)

This area was selected for the downstream of the C sub-basin. The groundwater in this area was assumed salty based on the existing borehole data. VESs were conducted at the sites where the bedrock was shallower along hilly side (T-19-1) and the soft-sedimentary layer (T-19-2). T-19-2 was finally selected because of its relatively better accessibility. This area was selected as the downstream of the A sub-basin. This site was selected in order to detect the continuity of aquifer in the soft-sediment area by comparison with the drilling site No. 16. The results of VES indicate that the soft-sedimentary layer is thick and the bedrock is lying at 120 m depth.

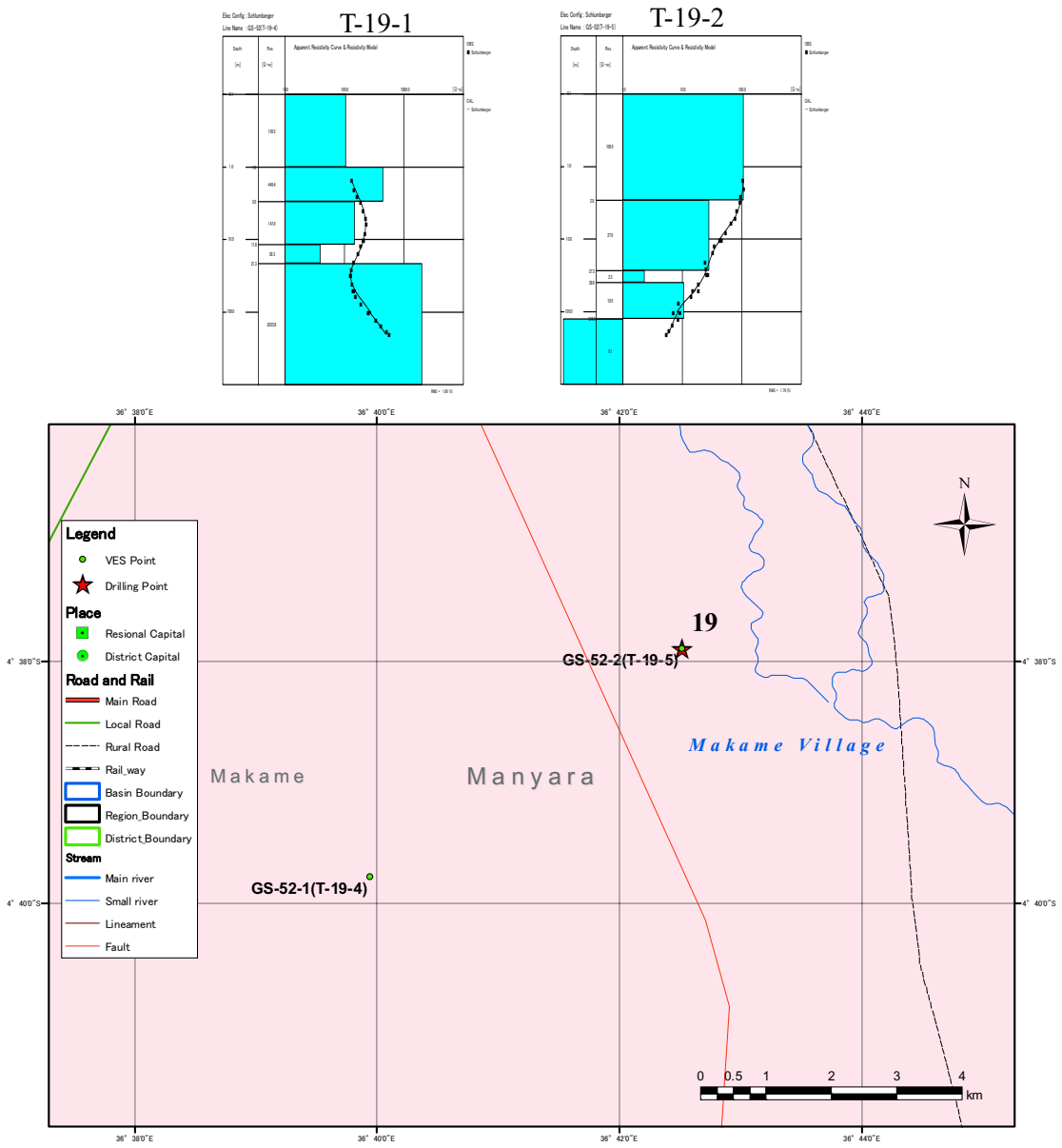

Figure 5-40 Location of Test Borehole Drilling No.19 and Survey Result

(20) Test Drilling No. 20 (Ngofila Village, Kishapu District, Shinyanga Region)

This area was selected as the downstream of the A sub-basin. This site was selected in order to detect the continuity of aquifer in the soft-sediment area by comparison with the drilling site No. 16. The results of VES indicate that the soft-sedimentary layer is thick and the bedrock is lying at 120 m depth.

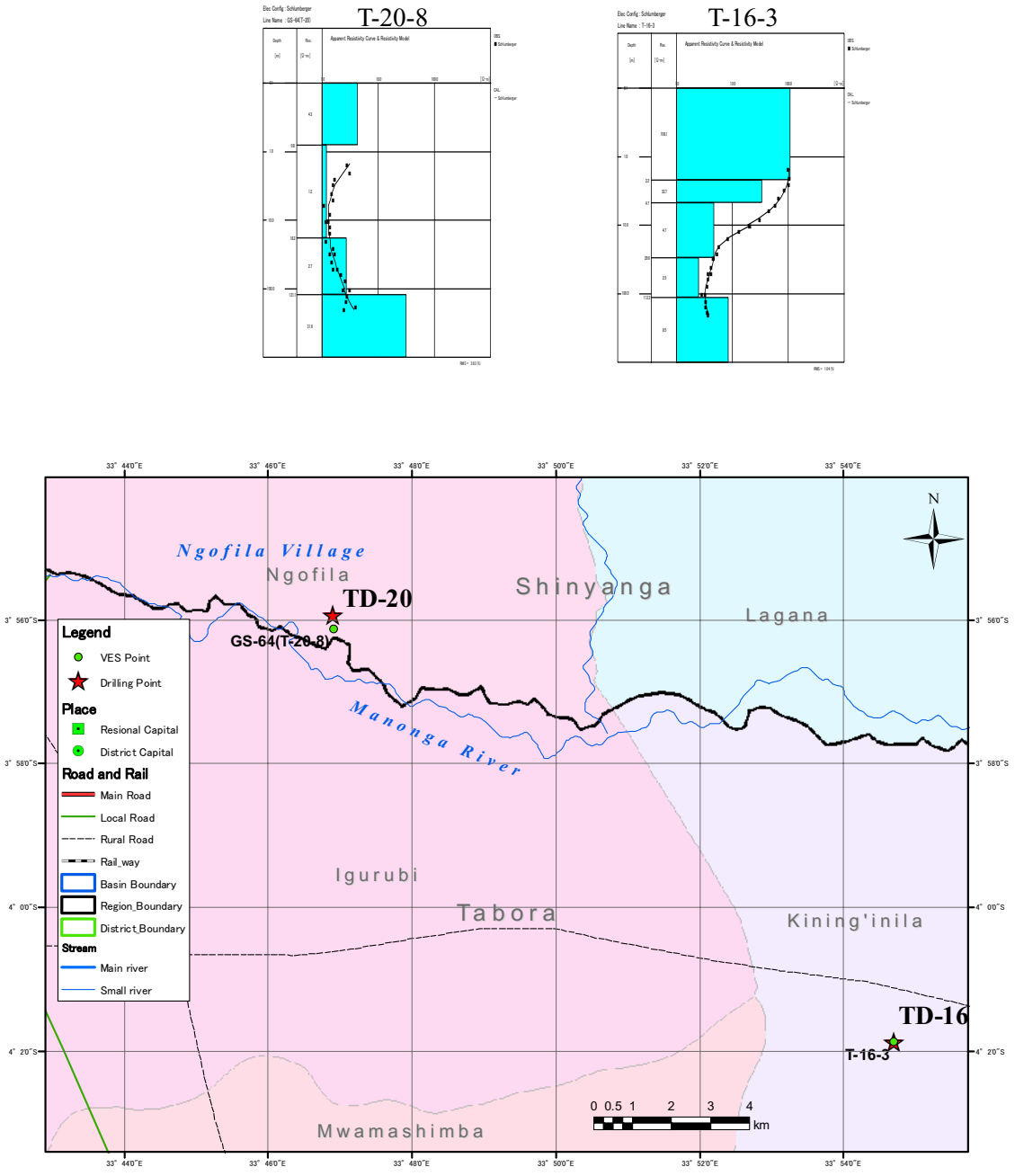

Figure 5-41 Location of Test Borehole Drilling No.20 and Survey Result

(21) Test Drilling No. 21 (Mwasayi Village, Maswa District, Shinyanga Region)

This area was selected as a granite area in north-west side of the A sub- basin. Any lineaments were not recognized by Satellite Image analysis in this area. And, this area has very few deep well information. Therefore, in order to know the hydrogeological condition in this area, this site was selected for test borehole drilling. VESs were conducted at the sites where the small river is flowing. First and second VES points (T-21-1 and T-21-2) show high resistivity from shallower part. In the magnetic survey result, small anomaly was appeared at the south-east of T-21-1. Third VES point (T-21-3) was selected by the magnetic survey result. In the VES result of T-21-3, low resistivity layer is lain deeper than the other points . Therefore, the drilling point was selected at T-21-3.

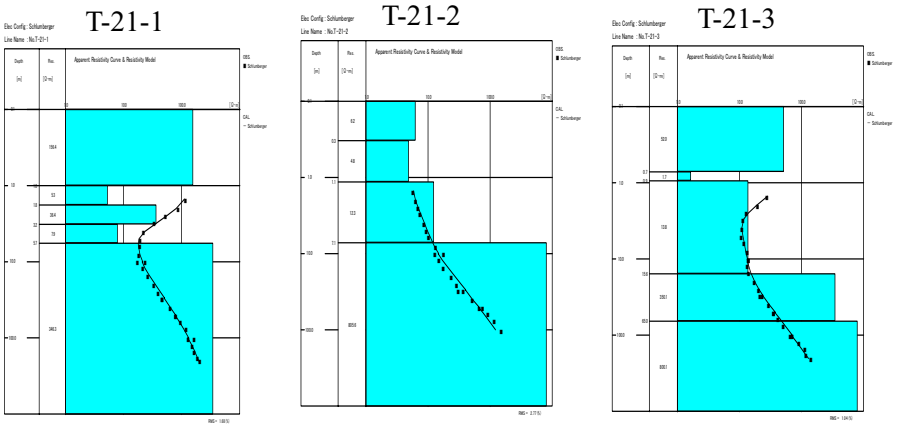

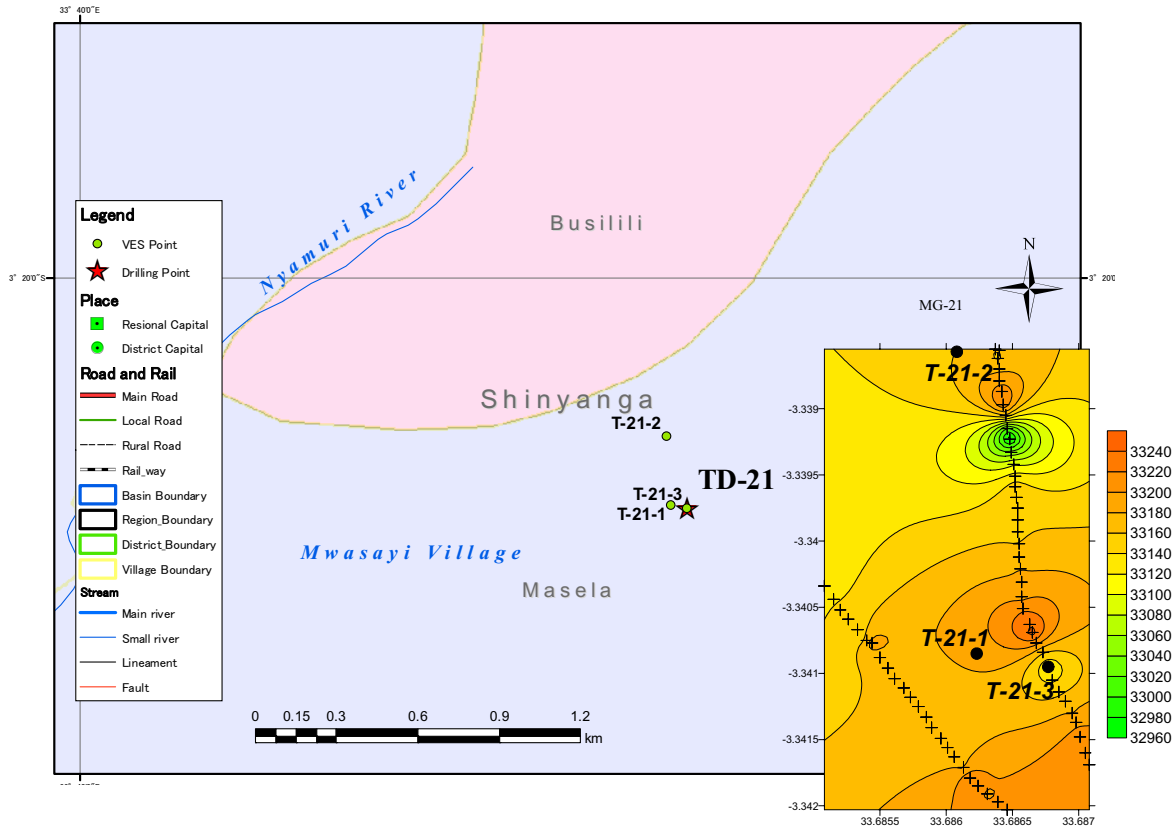

Figure 5-42 Location of Test Borehole Drilling No.21 and Survey Result

(22) Test Drilling No. 22 (Mwangudo Village, Meatu District, Shinyanga Region)

Typical granite area was selected for the test borehole drilling site in northern part of A sub-basin. This area has no existing borehole data. In order to know the hydrogeological information, this site was selected. VES results show very high resistivity granite zone. Drilling point was selected by low anomaly of magnetic survey result and its accessibility.

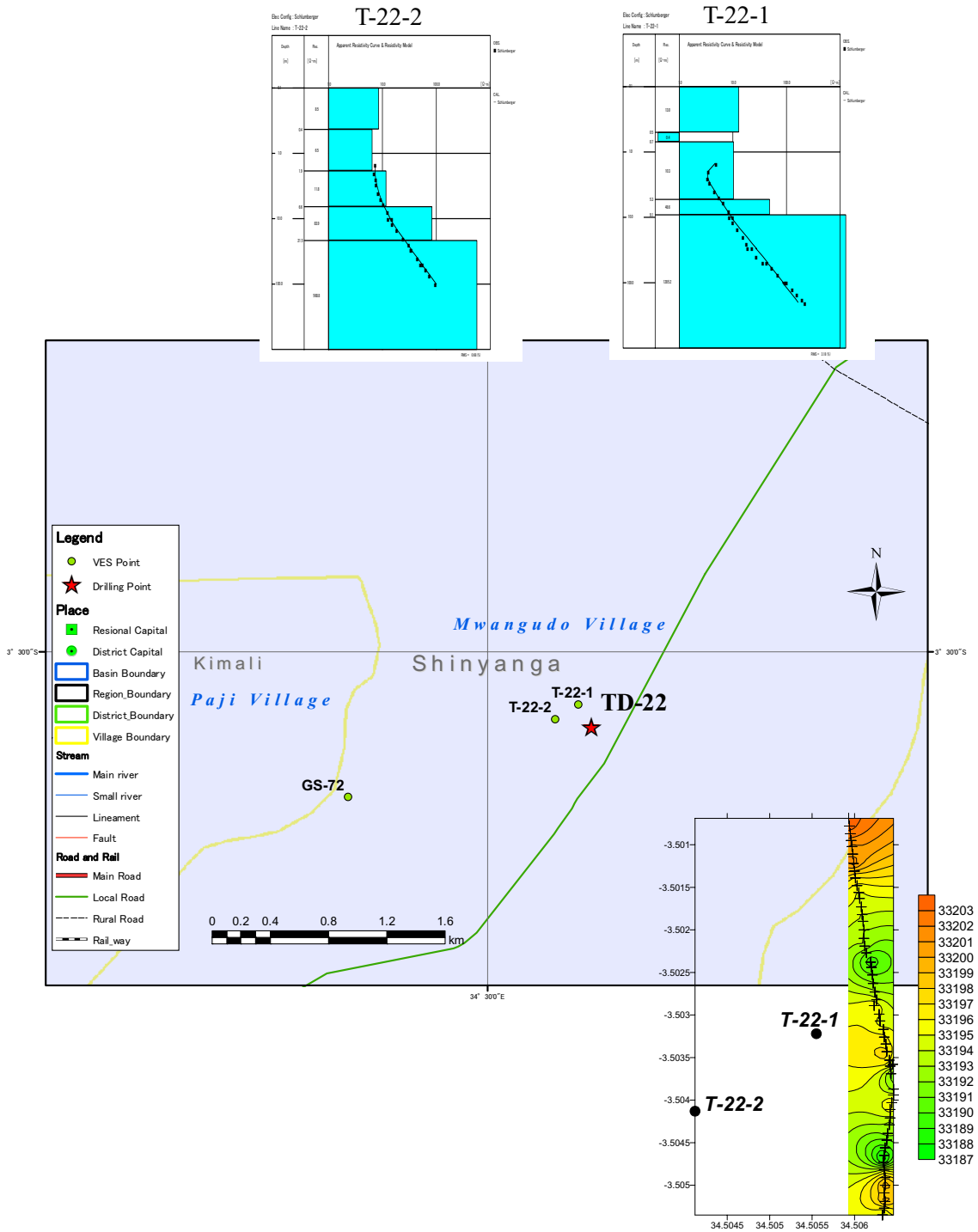

Figure 5-43 Location of Test Borehole Drilling No.22 and Survey Result

(23) Test Drilling No. 23 (Loliondo Village, Ngorongoro District, Arusha Region)

This site is the most northern part of IDB area, which is belonging in E sub-basin. This area is in the metamorphic rock (Xs) area. In this area, spring water is used for town water supply. Three VESs were conducted in this area. These three are along the axis of valley. Existing well is near the VES point T-23-1, it is used for dry season only. In the result of VES, bedrock is expected to encounter 45m approximately at the site T-23-1 and 2. There are 20 m layers on the upper part of the bedrock, and the layer is expected as aquifer. On the other hand, T-23-3 shows the bedrock depth is expected approximately 20m. And the upper layer which shows very low resistivity is expected as clayey layer. Therefore, T-23-2 was selected as a drilling site.

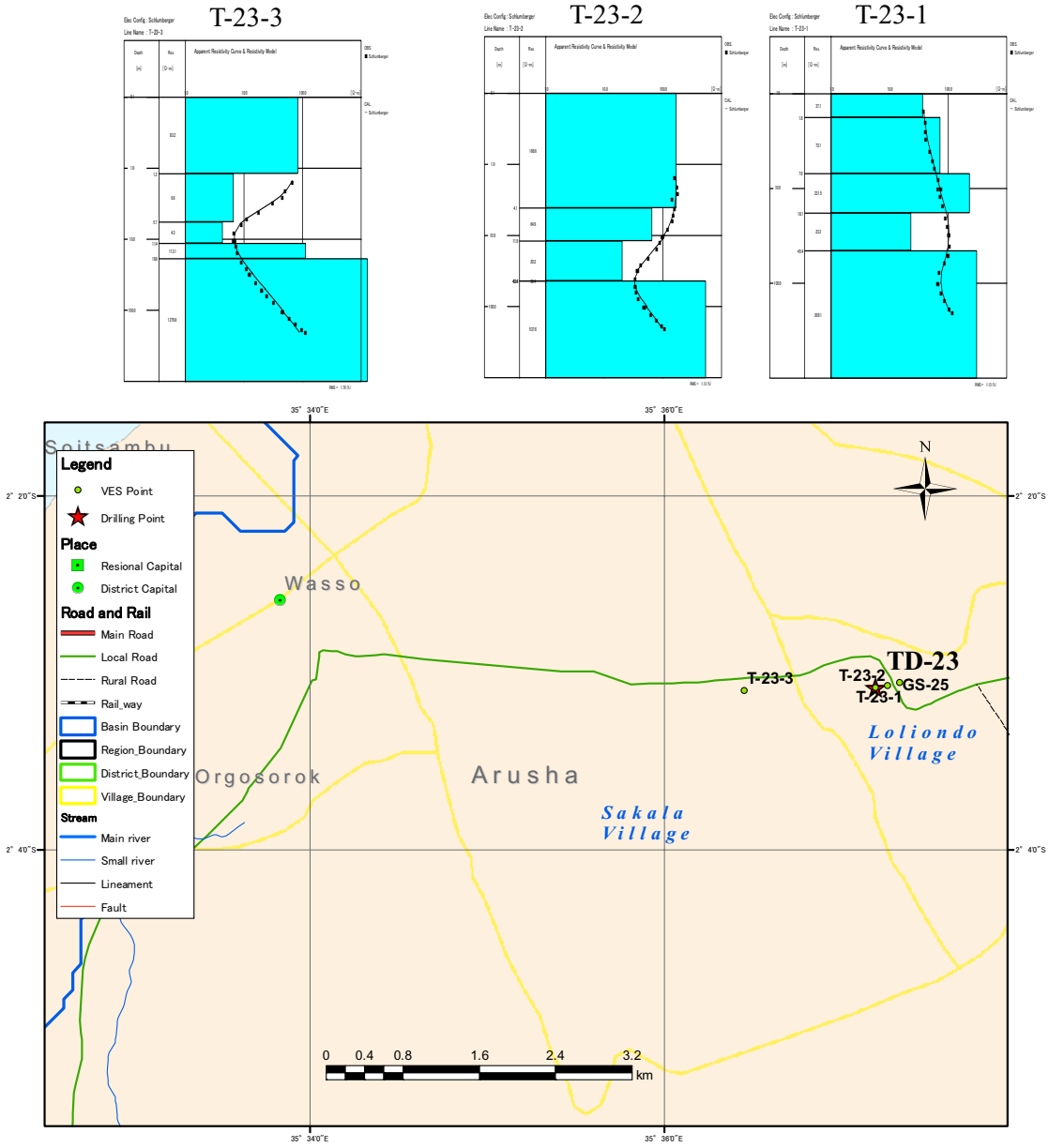

Figure 5-44 Location of Test Borehole Drilling No.23 and Survey Result

(24) Test Drilling No. 24 (Bassotu Village, Hanang District, Manyara Region)

This area was selected as an alternative site of Engarasero village, Ngorongoro District, Arusha Region. Engarasero site was selected as the deep well which fresh water will be taken from the fault of the Great Rift Valley in the contaminated area by fluoride. This Bassotu site is expected as the site which the water is also contaminated by fluoride from the volcanic ash of Mt. Hanang. The drilling site was selected near the fault escarpment which is continuing to Singida.

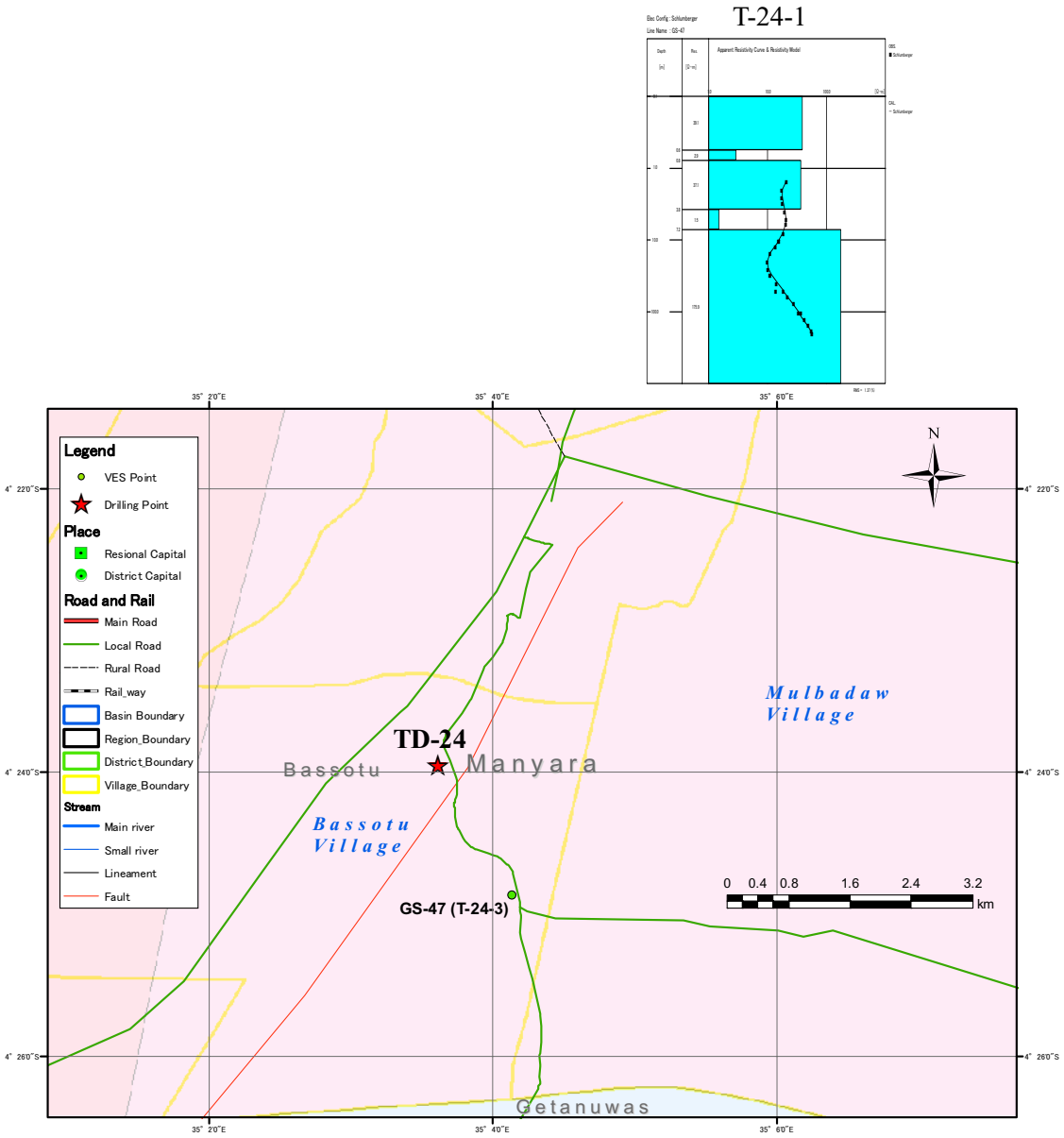

Figure 5-45 Location of Test Borehole Drilling No.24 and Survey Result

(25) Test Drilling No. 25 (Orkejuloongushu Village, Longido District, Arusha Region)

This area is the foot of Mt. Ketumbeine which is consist of basalt in C sub-basin. VESs were conducted three points in this area. T-25-1 and 2 are in lowland area. However, the resistivity results didn't show a good aquifer. T-25-3 was conducted at the hilly area near the fault line. The resistivity result shows good curve which has low resistivity layer. Therefore, T-25-3 was selected as a drilling point.

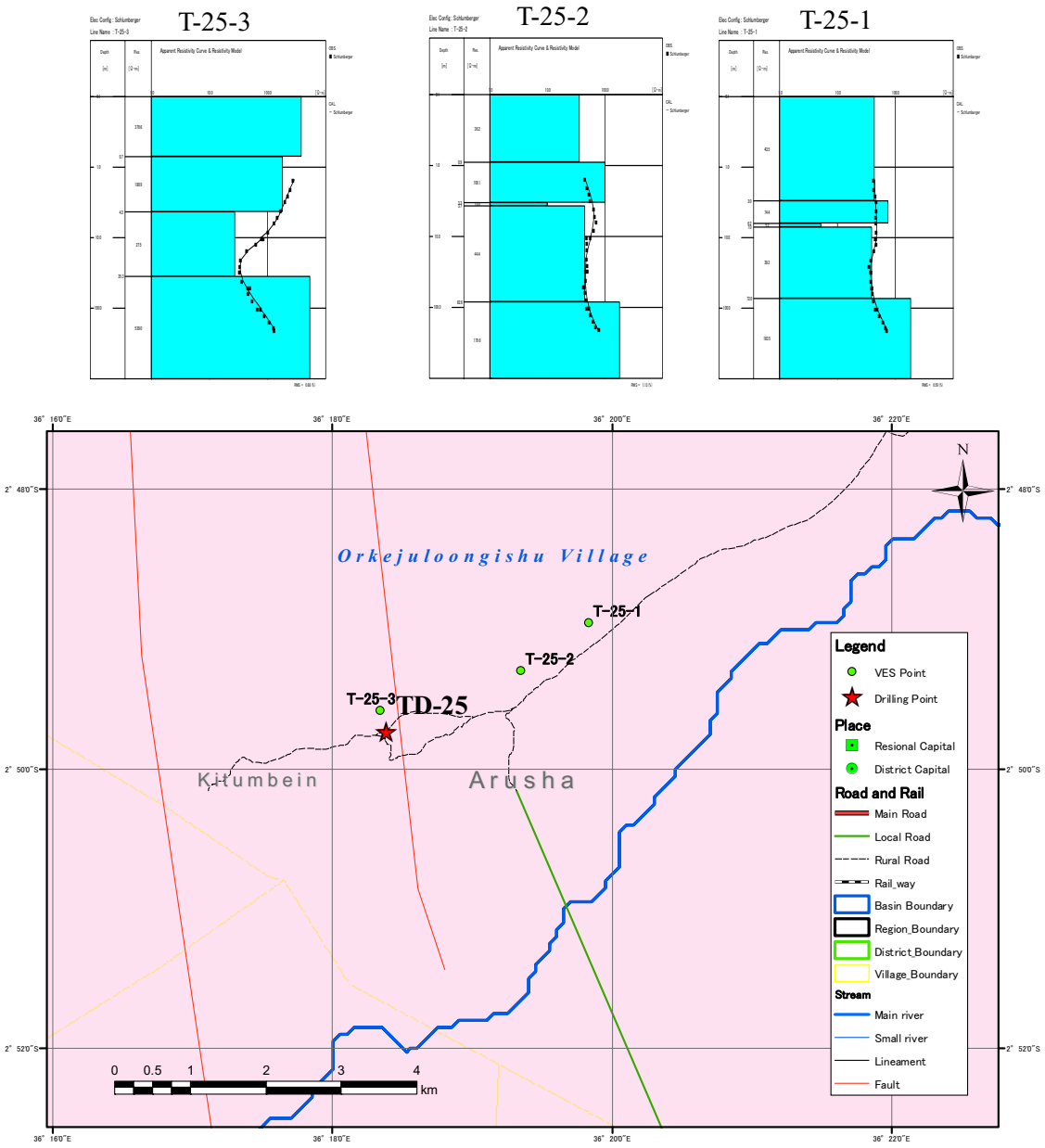

Figure 5-46 Location of Test Borehole Drilling No.25 and Survey Result

(26) Test Drilling No. 26 (Engaruka Chini Village, Monduli District, Arusha Region)

This site was selected as one area which is in the B sub-basin. This area is covered by volcanic ash. This village has some rivers which are flowing from Ngorongoro mountain area. Therefore, this area was expected to have much groundwater. T-26-1and 2 are conducted at the same point, but the direction of measurement line was perpendicular. These results were obtained almost same. This shows the area around the site has horizontal layered structure perfectly.

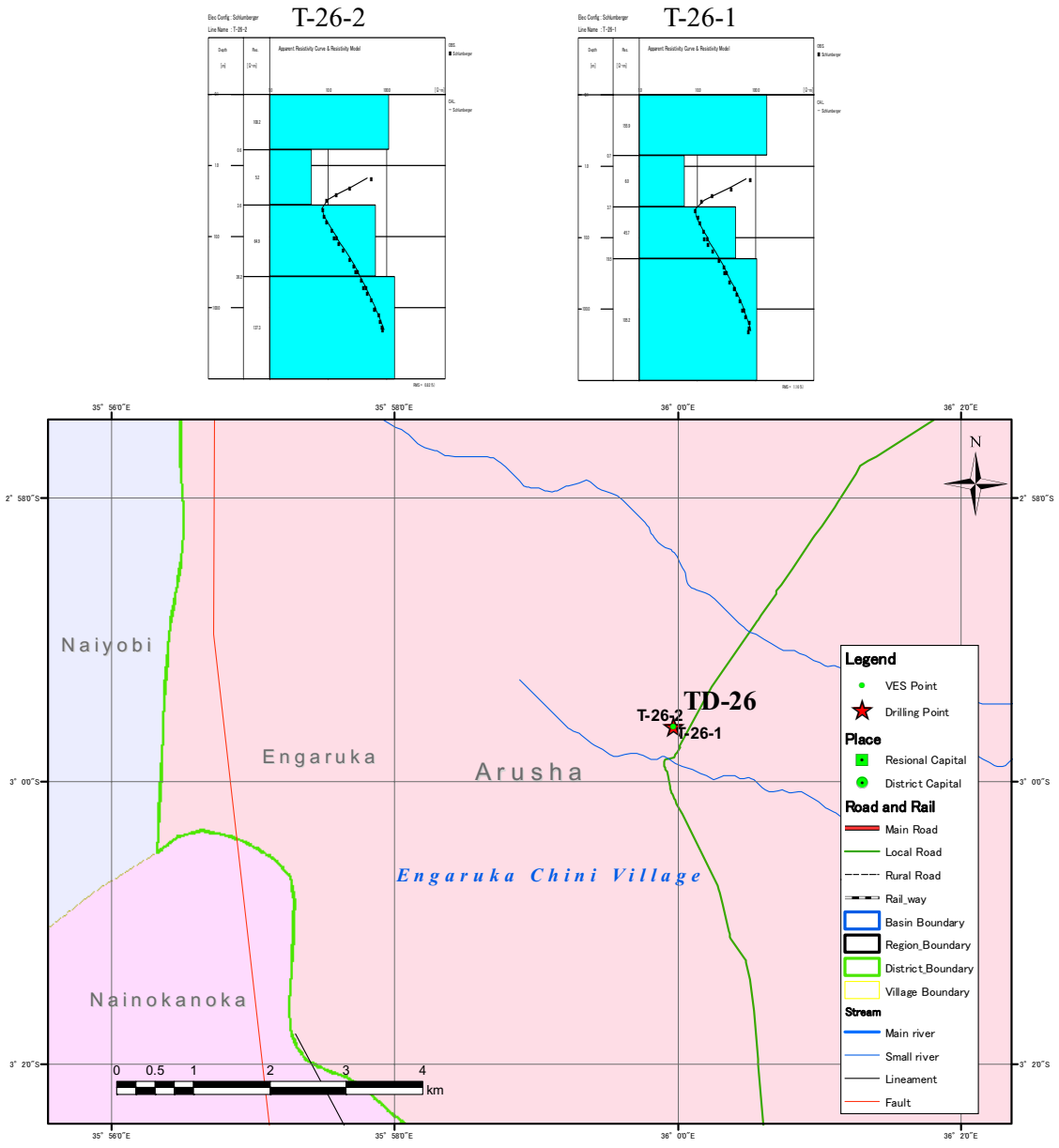

Figure 5-47 Location of Test Borehole Drilling No.26 and Survey Result

(27) Test Drilling No. 27 (Mfereji Village, Monduli District, Arusha Region)

This area is in the south-east of B sub-basin and the foot of Mt. Monduli. One of basalt lava flow made this hilly site. At the west side of this site, there is a escarpment of basalt lava. Many springs are flowing out from the escarpment. Existing water supply facility is taking water from the spring. But it was not accessible. Three VESs were conducted on the hilly area of basalt lava. And magnetic survey was conducted crossing the lava hill. The results of VESs are the similar; fresh basalt is expected to encounter 40 to 70 m depth. T-27-3 shows the deepest bedrock depth in the VES results. Magnetic survey result shows also negative anomaly around T-27-3. Therefore, T-27-3 was selected as the drilling point.

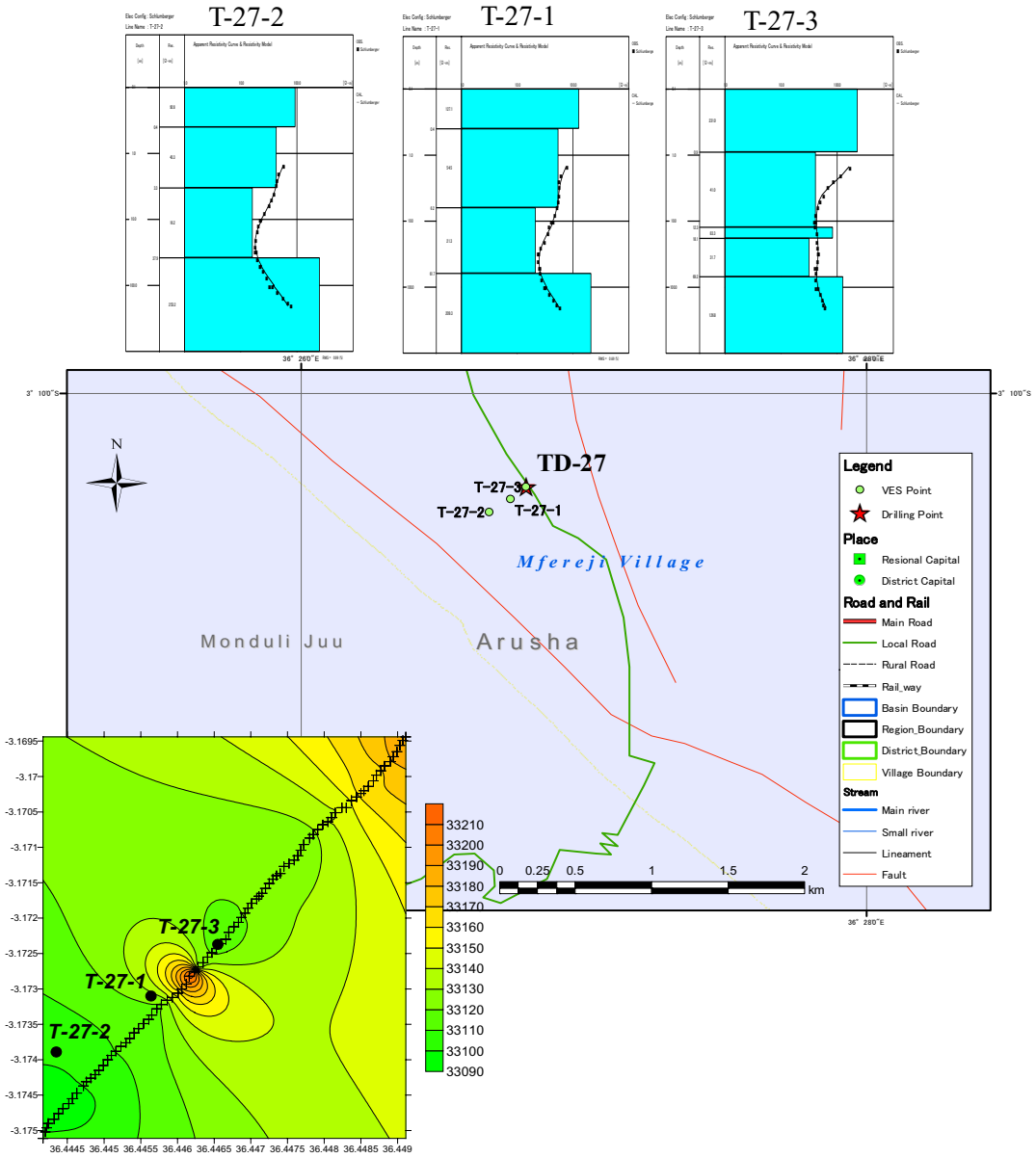

Figure 5-48 Location of Test Borehole Drilling No.27 and Survey Result

(28) Test Drilling No. 28 (Olmolog Village, Longido District, Arusha Region)

This area is in the I sub-basin and the foot of Mt. Kilimanjaro. There are many scoria cones around this area. Two VESs and magnetic survey were conducted in this site. The results of VESs showed that the bedrock which has high resistivity is encountered 10 m depth approximately. This high resistivity layer is expected as basalt lava. Generally, basalt lava has much fracture zone on its upper and lower side of lava flow. and the aquifer was expected in such a fracture part of the lava. Magnetic survey result shows the negative anomaly is near T-28-1. Therefore, T-28-1 was selected as a drilling point.

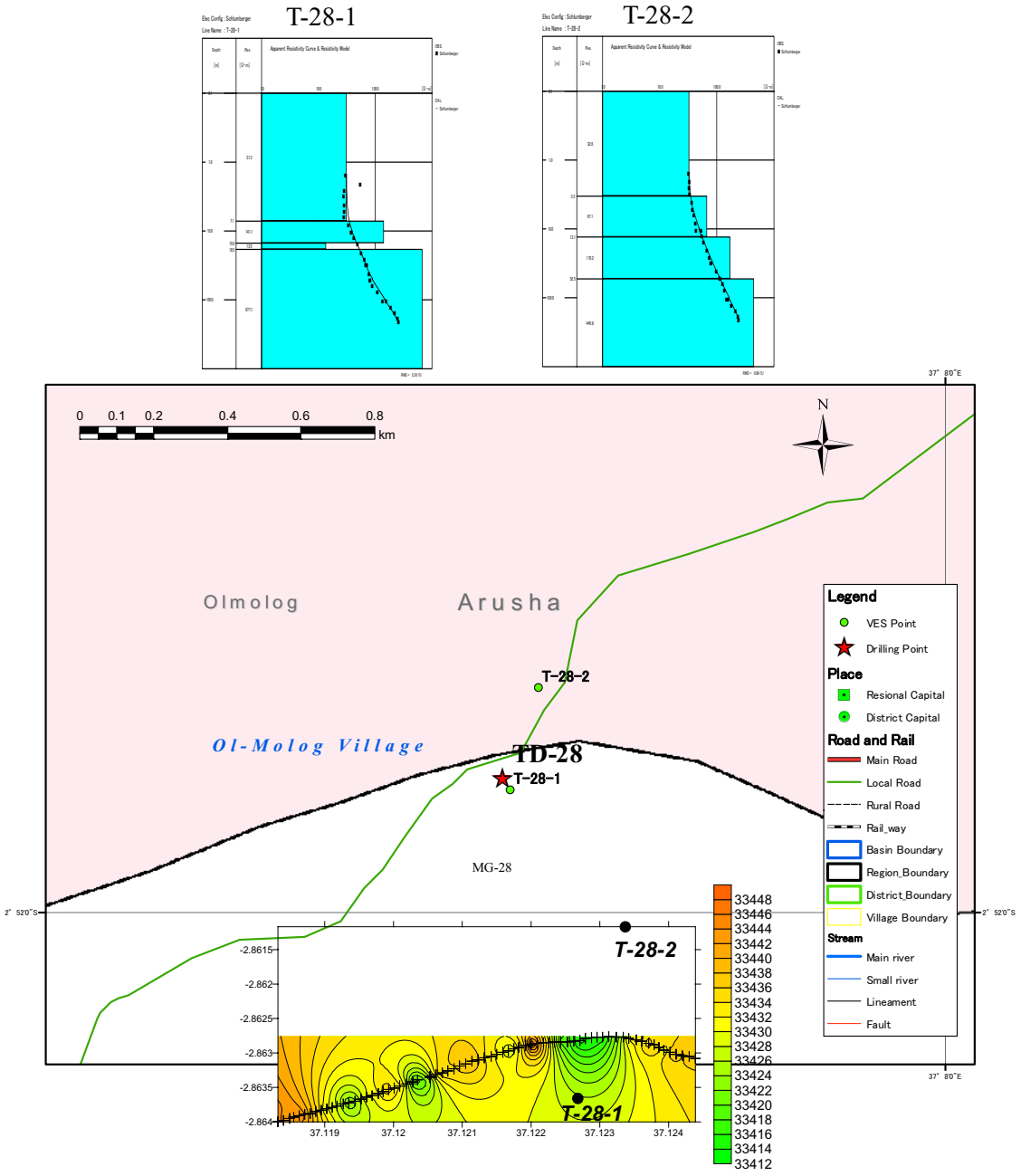

Figure 5-49 Location of Test Borehole Drilling No.28 and Survey Result

(29) Test Drilling No. 29 (Uwiro Village, Arumeru District, Arusha Region)

This area is in the I sub-basin and the northern foot of Mt. Meru. There are many springs in the foot of Mt. Meru, and the water is contaminated by much fluoride. To confirm the fluoride contents in groundwater in this area, this site was selected. Two VESs points was selected around the fault escarpment. The results of T-29-1 shows that the high resistivity layer is lain deeper than T-29-2. Magnetic survey result shows the negative anomaly around the fault escarpment. Finally, T-291 was selected as a drilling site.

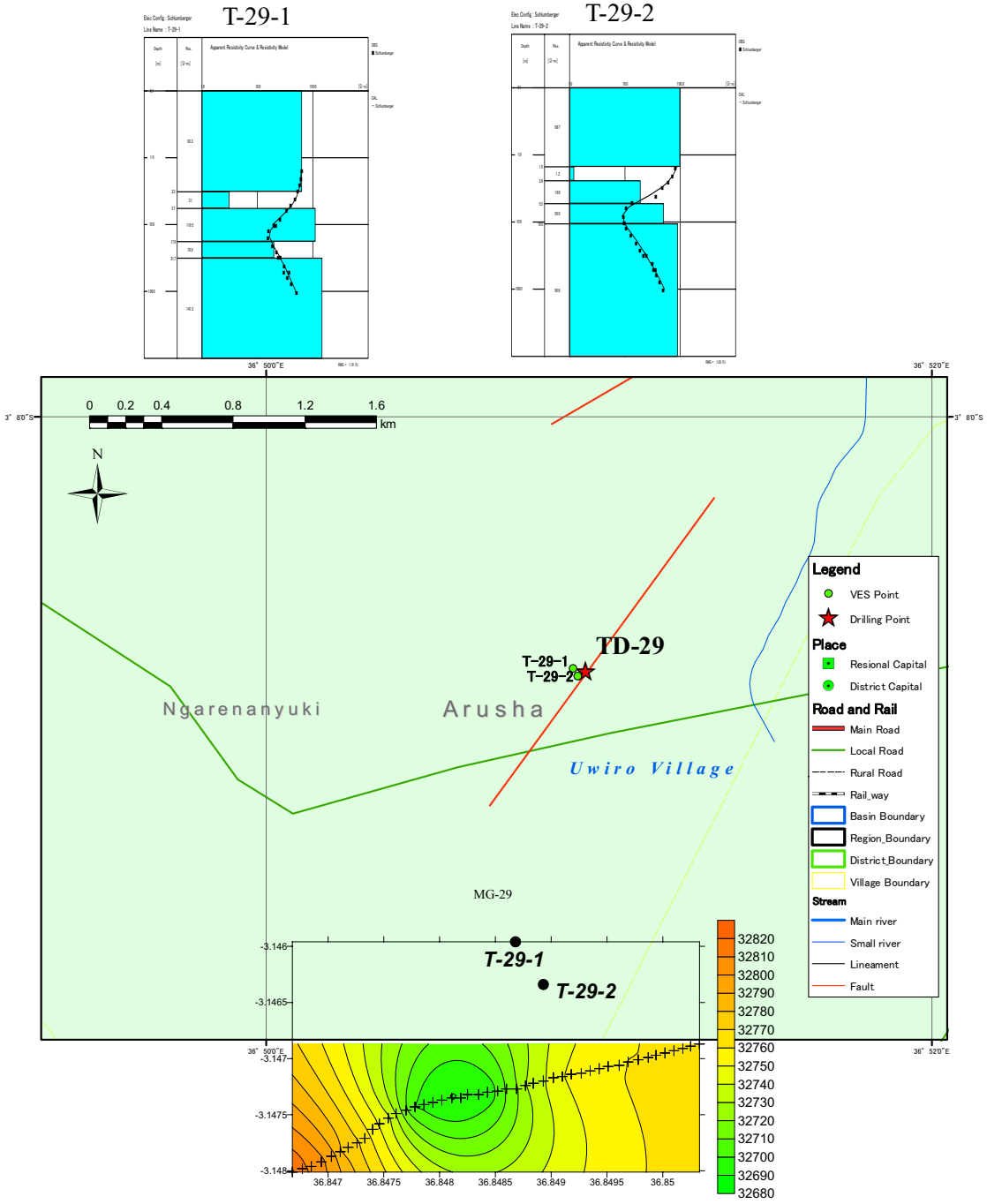

Figure 5-50 Location of Test Borehole Drilling No.29 and Survey Result

(30) Test Drilling No. 30 (Tingatinga Village, Longido District, Arusha Region)

This area was selected as the downstream of the I sub-basin. Two VESs were conducted in this village. The result of T-30-1shows very high resistivity, and it was not expected any layer has groundwater. The result of T-30-2 shows that the resistivity increases in deeper part, and it shows the good aquifer is not expected in the site. However, there is a spring in the southern part of this village, which is higher altitude than T-30-2. Groundwater was expected in the layer of the upper part of bedrock. T-30-2 was selected as a drilling point.

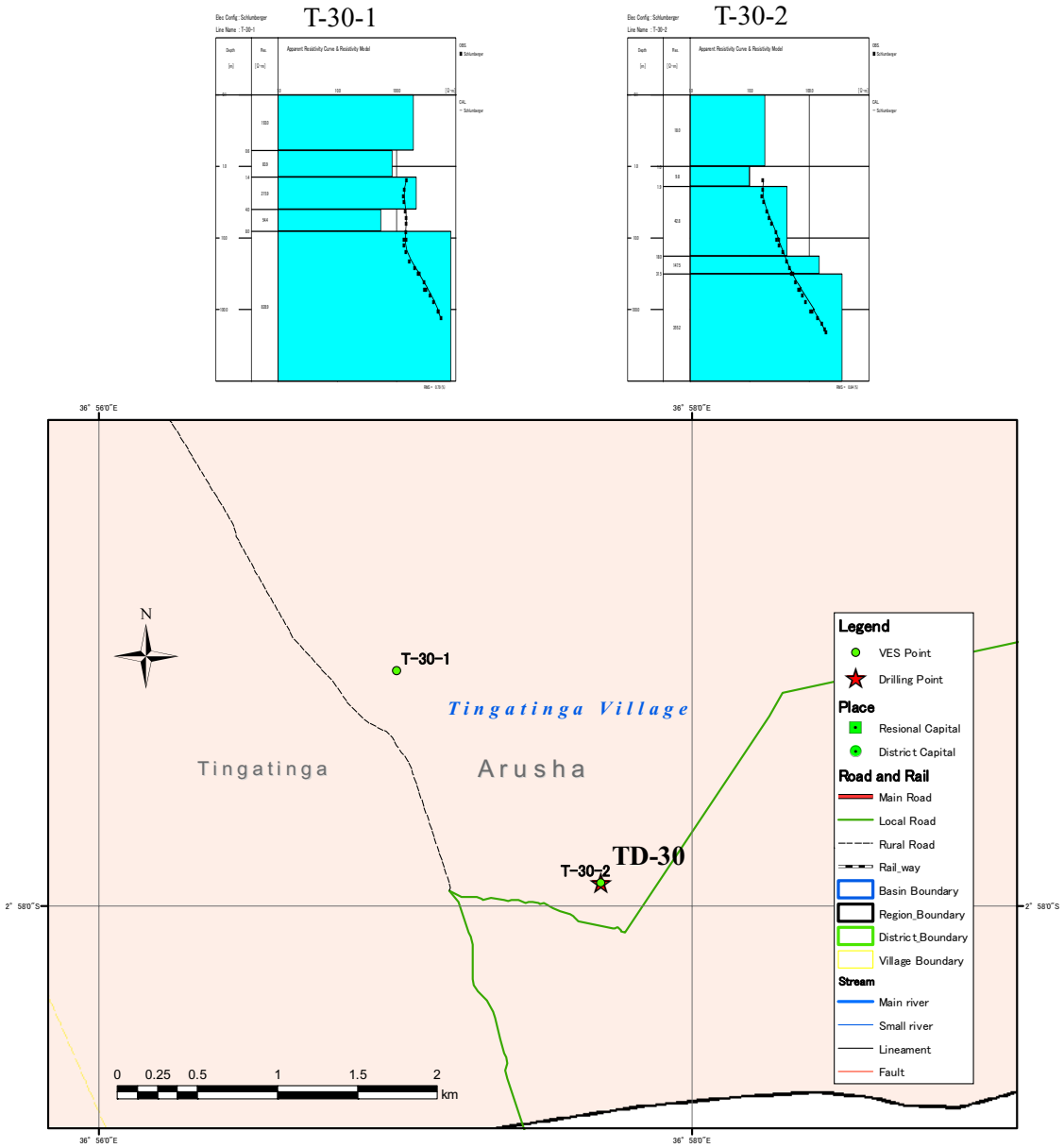

Figure 5-51 Location of Test Borehole Drilling No.30 and Survey Result